AD-A092 077 KANSAS UNIV/CENTER FOR RESEARCH INC LAWRENCE REMOTE --ETC F/G 17/9
CIRCULARLY POLARIZED MEASUREMENTS OF RADAR BACKSCATTER FROM TER--ETC(U)
JUL 80 W H STILES, F T ULABY, E A WILSON DAAK70-78-C-0121
UNCLASSIFIED CRINC/RSL-TR-393-2 ETL-0234 NL

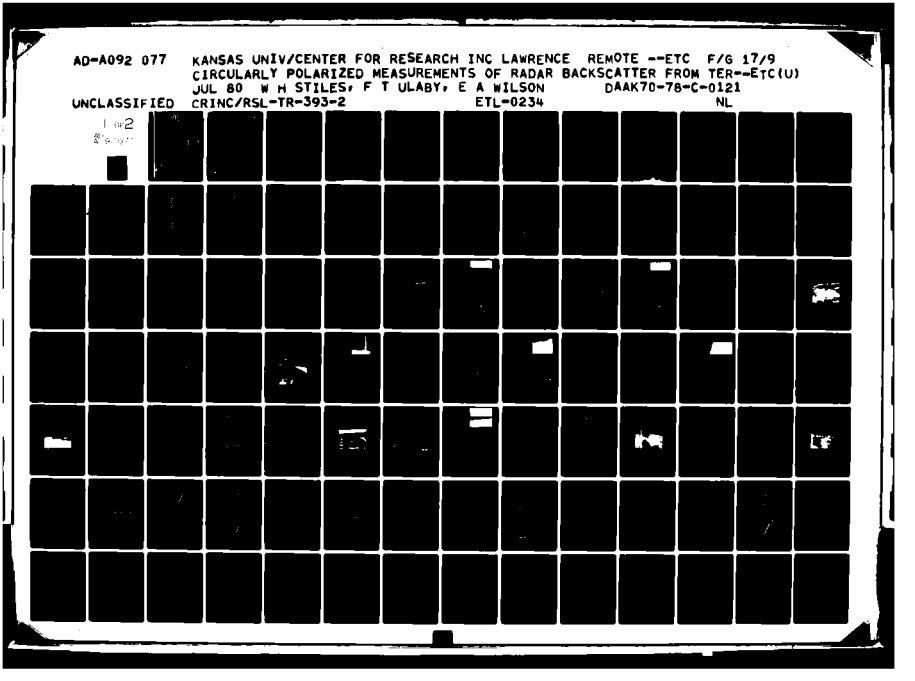

REMOTE SENSING LABORATORY

ETL-0234

CIRCULARLY POLARIZED MEASUREMENTS OF RADAR BACKSCATTER FROM TERRAIN AND SNOW-COVERED TERRAIN

W. H. Stiles
F. T. Ulaby
E. A. Wilson
J. C. Holtzman

July 1980

Prepared for:

U. S. Army Engineer Topographic Laboratories
Fort Belvoir, Virginia 22060

THE UNIVERSITY OF KANSAS CENTER FOR RESEARCH, INC.

2291 Irving Hill Drive—Campus West
Lawrence, Kansas 66045

Telephone: (913) 864-4832

(10)

ETL-0234

CIRCULARLY POLARIZED MEASUREMENTS OF RADAR BACKSCATTER FROM TERRAIN AND SNOW-COVERED TERRAIN

Remote Sensing Laboratory
RSL Technical Report 393-2

W. H. Stiles
F. T. Ulaby
E. A. Wilson
J. C. Holtzman

Fawwaz T. Ulaby, Principal Investigator

July 1980

Prepared for:

U. S. Army Engineer Topographic Laboratories
Fort Belvoir, Virginia 22060

DESTROY THIS REPORT WHEN NO LONGER NEEDED.
DO NOT RETURN IT TO THE ORIGINATOR.

THE FINDINGS IN THIS REPORT ARE NOT TO BE CONSTRUED AS AN OFFICIAL DEPARTMENT OF THE ARMY POSITION UNLESS SO DESIGNATED BY OTHER AUTHORIZED DOCUMENTS.

THE CITATION IN THIS REPORT OF TRADE NAMES OF COMMERCIALLY AVAILABLE PRODUCTS DOES NOT CONSTITUTE OFFICIAL ENDORSEMENT OR APPROVAL OF THE USE OF SUCH PRODUCTS.

(14) CRINC/RSL-TR-393-2

SECURITY CLASSIFICATION OF THIS PAGE (When Data Entered)

(19) REPORT DOCUMENTATION PAGE

READ INSTRUCTIONS BEFORE COMPLETING FORM

1. REPORT NUMBER (18) ETL-0234	2. GOVT ACCESSION NO. AD-A092077
3. RECIPIENT'S CATALOG NUMBER	
4. TITLE (and Subtitle) (6) CIRCULARLY POLARIZED MEASUREMENTS OF RADAR BACKSCATTER FROM TERRAIN AND SNOW-COVERED TERRAIN.	5. TYPE OF REPORT & PERIOD COVERED Contract Report (Final)
	6. PERFORMING ORG. REPORT NUMBER RSL Tech. Report 393-2
7. AUTHOR(s) (10) W. H. Stiles, F. T. Ulaby, E. A. Wilson and J. C. Holtzman	8. CONTRACT OR GRANT NUMBER(s) (15) DAAK70-78-C-0121
9. PERFORMING ORGANIZATION NAME AND ADDRESS University of Kansas Center for Research, Inc. Remote Sensing Laboratory - West Campus Lawrence, KS 66044	10. PROGRAM ELEMENT, PROJECT, TASK AREA & WORK UNIT NUMBERS (12) 147
11. CONTROLLING OFFICE NAME AND ADDRESS U. S. Army Engineer Topographic Laboratories Fort Belvoir, VA 22060	12. REPORT DATE (11) July 1980
	13. NUMBER OF PAGES 147
14. MONITORING AGENCY NAME & ADDRESS (if different from Controlling Office) (9) Final rpt.,	15. SECURITY CLASS. (of this report) Unclassified
	15a. DECLASSIFICATION/DOWNGRADING SCHEDULE

16. DISTRIBUTION STATEMENT (of this Report)

Approved for public release; distribution unlimited.

17. DISTRIBUTION STATEMENT (of the abstract entered in Block 20, if different from Report)

18. SUPPLEMENTARY NOTES

19. KEY WORDS (Continue on reverse side if necessary and identify by block number)

Backscatter, Microwave Remote Sensing, Radar Remote Sensing, Circular Polarization, Terrain, Snowcover

20. ABSTRACT (Continue on reverse side if necessary and identify by block number)

This report covers a measurement program to obtain circularly polarized radar backscatter coefficient (σ^0) data along with associated ground-truth information on snow-covered terrain. Snow-covered grass, asphalt and ice were observed at selected frequencies from 8 to 18 GHz for angles of incidence between 0° (nadir) and 80°. Also included are some analyses of the effects of snowcover on the backscatter from terrain.

* deg.

DD FORM 1 JAN 73 1473 EDITION OF 1 NOV 65 IS OBSOLETE S/N 0102-014-6601

UNCLASSIFIED

SECURITY CLASSIFICATION OF THIS PAGE (When Data Entered)

406688

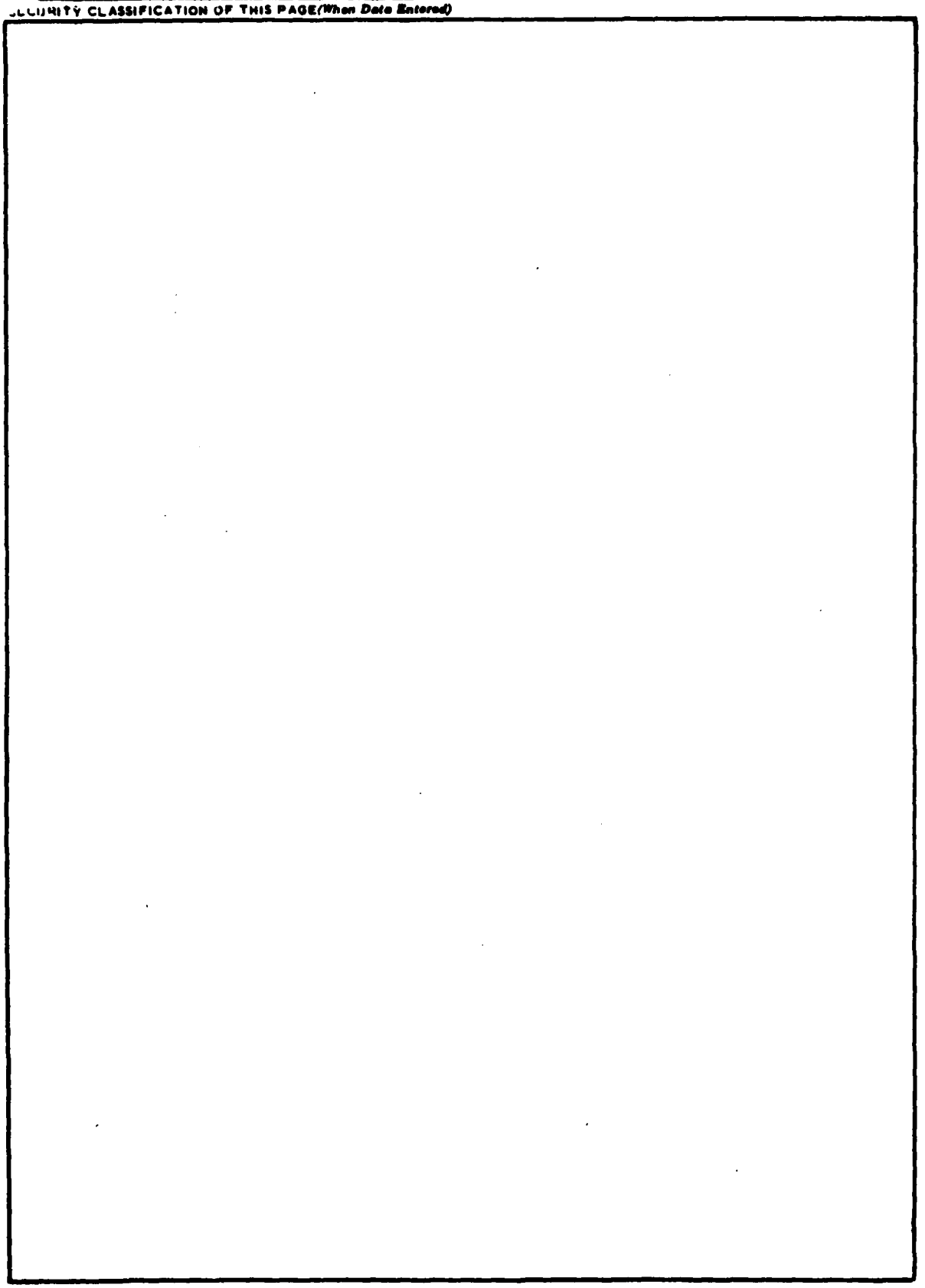

TABLE OF CONTENTS

PREFACE

The Remote Sensing Laboratory wishes to thank Mr. Jerry Patterson of the Steamboat Resort in Steamboat Springs, Colorado and Mr. Joe Reddick, Ranger of the Arapaho National Recreation Area for their cooperation in arranging the usage of their facilities. The participation and help of the following individuals in the data-acquisition and processing phases is appreciated:

Dennis Anderson
Dennis Carmichael
Chip Gabel
George Eger
John Williamson
Tom Near
Dan Barbour
Craig Dobson
Mohamed Abdel-Razik
Adnan Aslam

This report was prepared under Contract No. DAAK70-78-C-0121 for the U. S. Army Engineer Topographic Laboratories, Fort Belvoir, Virginia. The Contract Officers Representative (COR) was Mr. Richard A. Hevenor.

LIST OF FIGURES

LIST OF TABLES

1.0 INTRODUCTION

This report covers the conclusion of a measurement program to obtain circularly polarized radar backscatter coefficient (σ^o) data along with associated ground-truth information on terrain. A previous report [1] documented the circular polarization response of various types of tree-covers, road surfaces, and bare-soil targets. This report includes analyses of the previously reported backscatter coefficient data, measurements and observations on the effects of snow-cover on the various terrain classes, and recommendations for future studies in this area. Section 2, although by no means detailed, provides heuristic explanations for the different scattering coefficient responses reported in [1]. This section points to the need for more measurements and theoretical developments to provide a firmer basis for the given explanations. In Section 3, the snow-covered-terrain data is presented, along with discussions of the ground-truth data and the scattering behavior of snow. The final section points out areas of interest that are not well-understood and recommends experimental and theoretical programs designed to improve the understanding of the circularly polarized return from terrain and to remove some of the ambiguities observed in the data.

2.0 ANALYSES OF THE RADAR BACKSCATTER COEFFICIENT OF TERRAIN

In the initial phase of this program, measurements were taken on various types of terrain. The targets studied included coniferous and deciduous trees, asphalt and concrete surfaces, and plowed and bare ground. Data were acquired at six frequencies in the 8-18 GHz range using RR, RL, and LL circular polarization and at incidence angles from 0° to 80°.

This section will provide a brief review and interpretation of these terrain measurements. For more detailed information, refer to Wilson, et al. [1].

2.1 Coniferous and Deciduous Trees

All tree measurements for this program were taken at six sites in the Mark Twain National Forest located in southern Missouri. The sites were visited in August and in November.

2.1.1 Coniferous Trees

The type of coniferous tree studied was shortleaf pine. Data were acquired at three sites. Relevant ground truth is summarized in Table 2-1. Figure 2-1 compares the angular response of the three sites in August. For incidence angles less than 30°, Site 1, the densest, exhibits a higher return. Note also, however, that Sites 2 and 5 differ significantly in density, height, and circumference, yet their response is nearly identical. It is possible that the return from the densest site is dominated by the vegetation, even at low angles of incidence, while at the other two sites a significant ground-return is present, below 30°. One might argue that this ground-return at lower angles should result in a "peak" near vertical incidence. It must be recognized, however, that the observed response is strongly dependent on the "roughness" of the forest floor, which is covered with deadwood, various other types of vegetation, and fallen leaves. Another possible explanation is that Site 1 is so dense that the upper part of the canopy almost forms a surface. Figure 2-2 compares the angular response at Site 5 in August versus November. Considering the limits of system accuracy and precision, it appears that coniferous trees exhibit negligible seasonal change.

TABLE 2-1

Coniferous Tree Ground Truth

Site	Date	Height (m)	Height to Branches (m)	Average Trunk Circumference (m)	Tree Density (100 m^2)	Soil Moisture (0-2 cm)	Needle Moisture
1	AUG	7.5	2.5	0.33	80	22%	68%
2	AUG	10.4	4.3	0.58	60	22%	66%
5	AUG	3.5	0.6	0.30	30	16%	65%
5	NOV	3.5	0.6	0.30	30	23%	63%

TABLE 2-2

Deciduous Tree Ground Truth

Site	Date	Height (m)	Height to Branches (m)	Average Trunk Circumference (m)	Tree Density (100 m^2)	Soil Moisture (0-2 cm)	Leaf Moisture
3	AUG	6.5	3.2	0.89	30	26%	59%
6	AUG	6.0	0.6	0.39	35	12%	55%
3	NOV	6.5	3.2	0.89	30	29%	--
6	NOV	6.0	0.6	0.38	35	29%	--

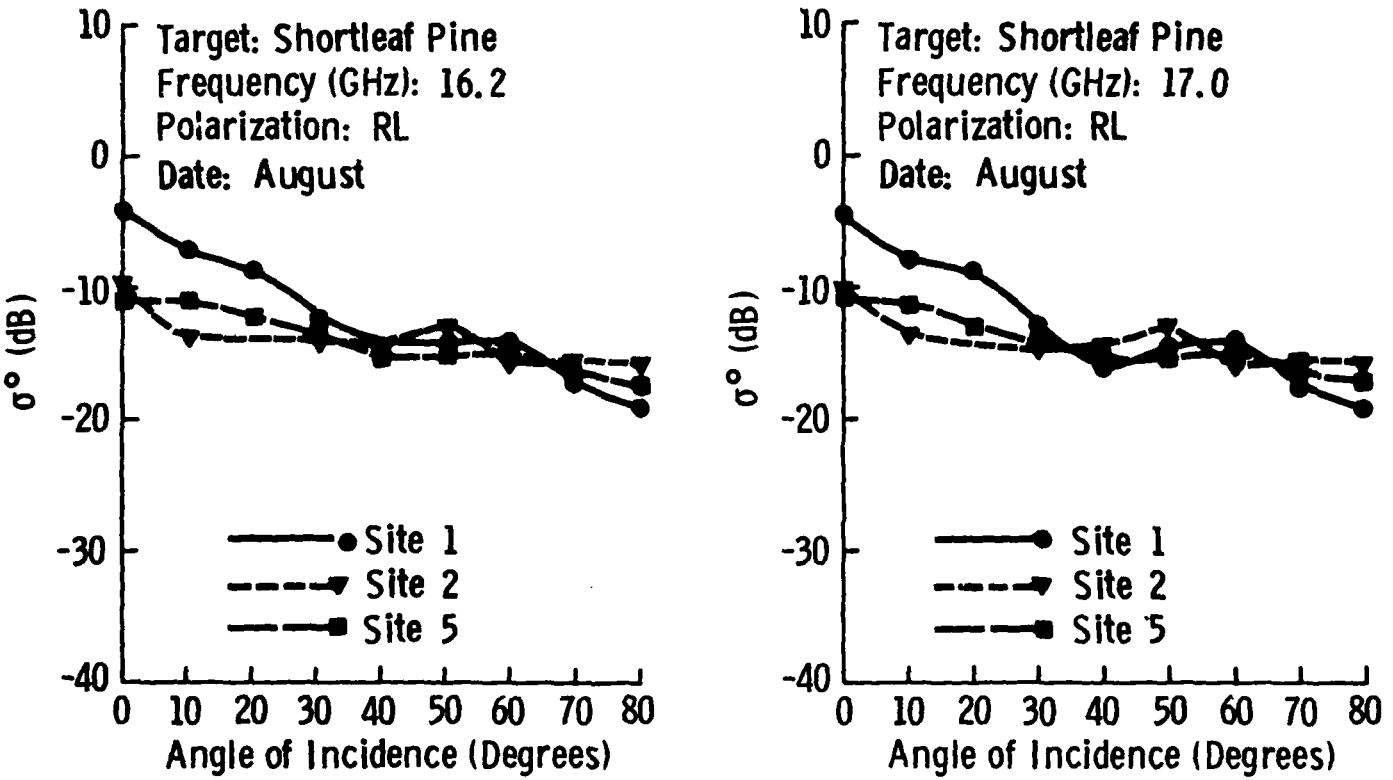

Figure 2-1 A comparison of the angular response of σ^{o} at 16.2 GHz and 17.0 GHz for shortleaf pine at three sites.

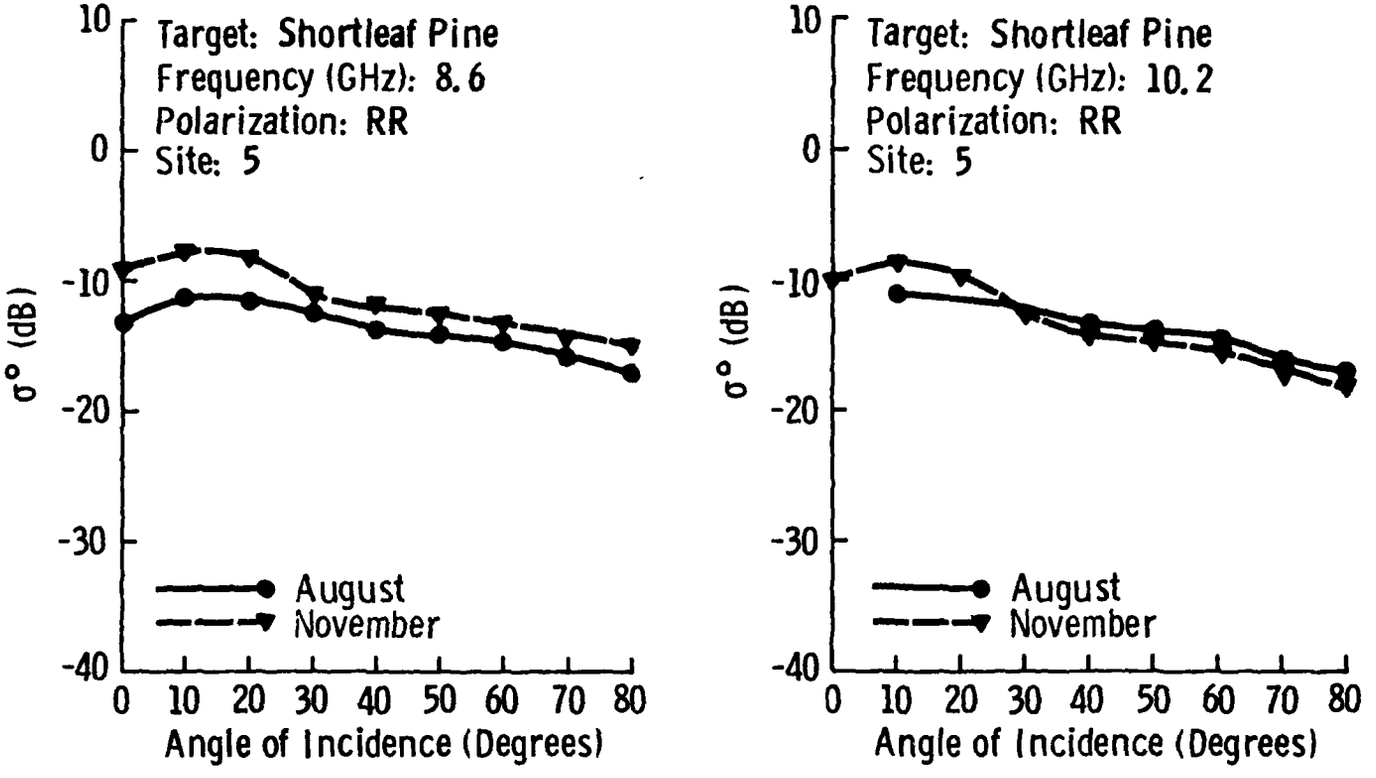

Figure 2-2 A comparison of the angular response of σ° at 8.6 GHz and 10.2 GHz for shortleaf pine at Site 5 in August and November.

2.1.2 Deciduous Trees

The type of deciduous trees studied was a mix of oak and hickory. Data were acquired "with leaves" at two sites in August and "without leaves" at the same two sites in November. Relevant ground truth is summarized in Table 2-2. Figure 2-3 compares the angular response of the two sites in August. The plots reveal a rather wide spread in level between the two sites at all angles of incidence. The density of trees per unit area and the average tree height were about the same for both sites, but the tree "volumes" were quite different. The canopy volume (branches) for Site 6 extended from 0.6 m above the ground to the top of the canopy while the canopy of Site 3 had essentially no branches in the lower three meters. Consequently, it is conceivable that the greater range of volume scatterers in Site 6 is responsible for the higher values of σ^{o}. It is possible also that the cause may be due to some other geometrical difference between the trees of the two canopies. In order to resolve such questions and to improve the understanding of the mechanisms responsible for the backscatter from tree canopies, it is necessary to conduct measurements with a high-resolution system capable of measuring the backscatter contribution as a function of range into the canopy. This recommendation is discussed in more detail in Section 4.

Figure 2-4 compares the response at Site 6 in August versus November. At the higher angles of incidence, the defoliation has resulted in a reduction in level of approximately 4-5 dB; at the lower angles of incidence, the moist November soil has apparently caused the level to rise above that of the August data.

2.1.3 Mixed Deciduous and Coniferous Trees

An area of mixed oak, hickory and shortleaf pine also was studied during this experimental program. Although it was not possible to determine the exact percentage of each type of tree, the site appeared to be approximately 60%-70% deciduous. The response of this site was similar to that of Site 6 which was totally deciduous.

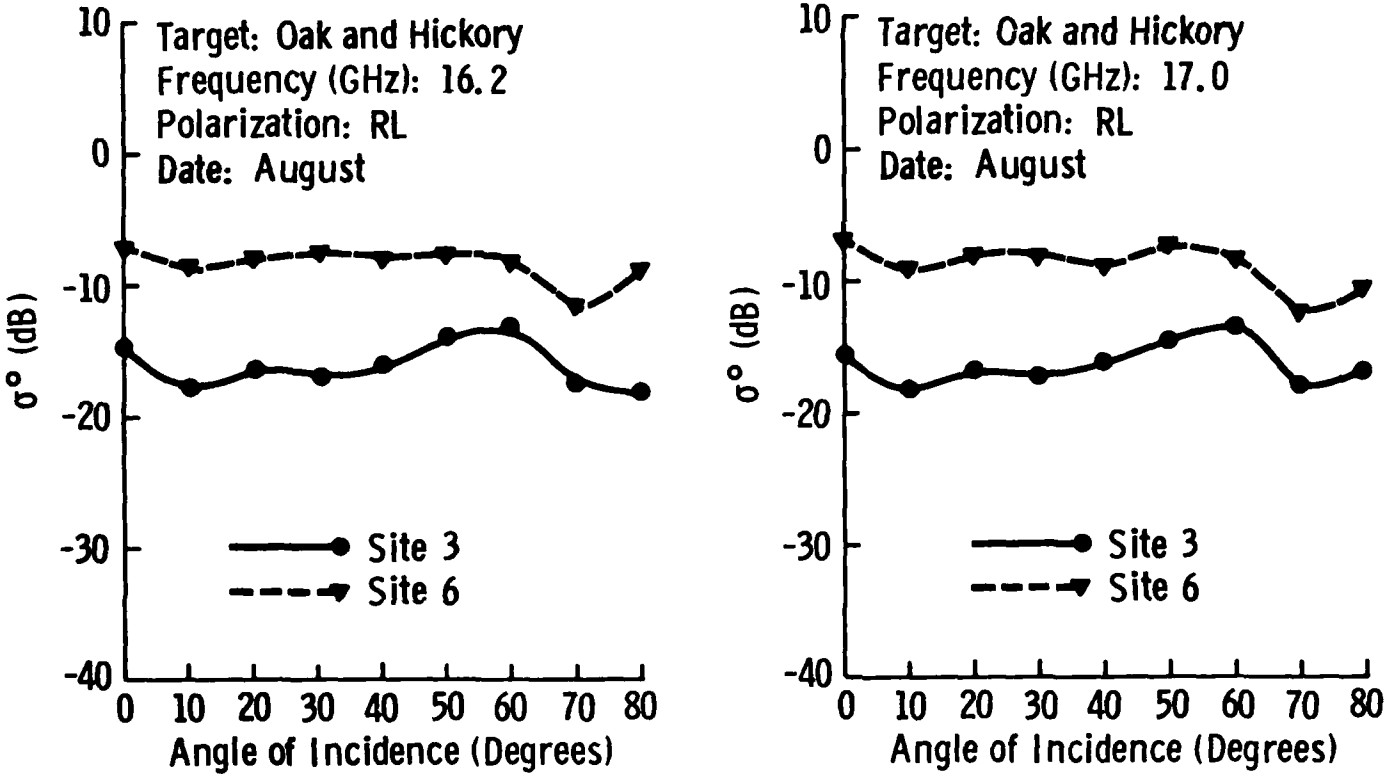

Figure 2-3 A comparison of the angular response of σ^{o} at 16.2 GHz and 17.0 GHz for oak and hickory at two sites.

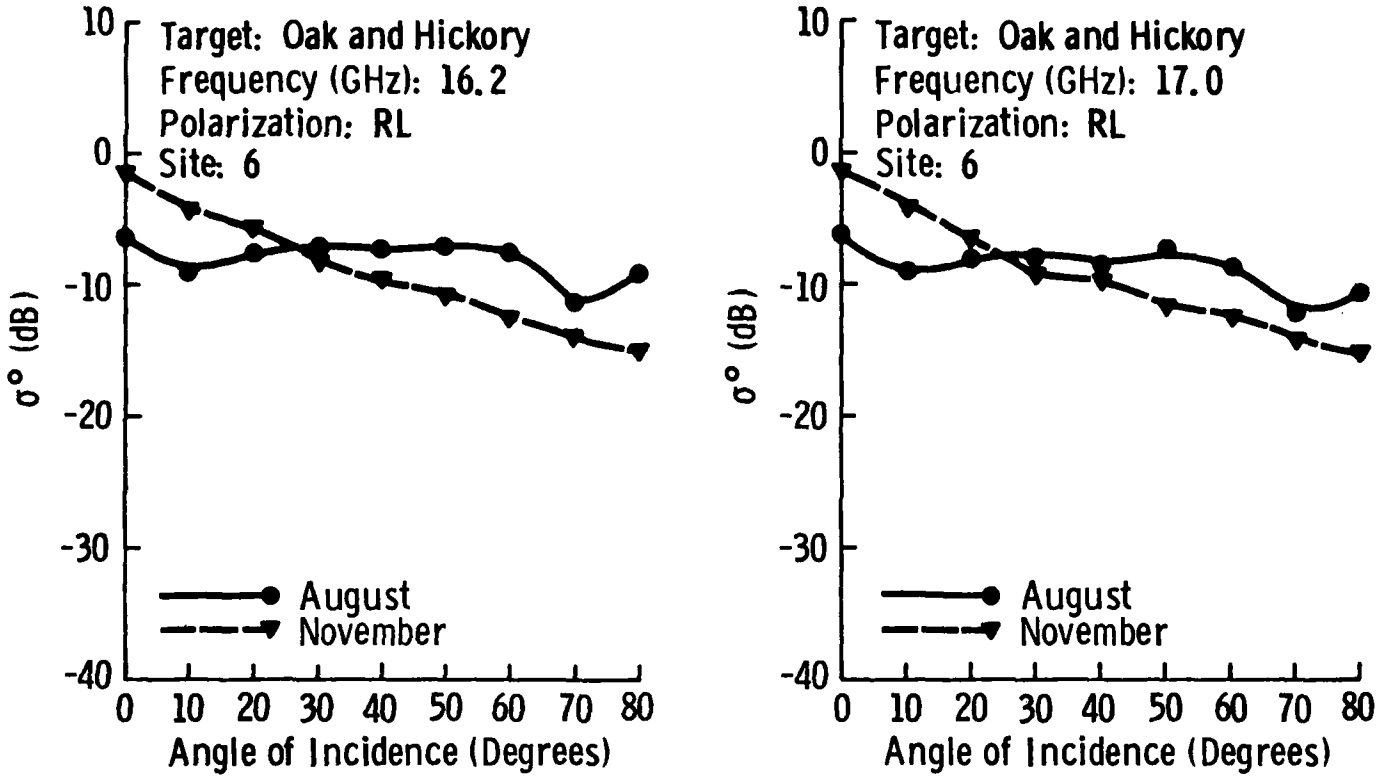

Figure 2-4 A comparison of the angular response of σ^{o} at 16.2 GHz and 17.0 GHz for oak and hickory at Site 6 in August and November.

2.1.4 Comparison of Deciduous and Coniferous Trees

Figure 2-5 compares the response of coniferous, deciduous, and mixed stands of trees. Over most of the angular range investigated, the response of the coniferous-tree site is approximately 5 dB below that of the other two sites.

This comparison is based upon August data; a similar comparison for November data would show little difference in level among the tree-types, except near nadir where apparently there is a significant ground-return associated with the defoliated deciduous trees.

2.2 Asphalt and Concrete Surfaces

Measurements on asphalt and concrete surfaces were conducted at Johnson County Industrial Airport near Olathe, Kansas. Both surfaces were measured under wet and dry conditions. In general, one would expect that the addition of water to an asphalt or concrete surface should have two effects: (1) the average dielectric constant should increase and (2) the water should tend to "smooth" the surface. The angular response of σ^{o} for wet and dry concrete, however, showed little difference between the two conditions; the same was true for asphalt, except at nadir where the wet surface gave approximately a 5 dB greater return than the dry surface. These measurements suggest that there was little effect due to changes in dielectric constant, especially on concrete. The 5 dB increase at nadir on asphalt may be due to a "smoothing" effect, but quite likely it reflects the difficulty of making precise measurements at nadir on a smooth surface where a slight angular error causes a significant drop in the large coherent component of the return. Comparison of dry concrete versus dry asphalt indicates that the asphalt is slightly rougher, as expected from physical observation (Figure 2-6); comparison of the two surfaces when wet shows little difference in roughness.

2.3 Plowed and Bare Ground

Measurements on plowed and bare ground were conducted north of Lawrence, Kansas. As with other surfaces, the return should be a

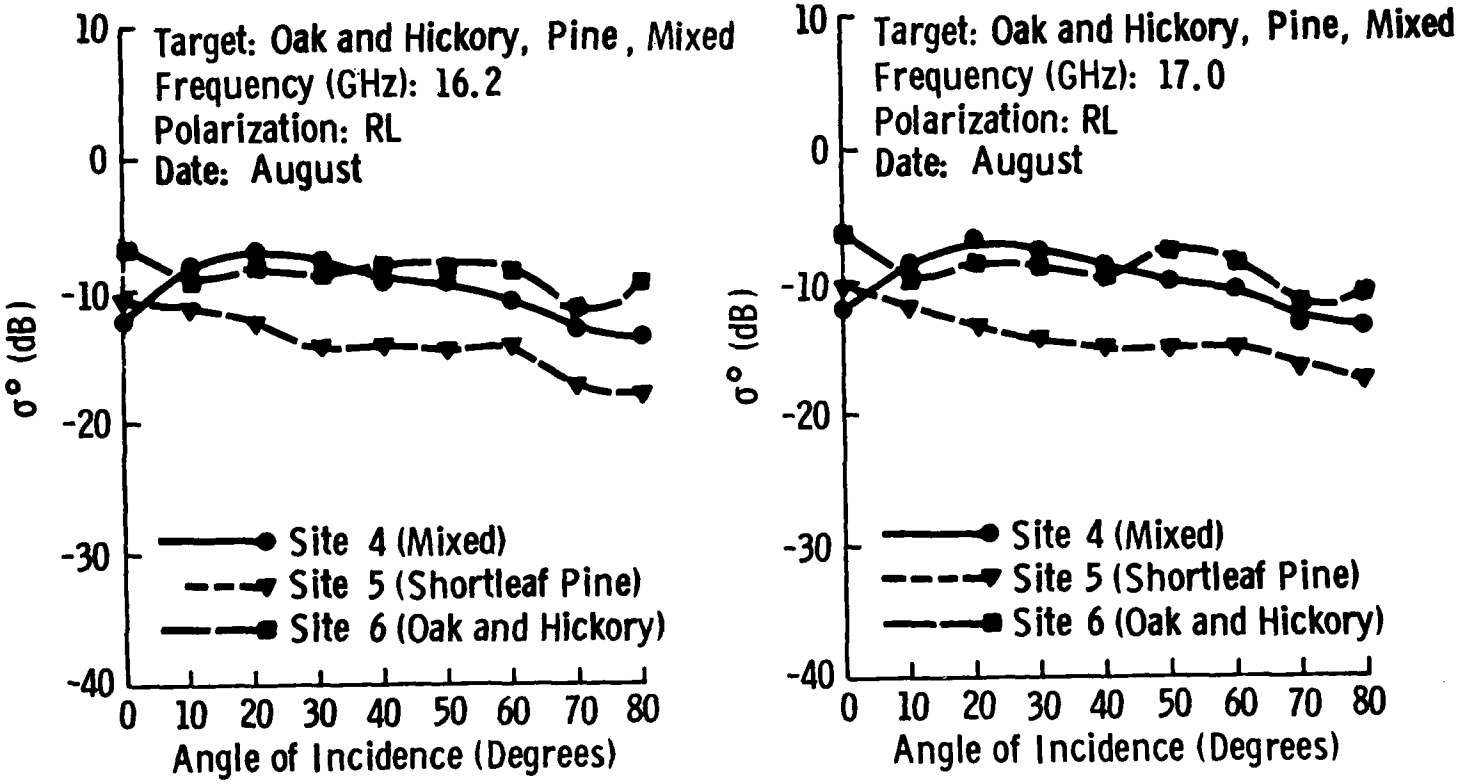

Figure 2-5 A comparison of the angular response of σ^{o} at 16.2 GHz and 17.0 GHz for oak and hickory, shortleaf pine, and mixed oak, hickory and shortleaf pine.

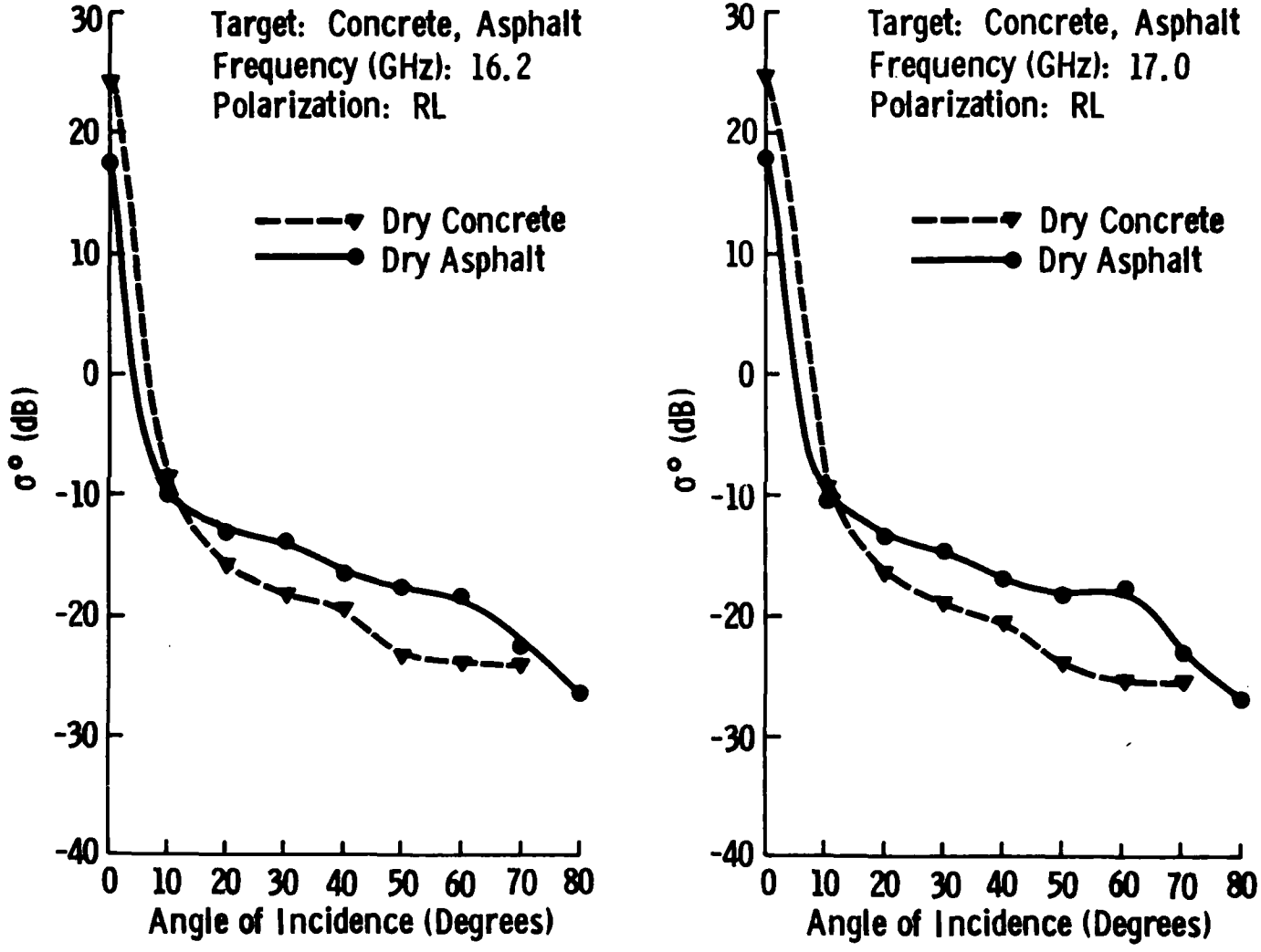

Figure 2-6 A comparision of the angular response of σ^{o} at 16.2 GHz and 17.0 GHz for dry concrete and dry asphalt.

function of (1) the surface dielectric constant, which is governed primarily by the soil moisture, and (2) the surface roughness.

During the period of time that the two sites were available for observation, the soil moisture varied over a rather narrow range, so the effect of dielectric-constant changes was minimal. There was, however, a dramatic difference in surface roughness between the two sites on both a micro- and macro-scale; this difference in roughness is quite evident from the backscatter data such as that presented in Figure 2-7.

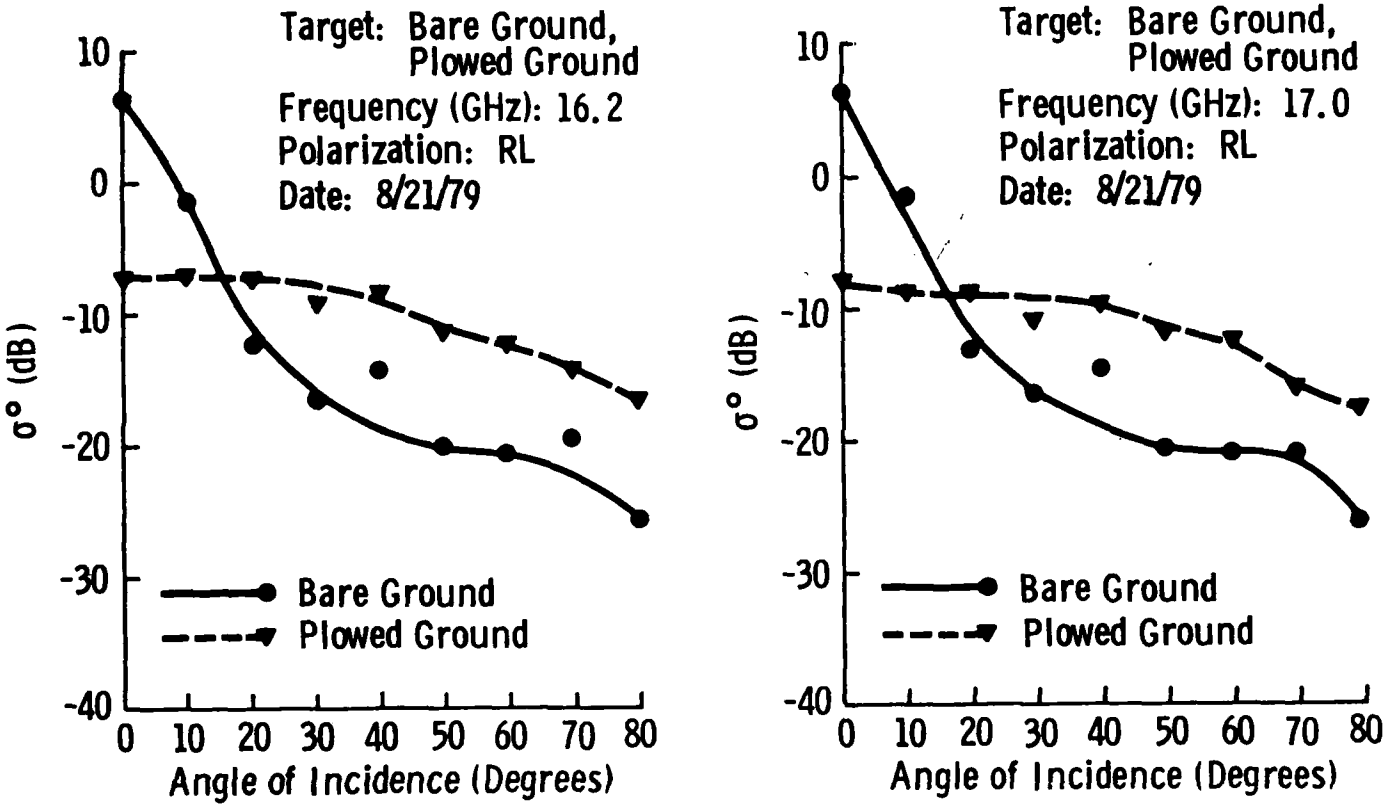

Figure 2-7 A comparison of the angular response of σ^{o} at 16.2 GHz and 17.0 GHz for bare ground and plowed ground.

3.0 RADAR BACKSCATTER COEFFICIENT OF SNOW-COVERED TERRAIN

These additional measurements were conducted by the University of Kansas Center for Research, Inc., Remote Sensing Laboratory, using the MAS 8-18/35 microwave scatterometer system which was described in detail in the previous report [1]. The system specifications, precision and calibration methods were identical for this program and therefore will not be repeated. Briefly, however, the systems cover six frequencies between 8 and 18 GHz, operate in three circular polarization states (RR, RL, LL) and can observe angles of incidence from 0° (nadir) to 80°.

Data were acquired on three groups of terrain classes with snow cover: (1) Grass, (2) Road Surfaces, and (3) Snow and Ice. Four test sites were examined in the measurements. All sites were located in the Colorado mountains; the locations are illustrated in Figure 3-1a. Figures 3-1b, c and d give the test-site locations at a larger scale. Test Site No. 1 was a short-grass (hay) field. Test Sites Nos. 2 and 3 were asphalt and Test Site No. 4 was an ice- and snow-covered lake. More detailed descriptions are given in later sections. The radar backscatter coefficient data are given in Appendices A and B.

3.1 Ground-Truth Measurements Applicable to Snow Cover

The choice of the ground-truth parameters measured is determined by the significance that parameter is expected to play in the wave-target interaction mechanism and by the time and manpower restrictions associated with the data acquisition. The snow measurements were obtained at each site from a snow-pit dug down to ground level. Photographs of these areas are shown in several of the ground-truth tables. These pits allow access to the snow in order to obtain snow samples and to observe the layering of the snow. The following snow parameters were measured:

1. Depth
2. Stratification
3. Density
4. Water Equivalent

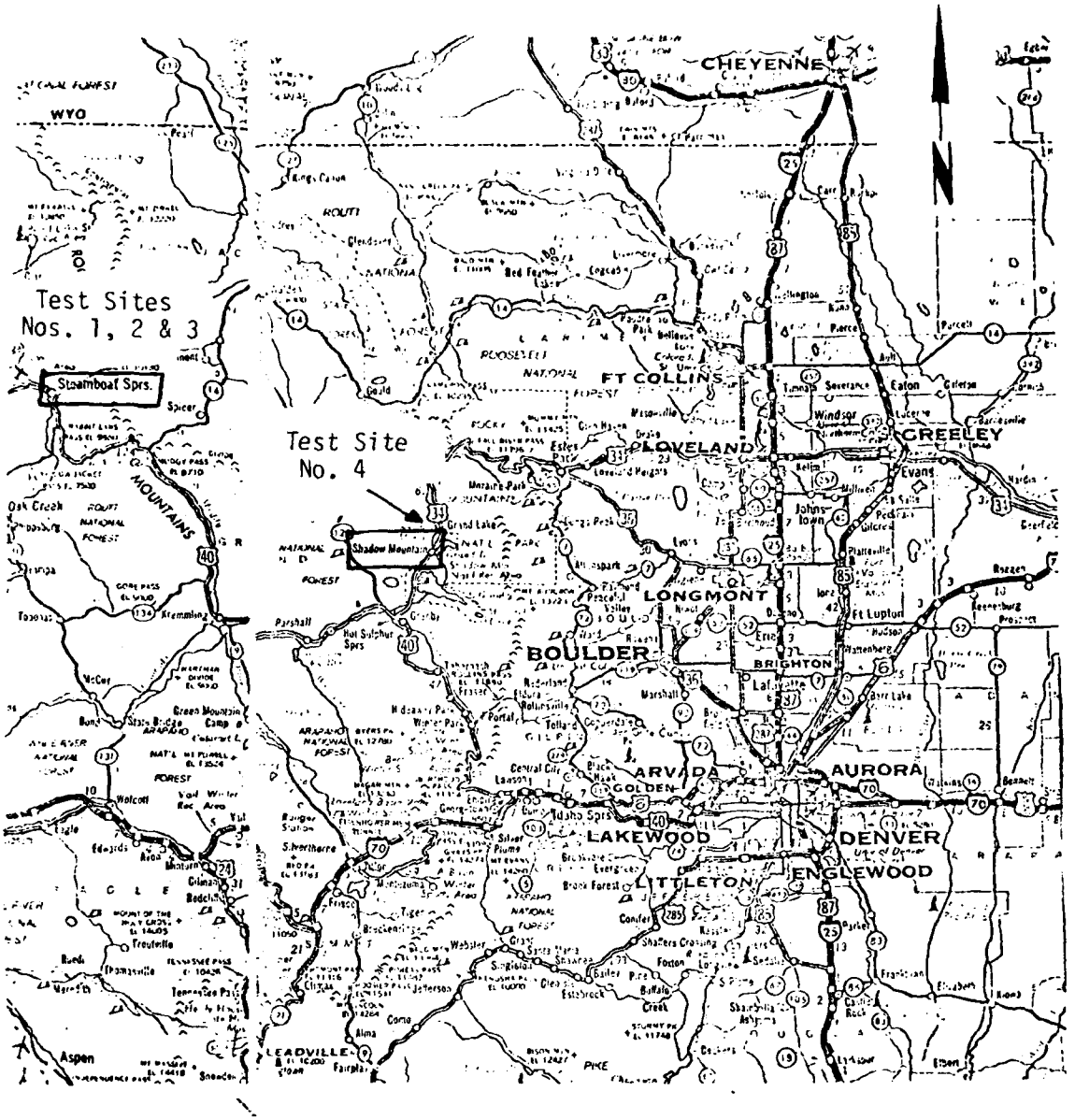

Figure 3-1a Location of Test Sites for the Snowcover Measurements.

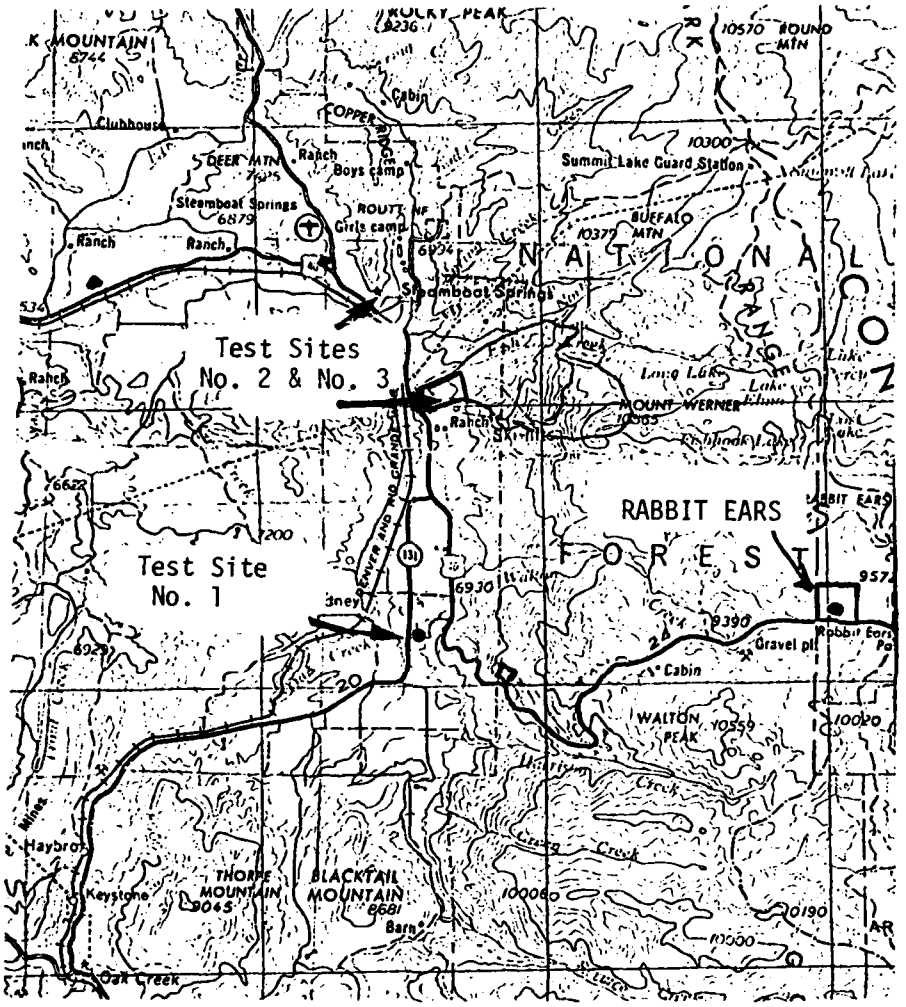

Figure 3-1b Location of the Three Test Sites in the Steamboat Springs, Colorado Area.

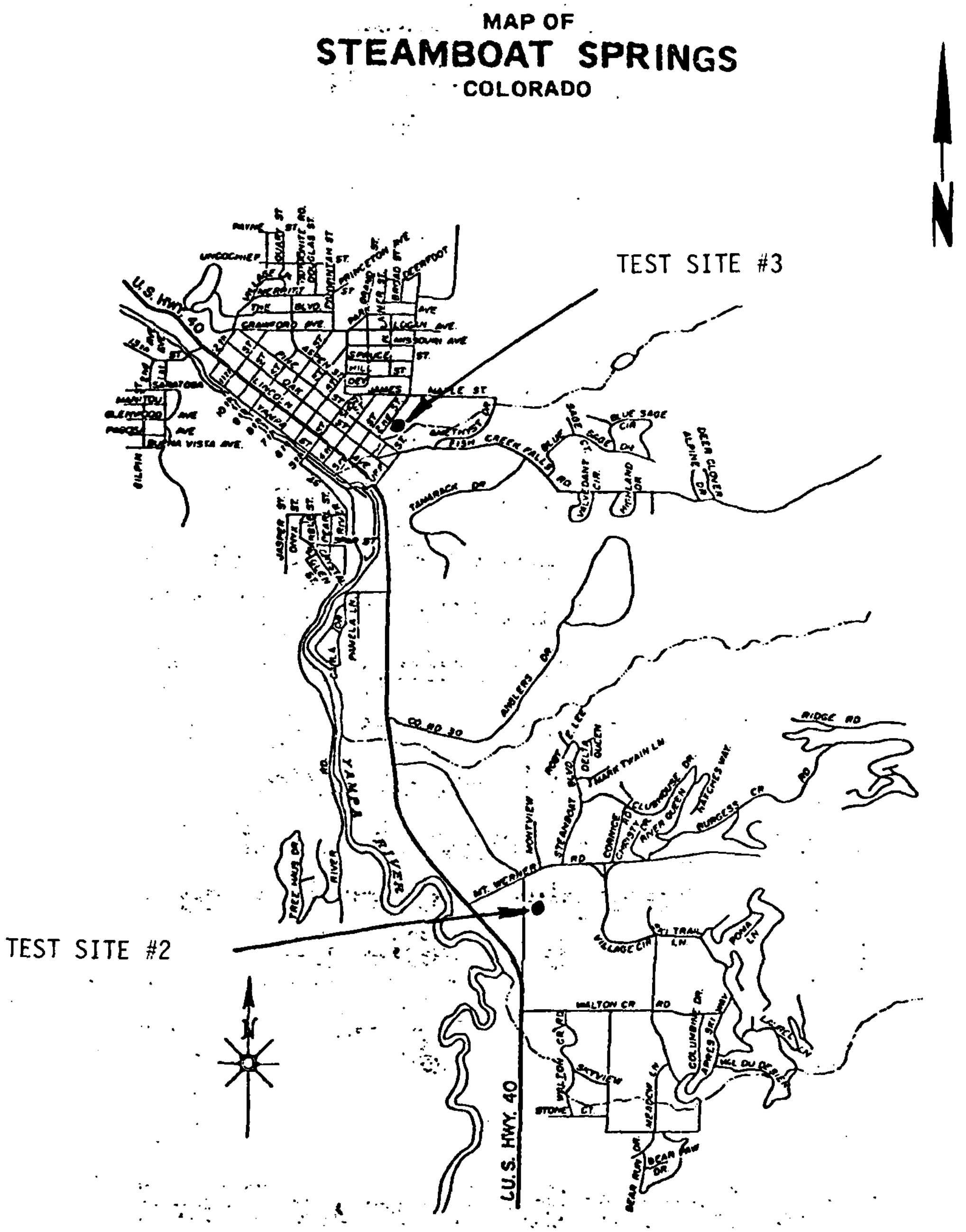

Figure 3-1c Location of the Test Sites within Steamboat Springs, Colorado.

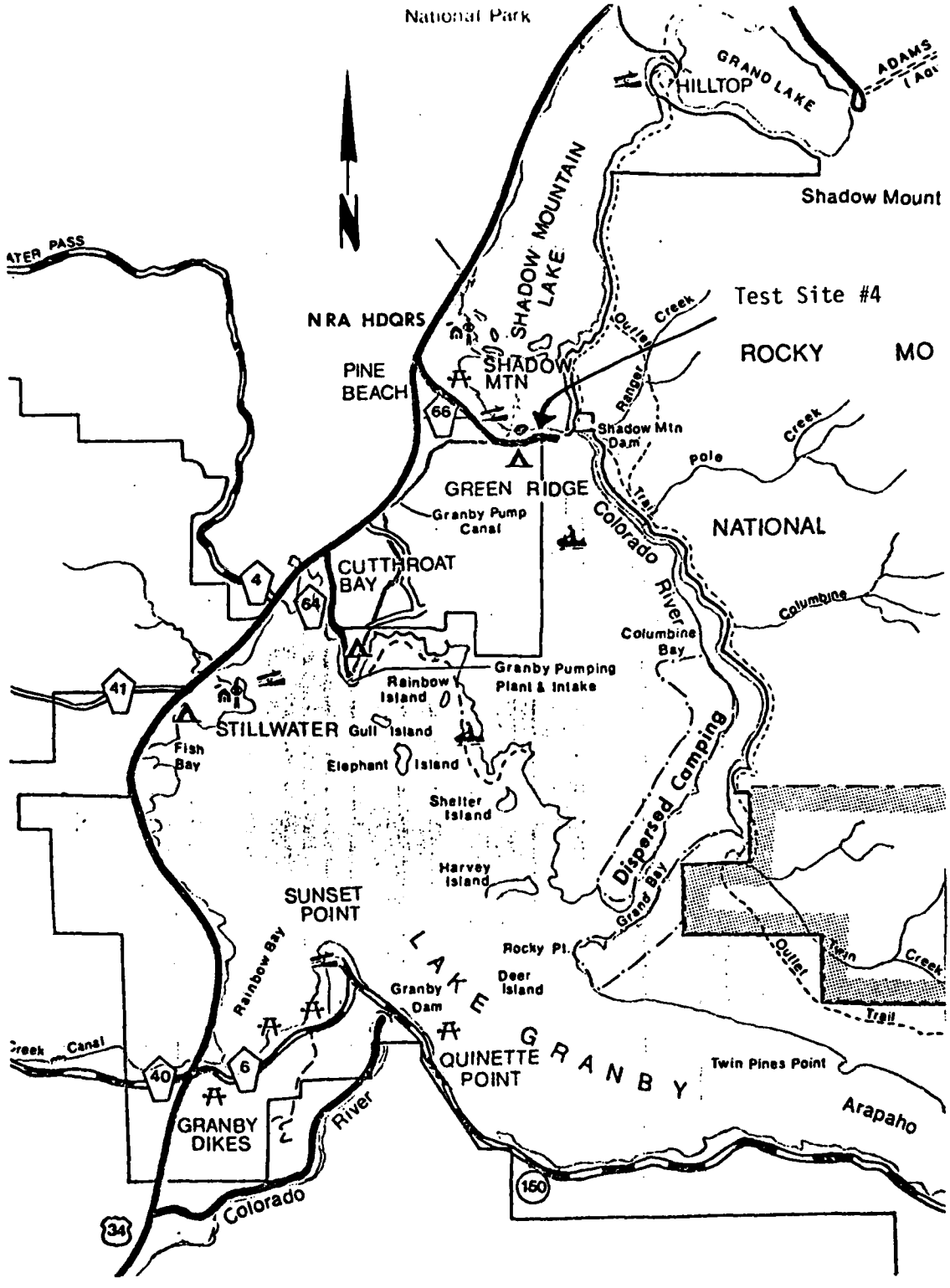

Figure 3-1d Location of the Lake-Ice Test Site at Shadow Mountain Lake in Colorado.

5. Wetness
6. Temperature
7. Grain Size
8. Surface Roughness Photograph

Detailed explanations of technique and procedure on the above measurements may be found in another report [2].

The depth (d) and stratification were determined with a meter stick. Two techniques were used to enhance the layer boundaries for their determination. Visual observations found most layer boundaries. However, for slight gradations in density, this technique was augmented by sliding a plastic card vertically through the snow and feeling the resistance to its motion at the layer boundaries. The snow density (ρ) was determined for each layer by taking a known volume of snow and finding its weight. The water equivalent (W) of snow is defined as the depth of water that would be obtained from the complete melt of a column of snow. The relationship between depth, density, and water equivalent is given by

$$W = \frac{\rho_{snow}}{\rho_{water}} d \quad cm$$

where ρ_{water} is approximately unity, therefore

$$W = \rho_{snow} d \quad cm$$

The snow wetness or percent liquid water within the snowpack is by far the most difficult snow parameter to measure. The most accurate method developed thus far is the freezing calorimeter. Calorimetric techniques have been employed for many years by physicists and chemists. The method was adapted to field-use by Leaf [3]. The basis for operation is to have a known volume of solvent with known heat capacity in an insulating container (thermos bottle) with provisions for measuring temperature. The solvent used was a silicone compound which remains in the liquid state at -40°C, which is its initial temperature. If a known weight of wet snow is then added and the solution is allowed to reach an equilibrium temperature, then by knowing the weights of solvent and wet snow, the initial and final temperatures within the calorimeter, and the latent heat of fusion of water, the liquid water content

can be calculated. The following equation gives the liquid water content by weight (m_w):

$$\frac{m_w}{100} = \frac{(W_i + E)(T_f - T_i)\, C_{si}}{W_s L_f} + \frac{T_f C_s}{L_f}$$

where

W_i = weight of silicone fluid

E = calorimeter constant

T_f = final temperature of solution

T_i = initial temperature of silicone

C_{si} = specific heat of silicone

C_s = specific heat of ice

L_f = latent heat of fusion

W_s = *weight of snow*

The snow wetness by volume (m_v) is then calculated from m_w and the snow density ρ_{snow}:

$$m_v = \rho_{snow}\, m_w$$

The snow temperature profile was measured with a digital thermometer and grain sizes were determined visually. Macrostructure roughness can be seen from roughness grid photographs. Soil moisture was measured for the grass targets.

3.2 Backscatter Measurements

This section covers the backscatter and ground-truth data obtained from snow-covered terrain.

3.2.1 Snow of Various Depths on Top of Grass

This field (Test Site No. 1) was a very flat, 40-acre field in the valley south of Steamboat Springs, Colorado. The location is shown in Figure 3-1b. The grass (hay) was in its winter-dormant state and had been cut to approximately 2.5 cm. This test site was observed under three different snow conditions. The overall view of the test site is given in Figure 3-2. Close-up photographs are given for each data set in Tables 3-1 to 3-3. Snow of greater than 6-inch depth was observed on two different days (2/14/80 and 2/16/80). Although the snow depths were the same for each of these data sets (64 and 63 cm), the angular and spectral responses are quite different as a result of the influence of snow wetness (m_v).

Figures 3-3 and 3-4 give the angular and spectral response of σ^o for a case in which the surface layer (0-5 cm) of the snow is slightly wet (m_v = 1.41%), while the interior of the snowpack is dry (m_v = 0). The dryness of the snowpack is inferred from the snow temperature profile shown in Table 3-1.

Figures 3-5 and 3-6 give the angular and spectral responses to the same snowpack under isothermal conditions. In this case, the entire snowpack is at 0°C (Table 3-2) and therefore, wetness exists at all levels. The snow wetness in the surface layer is very high at 5.2% by volume.

The same test site also was observed with a trace of snow. These conditions were obtained by clearing an area on the field. Figure 3-7 illustrates this area. The angular and spectral responses of σ^o are given in Figures 3-8 and 3-9. The ground-truth data are given by Table 3-3.

As a result of other constraints on the use of the MAS systems and as a result of uncooperative weather conditions, these were the only sets obtained over grass. Analyses of these data sets are furnished in Section 3.3.

Figure 3-2 Overall view of Test Site No. 1 shown on 2/14/80, deep snow over grass.

[redacted]

DATE: 2/14/80

TIME: 1245-1535

TARGET: Grass

TYPE OF SET: Snow ≥ 6-inch

LOCATION: Hibbert's
Steamboat Springs, CO
Test Site #1

Grid Size 2.4 cm

Layer Number (From Ground)	Depth (cm) (To Layer Top)	Density ρ(g/cm^3)	Water Equivalent W(cm)	Grain Size (mm)
Overall	64	--	16.1	NA
8	64	0.226	--	0.5
7	59	0.214	--	1
6	46.5	0.335	--	1
5	35	0.414	--	1-1.5
4	32	0.313	--	1-1.5
3	27	0.400	--	1-1.5
2	25	0.279	--	2-3
1	10	0.246	--	2-3

TARGET CONDITIONS

Height (cm): 2.5

Soil Moisture (0-5 cm): 52.8% by wt.

Temperature °C: 0.2 (Ground)

WEATHER OBSERVATIONS

Air Temperature °C: 3.0

Relative Humidity: 85%

General:

Cloudy, warm and humid

Light snow during set

SNOW WETNESS m_v

0-2 cm: 1.41%

2-5 cm: 0.65%

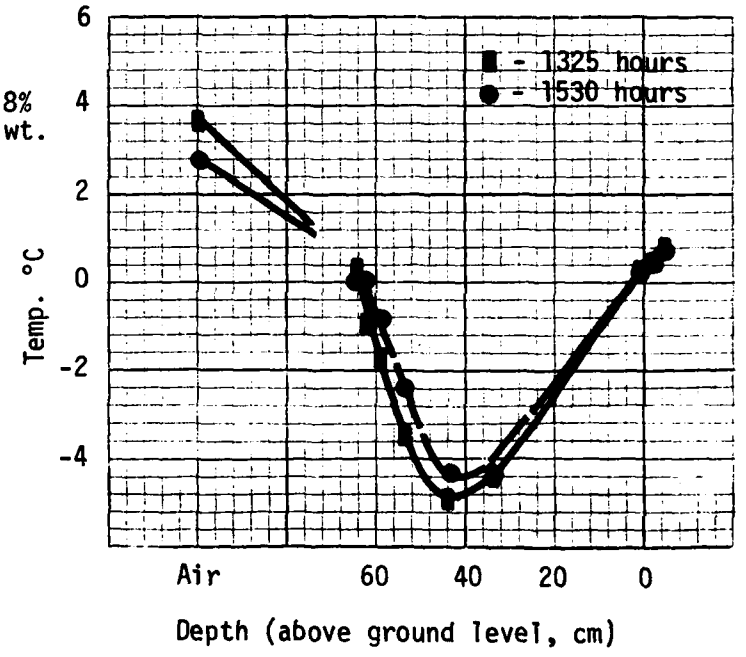

TABLE 3-1

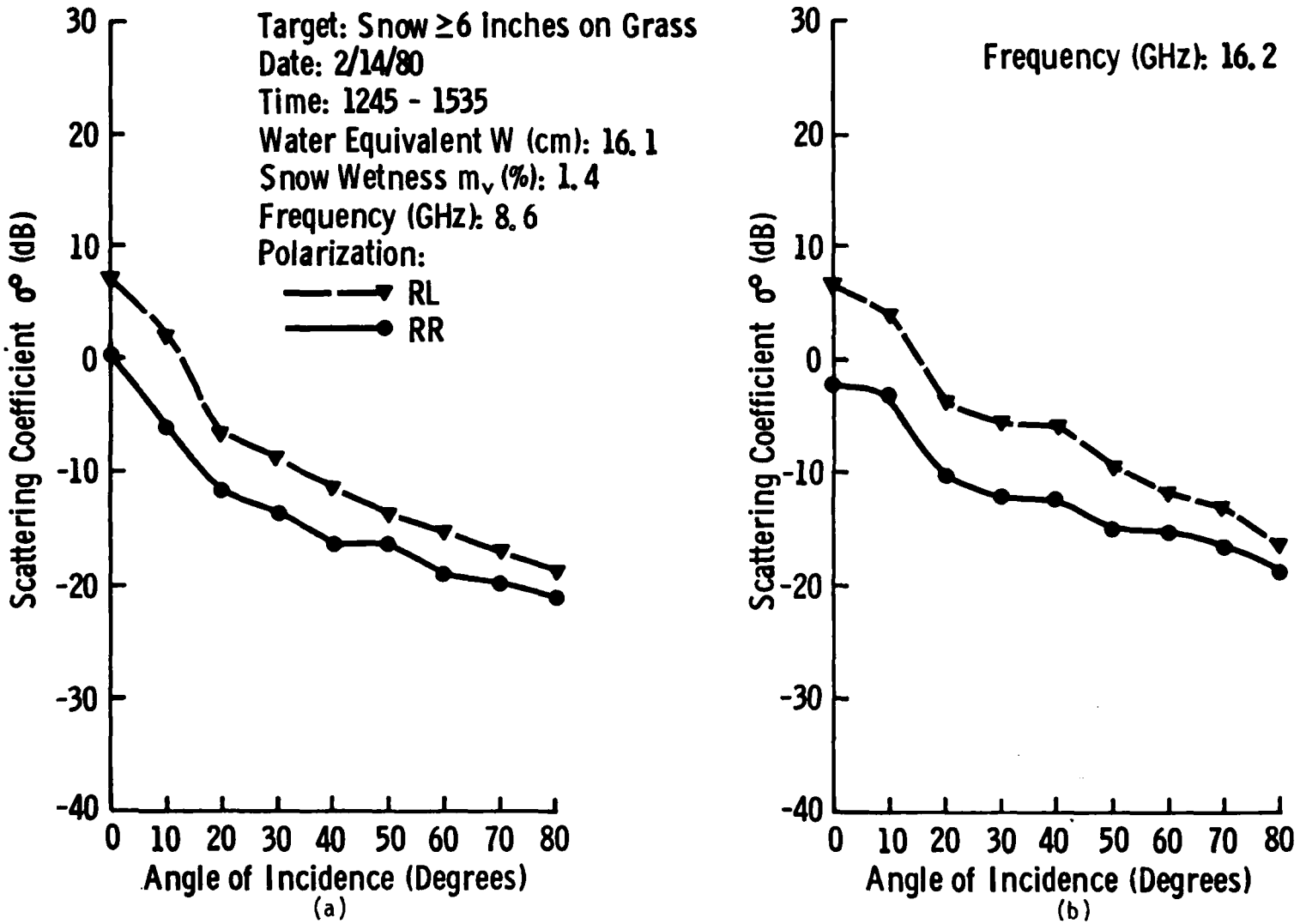

Figure 3-3 Angular response of σ^{o} of snow ≥ 6 inches on grass.

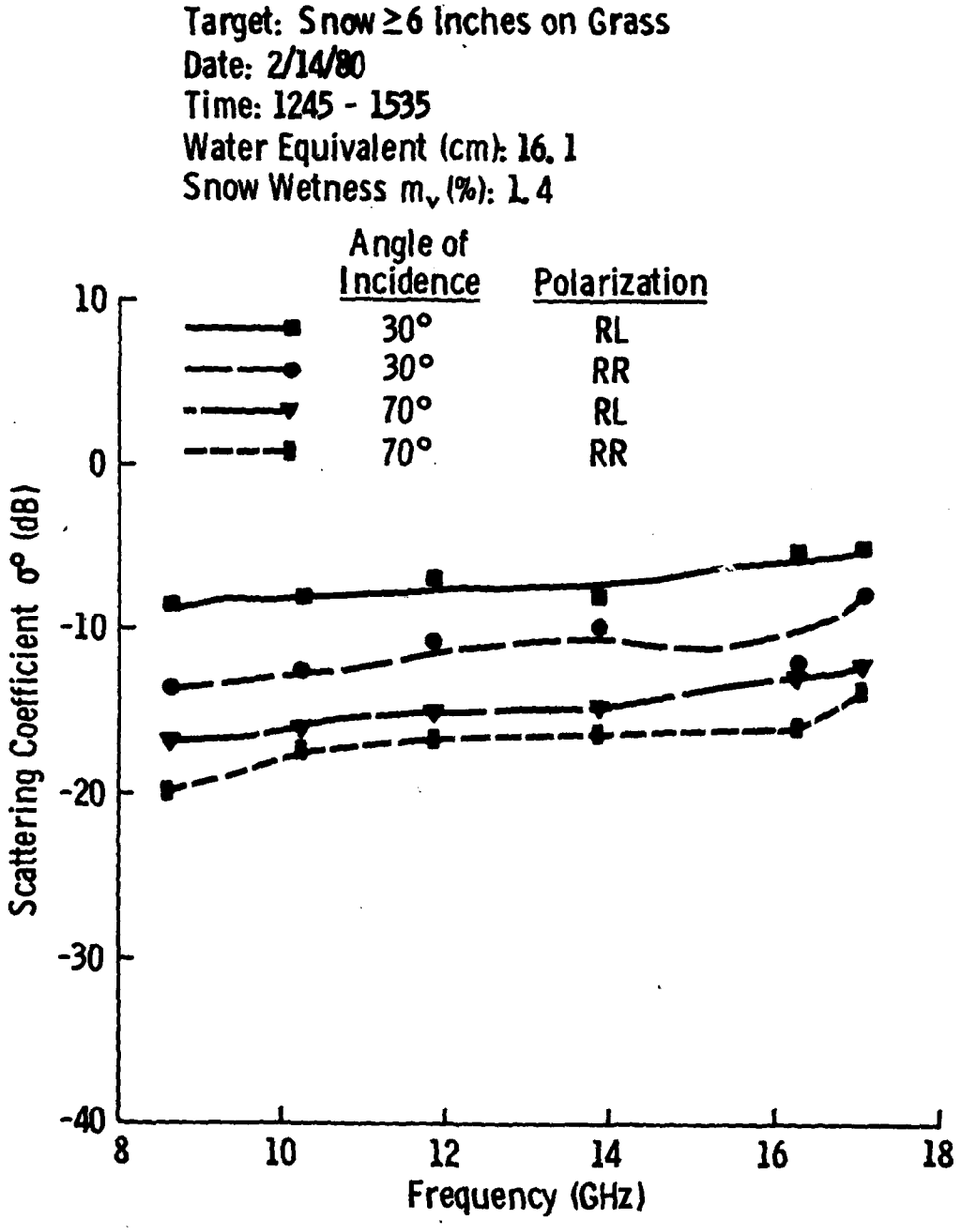

Figure 3-4 Spectral response of σ^{o} of snow ≥ 6 inches on grass.

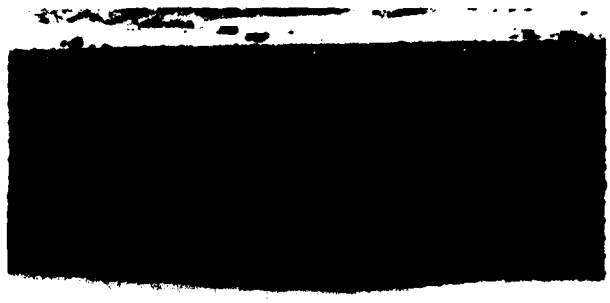

DATE: 2/16/80

TIME: 1400-1630

TARGET: Grass

TYPE OF SET: Snow ≥ 6-inch

LOCATION: Hibbert's
Steamboat Springs, CO
Test Site #1

Grid Size 2.4 cm

Layer Number (From Ground)	Depth (cm) (To Layer Top)	Density ρ(g/cm^3)	Water Equivalent W(cm)	Grain Size (mm)
Overall	63	--	16.9	NA
9				
8	63	0.350	--	1
7	57	0.214	--	1
6	45	0.322	--	1-2
5	35	0.408	--	1
4	32	0.331	--	1-1.5
3	27	0.400	--	1
2	25	0.279	--	2-3
1	10	0.246	--	2-4

TARGET CONDITIONS

Height (cm): 2.5

Soil Moisture (0-5 cm): 52.4% by wt.

Temperature °C: 0.2 (Ground)

WEATHER OBSERVATIONS

Air Temperature °C: 2.8

Relative Humidity: 63%

General:

Warm, partly cloudy

SNOW WETNESS m_v

0-5 cm: 5.2%

5-10 cm: 0.24%

10-15 cm: 1.78%

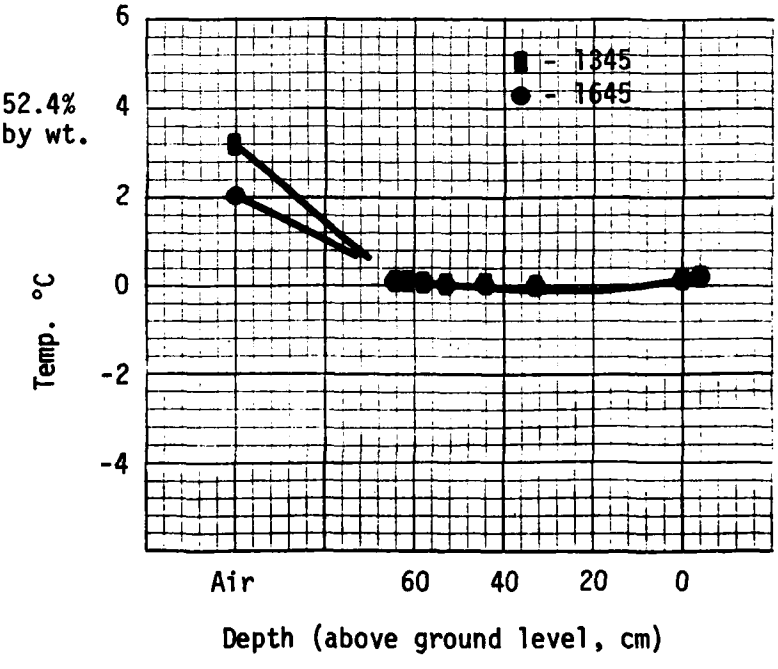

TABLE 3-2

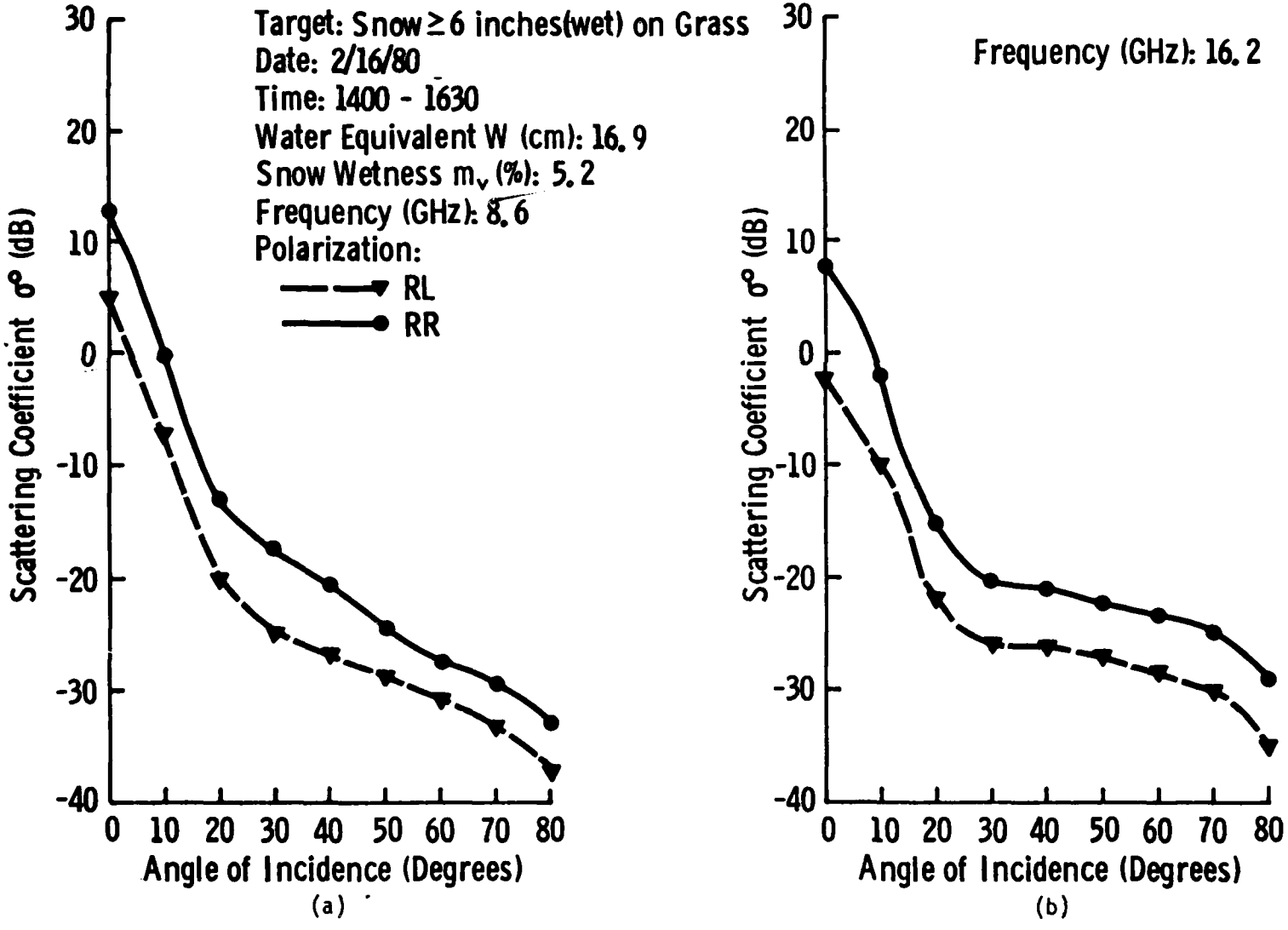

Figure 3-5 Angular response of σ^{o} of snow ≥ 6 inches (wet) on grass.

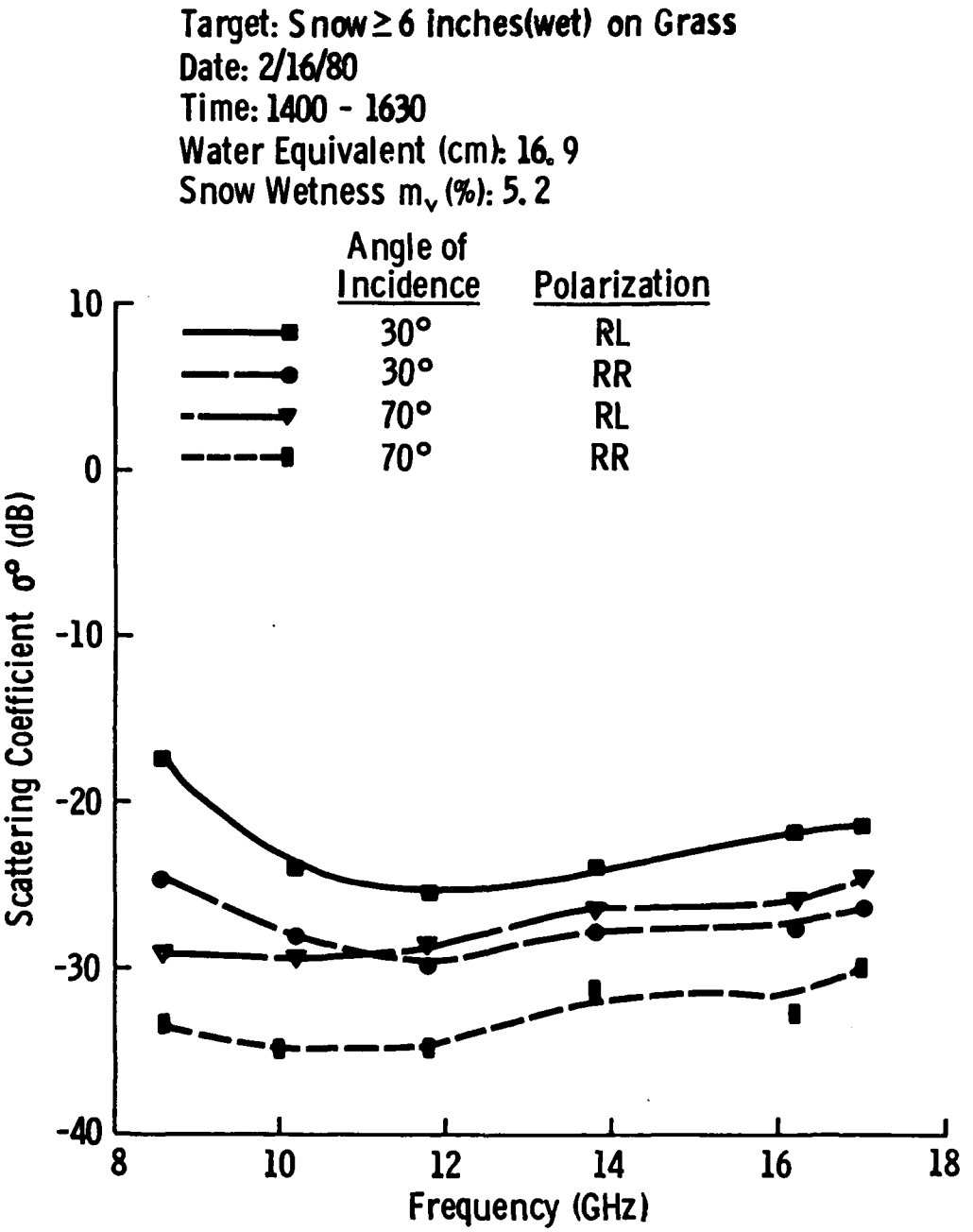

Figure 3-6 Spectral response of σ^{o} of snow ≥ 6 inches (wet) on grass.

Figure 3-7 View of Test Site No. 1 on 2/25/80 after the deep snow was cleared, leaving a trace of snow.

DATE; 2/25/80

TIME: 1730-1930

TARGET: Grass

See Figure 3-7

TYPE OF SET: Snow Trace

LOCATION: Hibbert's
Steamboat Springs, CO
Test Site #1

Layer Number (From Ground)	Depth (cm) (To Layer Top)	Density ρ(g/cm^3)	Water Equivalent W(cm)	Grain Size (mm)
Overall	0-1	--	0-1	NA
9				
8				
7				
6				
5				
4				
3				
2				
1	0-1	--	--	2-3

TARGET CONDITIONS:

Height (cm): 2.5

Soil Moisture (0-5 cm): 33.8% by wt.

Temperature °C: 0.1 (Ground)

WEATHER OBSERVATIONS

Air Temperature °C: 0.0

Relative Humidity: 67%

General:

Clear, cooling towards end of data set

SNOW WETNESS m_v

Wet but not measurable due to sample size

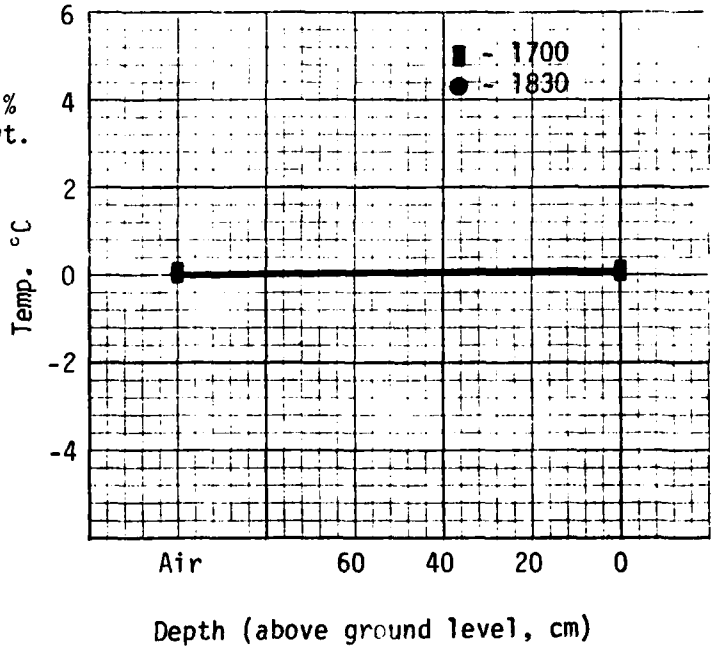

TABLE 3-3

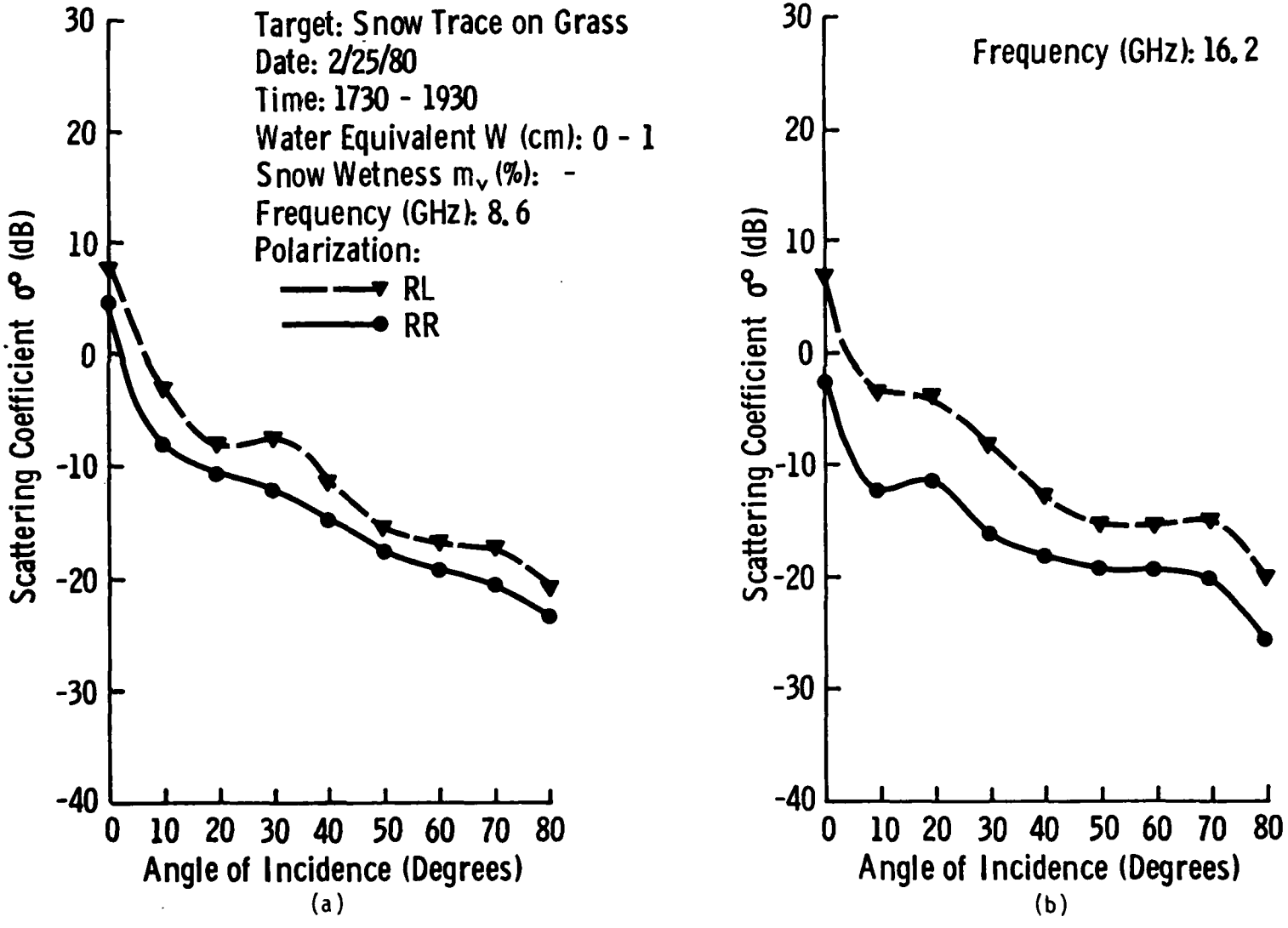

Figure 3-8 Angular response of σ^{o} of snow-trace on grass.

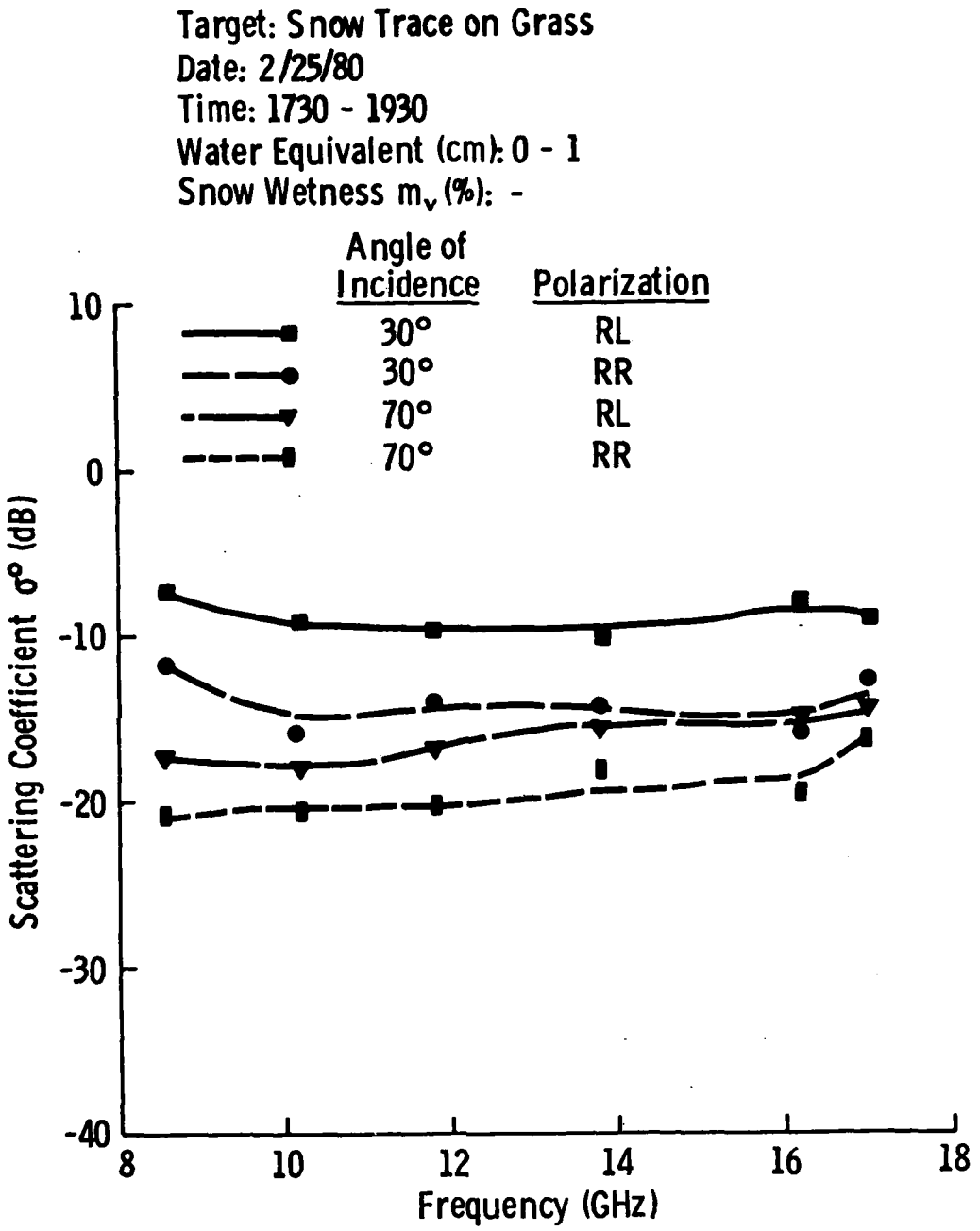

Figure 3-9 Spectral response of σ^o of snow-trace on grass.

3.2.2 Snow of Various Depths on Top of Roads

3.2.2.1 Asphalt

Two asphalt areas were observed: Site No. 2 and Site No. 3 (Figure 3-1c). Test Site No. 2 was the model-airplane runway at the Steamboat ski resort at Steamboat Springs, Colorado. This runway is approximately 150 m in length and 15 m wide. It is unused and normally snow-covered during the winter months. Three depths of snow were observed at this site. Figure 3-10 shows this area before and after it had been cleared.

When this runway was in its normal snow-covered state (before clearing), a data-set was obtained. Figures 3-11 and 3-12 give the angular and spectral responses of σ^o for wet snow (m_v = 3.75%) and an isothermal snowpack. Ground-truth data are given in Table 3-4.

Figures 3-13 and 3-14 present the angular and spectral response of σ^o over 6-inch, slightly wet snow (m_v = 1.0%). This snowcover was the result of two snowfalls that occurred on consecutive days and therefore, a boundary was not apparent between the snowfalls. The previous day, 2/21/80, a 3-inch layer was observed. The angular and spectral responses of σ^o to this very-wet-snow case (m_v = 4.23%) are shown in Figures 3-15 and 3-16. System problems were encountered during the data set requiring an abbreviated measurement set. The ground-truth data for these two sets are given in Tables 3-5 and 3-6.

The other asphalt area observed was the high-school parking lot at Steamboat Springs, Colorado (Test Site No. 3). It was snowing during the data set, but the weather was very warm and only a trace of snow was on the parking lot. Figure 3-17 shows this area. Figures 3-18 and 3-19 show the angular and spectral responses of σ^o. The ground-truth data are given in Table 3-7.

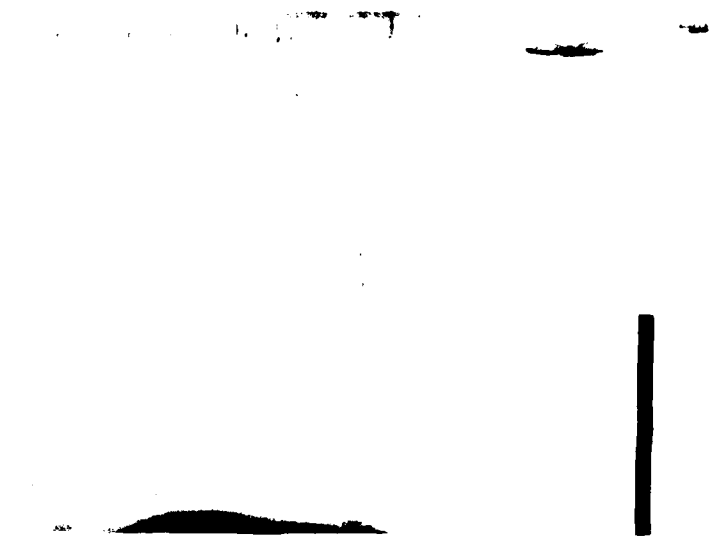

(a)

(b)

Figure 3-10 View of Test Site No. 2 with deep snow on 2/15/80 and after clearing and a 6-inch snowfall of 2/22/80.

DATE: 2/15/80

TIME: 1315-1600

TARGET: Asphalt

TYPE OF SET: Snow ≥ 6-inch

LOCATION: Model Airplane Runway
LTV Resort
Steamboat Springs, CO
Test Site #2

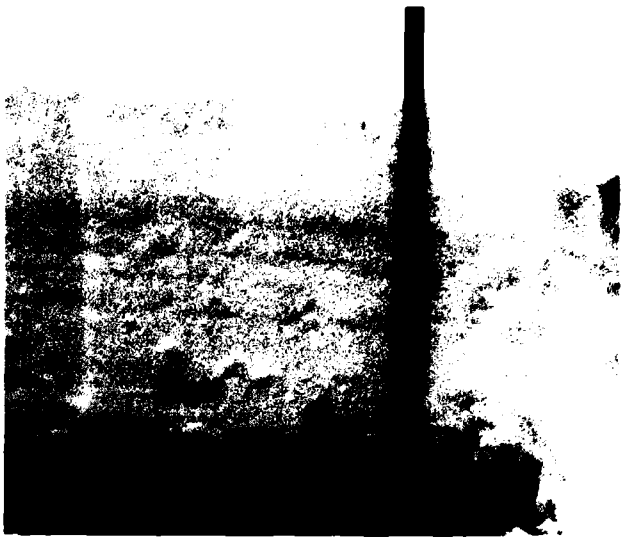

Layer Number (From Ground)	Depth (cm) (To Layer Top)	Density $\rho(g/cm^3)$	Water Equivalent W(cm)	Grain Size (mm)
Overall	55	--	15.7	NA
9				
8				
7				
6	55	0.246	--	
5	40	0.260	--	
4	34	0.280	--	
3	20	0.327	--	
2	15	0.333	--	
1	14	0.357	--	

TARGET CONDITIONS

Height (cm): NA

Soil Moisture (0-5 cm): NA

Temperature °C: 0.0
(Ground)

WEATHER OBSERVATIONS

Air Temperature °C: 2.7

Relative Humidity: 86%

General:

Warm and clear

SNOW WETNESS m_v

0-5 cm: 3.75%

5-10 cm: 0.27%

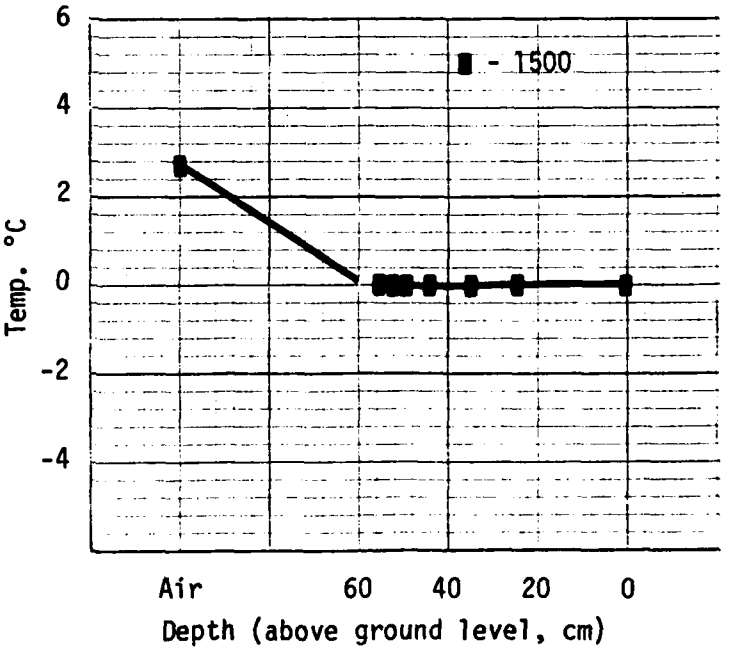

TABLE 3-4

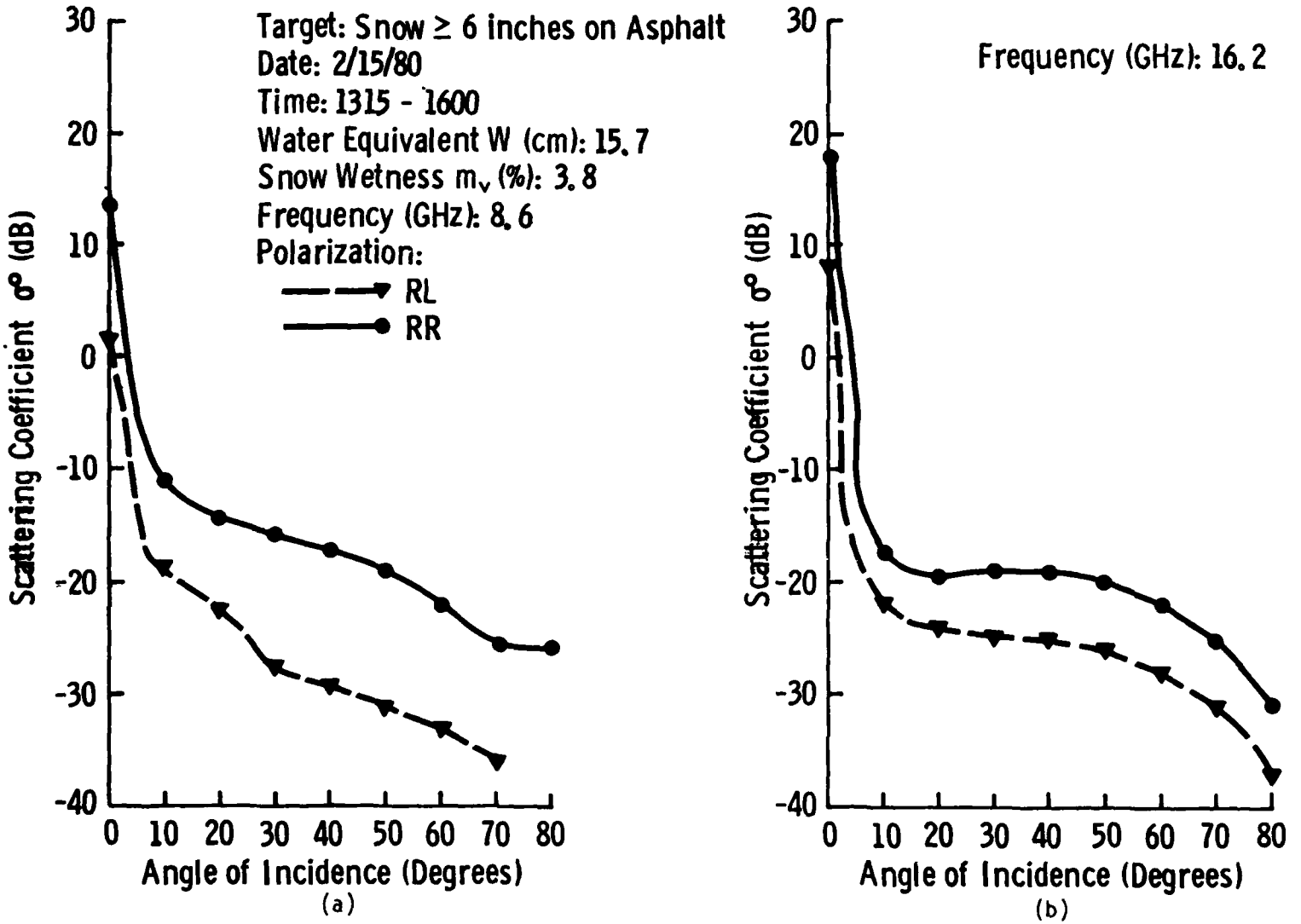

Figure 3-11 Angular response of σ^o of snow ≥ 6 inches on asphalt.

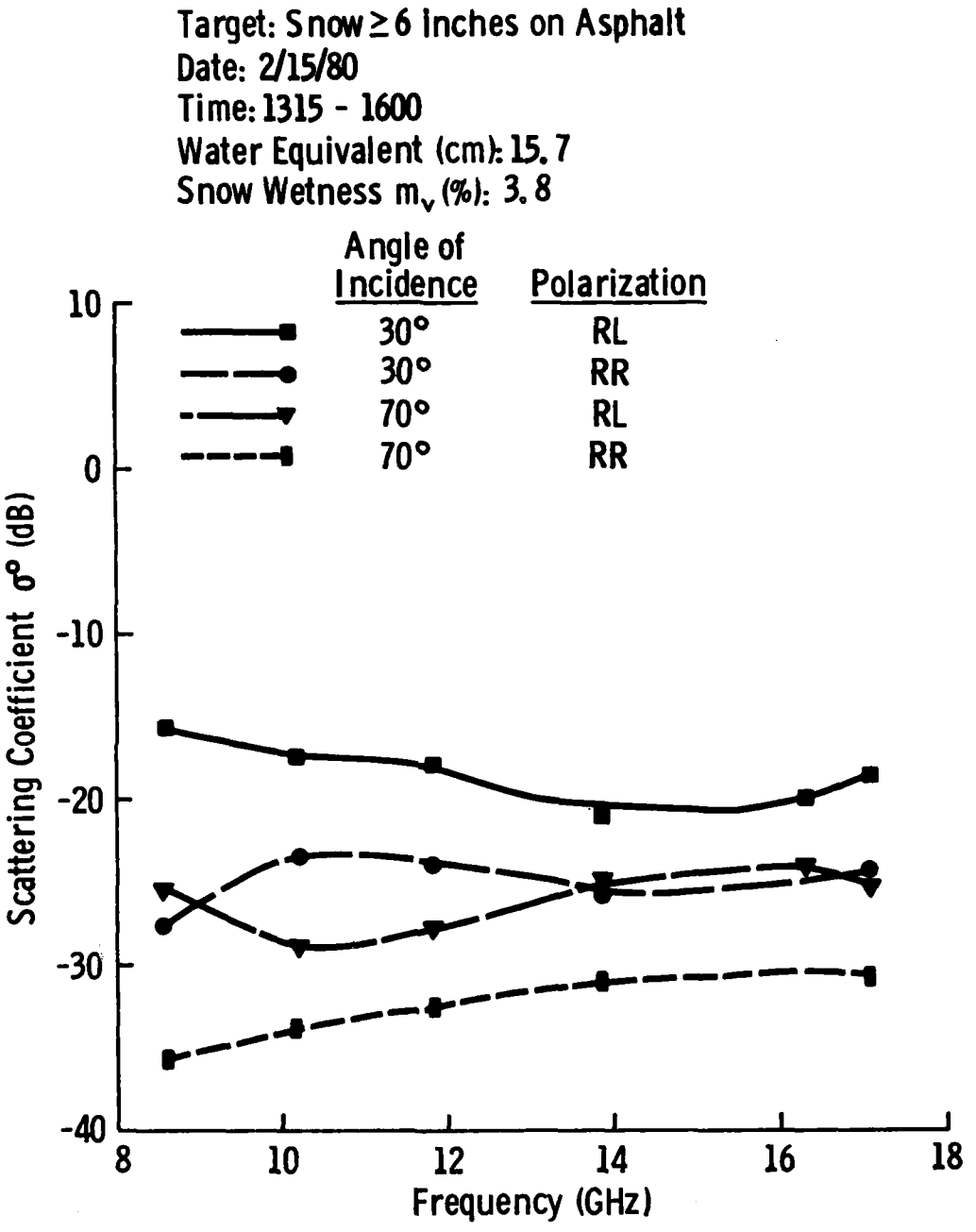

Figure 3-12 Spectral response of σ^{o} of snow ≥ 6 inches on asphalt.

DATE: 2/22/80

TIME: 0945-1400

TARGET: Asphalt

TYPE OF SET: Snow, 6-inch

LOCATION: Model Airplane Runway
LTV Resort
Steamboat Springs, CO
Test Site #2

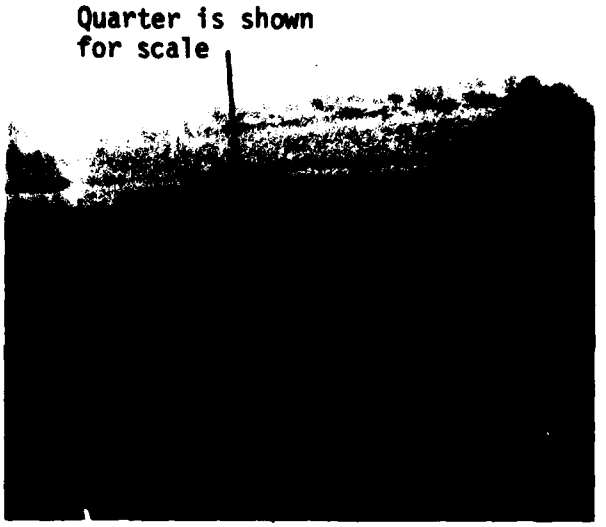

Layer Number (From Ground)	Depth (cm) (To Layer Top)	Density ρ(g/cm^3)	Water Equivalent W(cm)	Grain Size (mm)
Overall	14.5	--	2.62	NA
9				
8				
7				
6				
5				
4				
3				
2				
1	14.5	0.181	--	0.5-1

TARGET CONDITIONS

Height (cm): NA

Soil Moisture (0-5 cm): NA

Temperature °C: 0.0
(Ground)

WEATHER OBSERVATIONS

Air Temperature °C: -0.2

Relative Humidity: 100%

General:

SNOW WETNESS m_v

0-5 cm: 1.0%

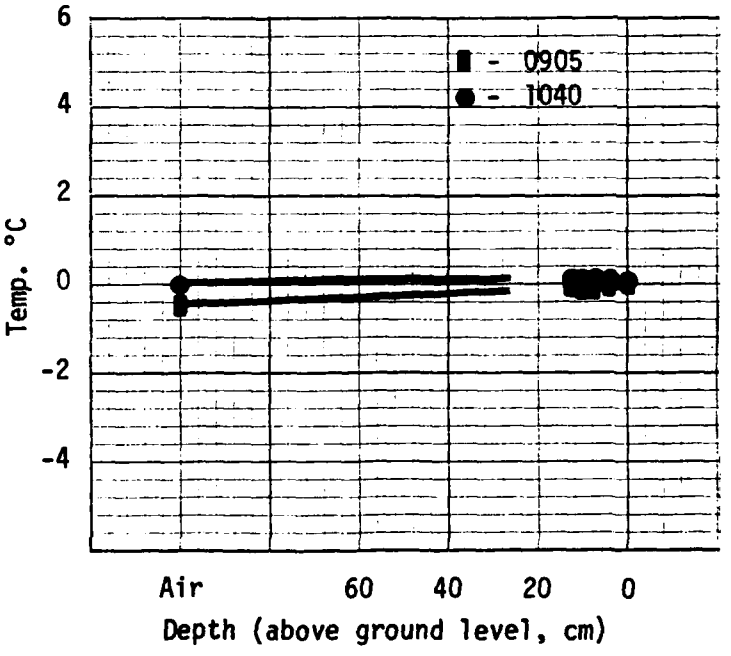

TABLE 3-5

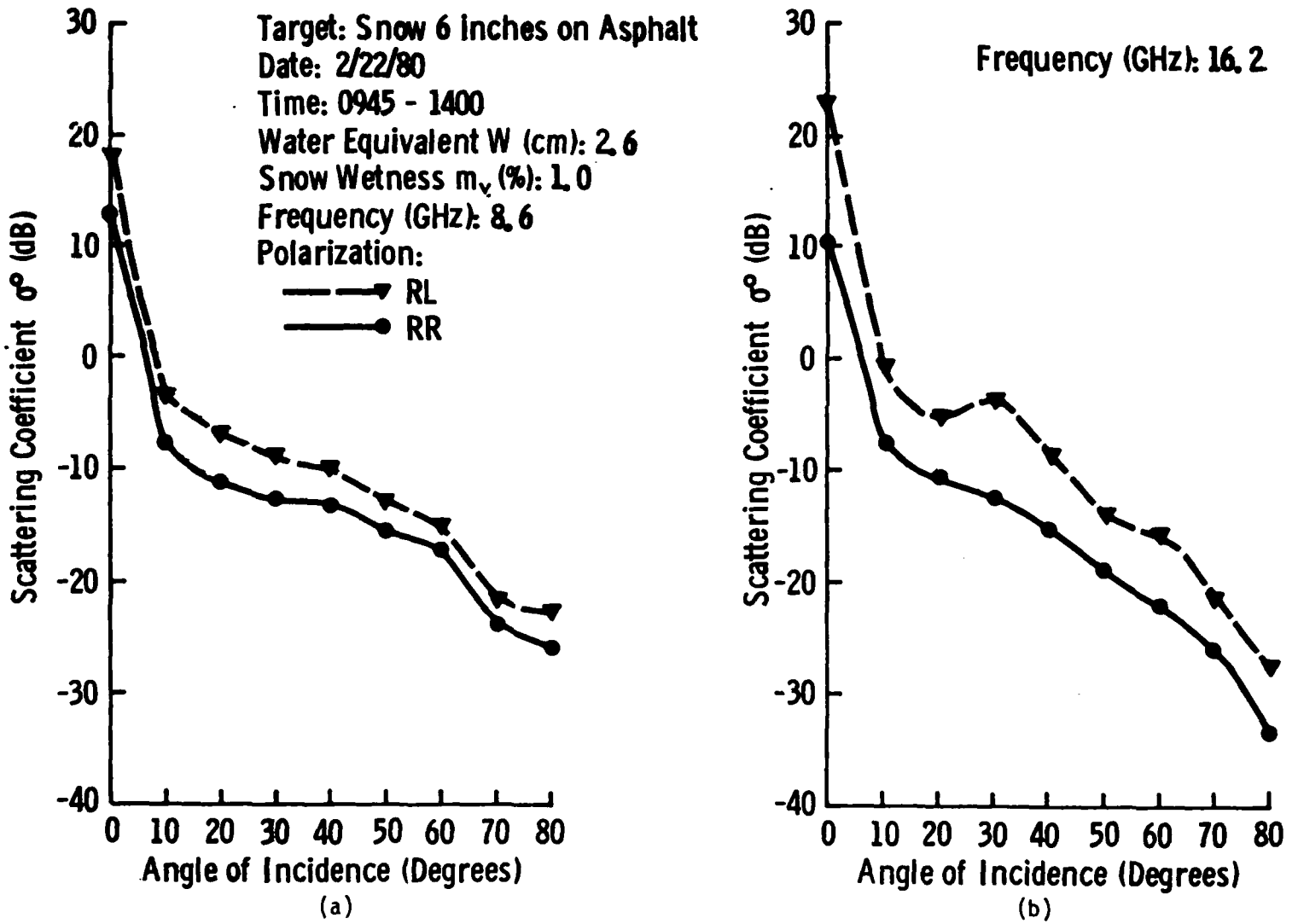

Figure 3-13 Angular response of σ^o of snow 6 inches on asphalt.

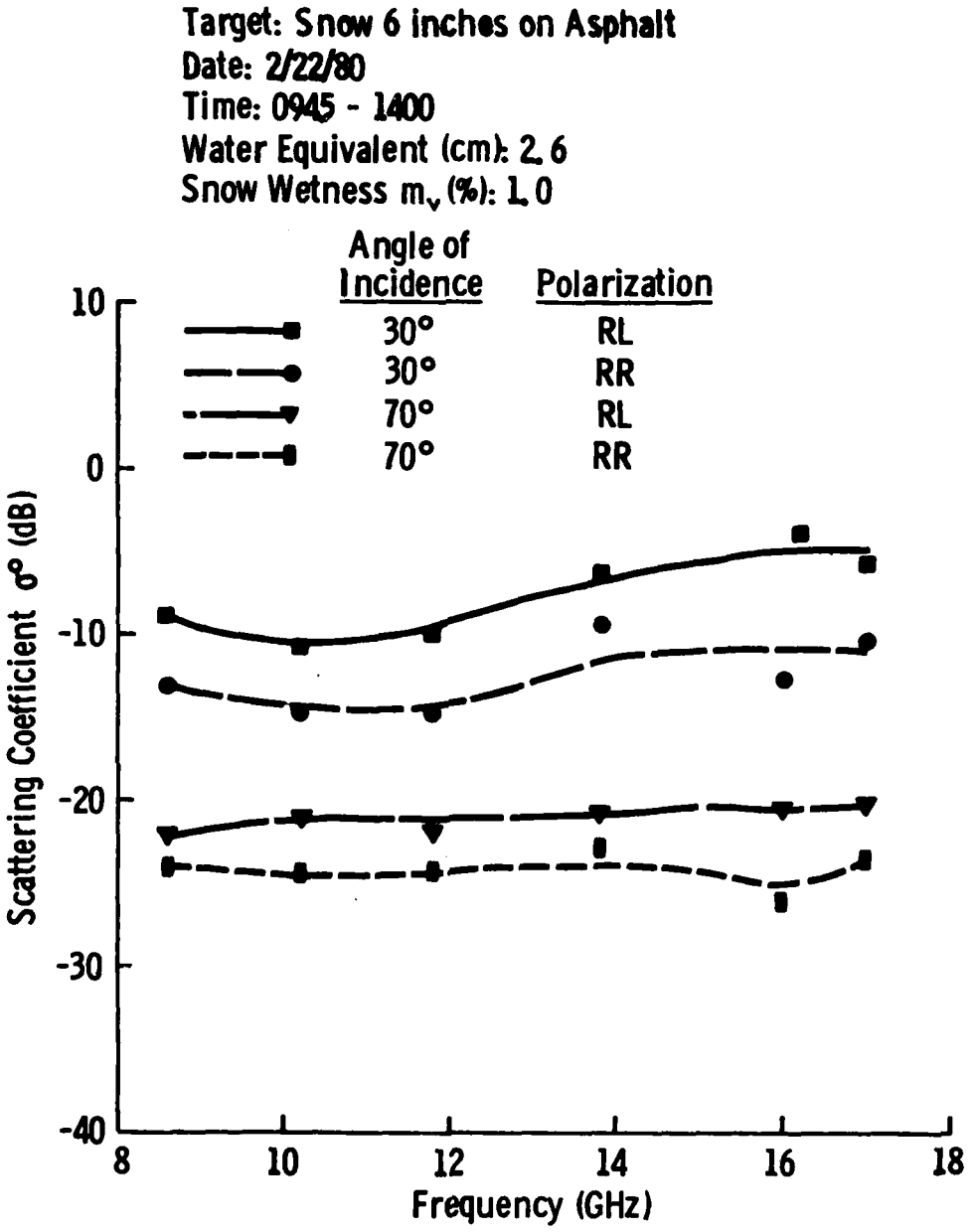

Figure 3-14 Spectral response of σ^{o} of snow 6 inches on asphalt.

DATE: 2/21/80

TIME: 1430-1600

TARGET: Asphalt

TYPE OF SET: Snow: 3-inch

LOCATION: Model Airplane Runway
LTV Resort
Steamboat Springs, CO
Test Site #2

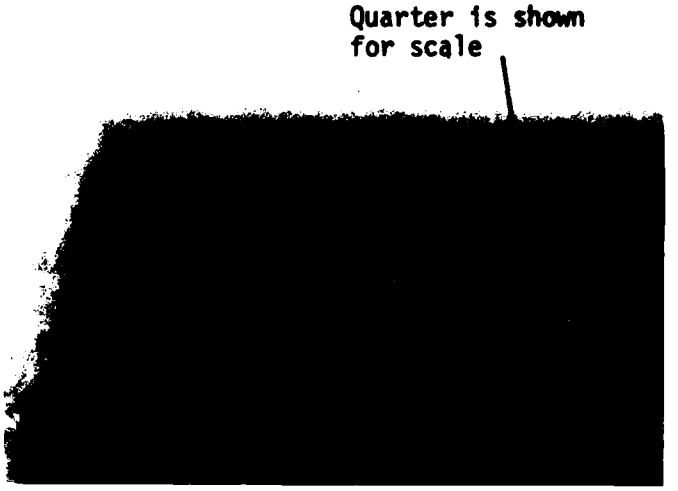

Layer Number (From Ground)	Depth (cm) (To Layer Top)	Density $\rho(g/cm^3)$	Water Equivalent W(cm)	Grain Size (mm)
Overall	8	--	2.0	NA
9				
8				
7				
6				
5				
4				
3				
2				
1	8	0.26	--	0.5-1

TARGET CONDITIONS

Height (cm): NA

Soil Moisture (0-5 cm): NA

Temperature °C: 2.0
(Ground)

WEATHER OBSERVATIONS

Air Temperature °C: 1.0

Relative Humidity: 52%

General:

Warm, clear

SNOW WETNESS m_v

0-8 cm: 4.23%

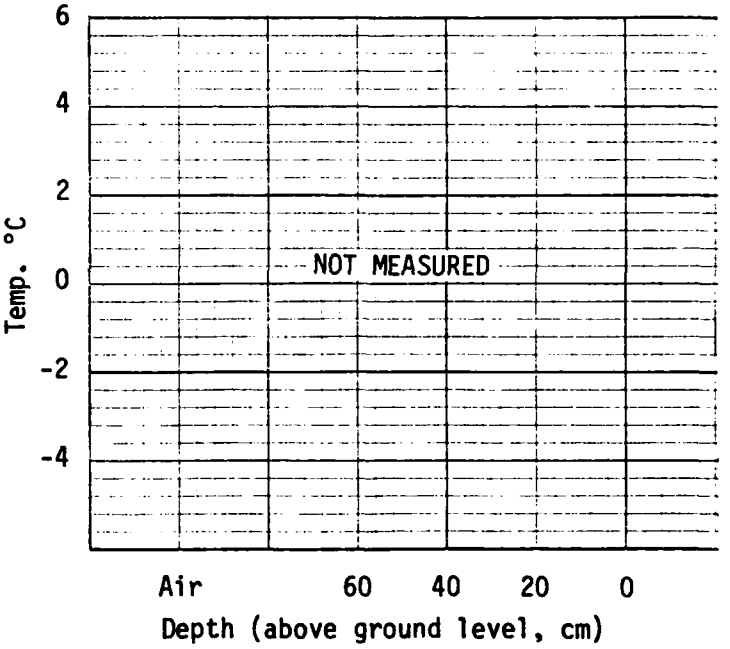

TABLE 3-6

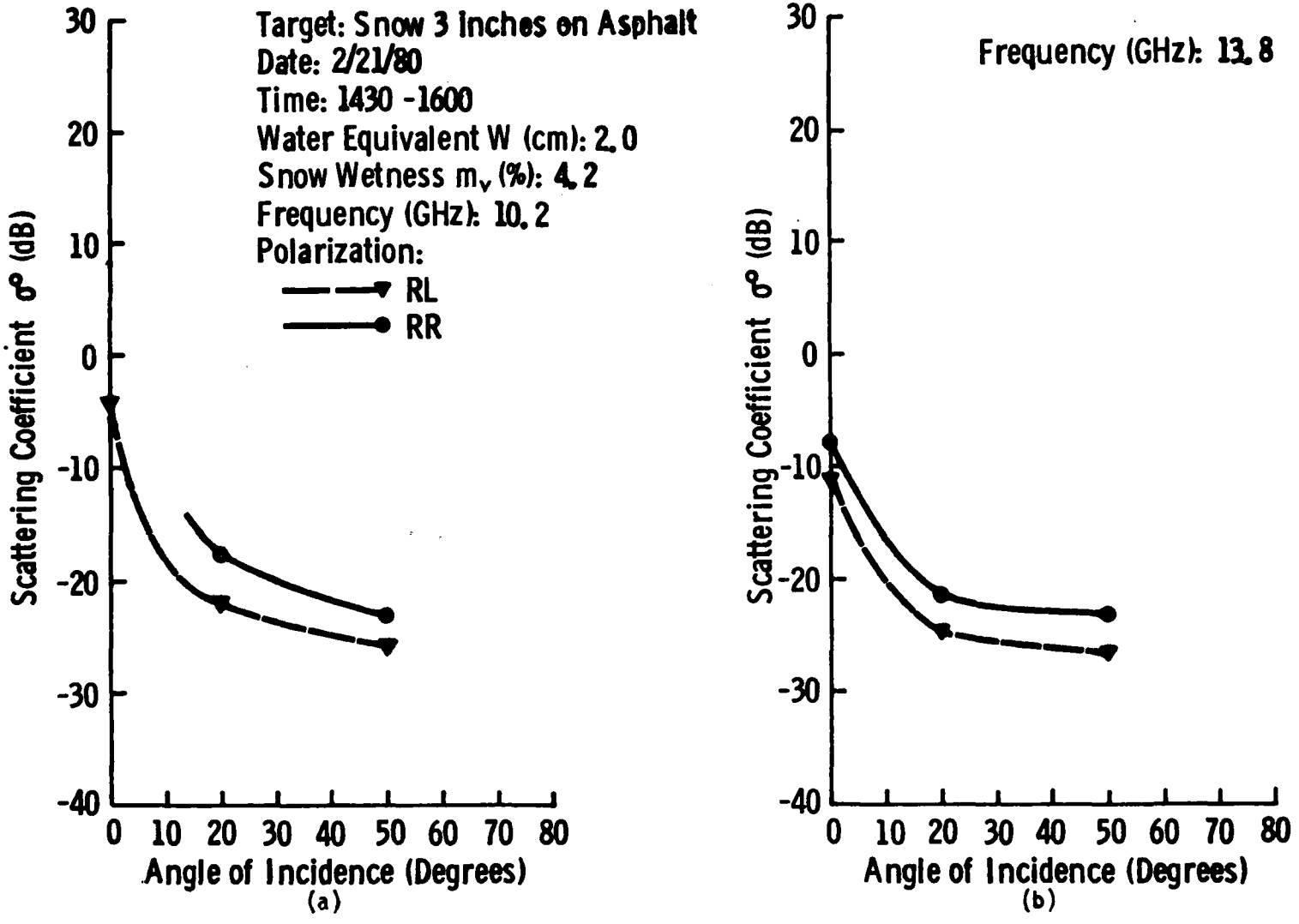

Figure 3-15 Angular response of σ^{o} of snow 3 inches on asphalt.

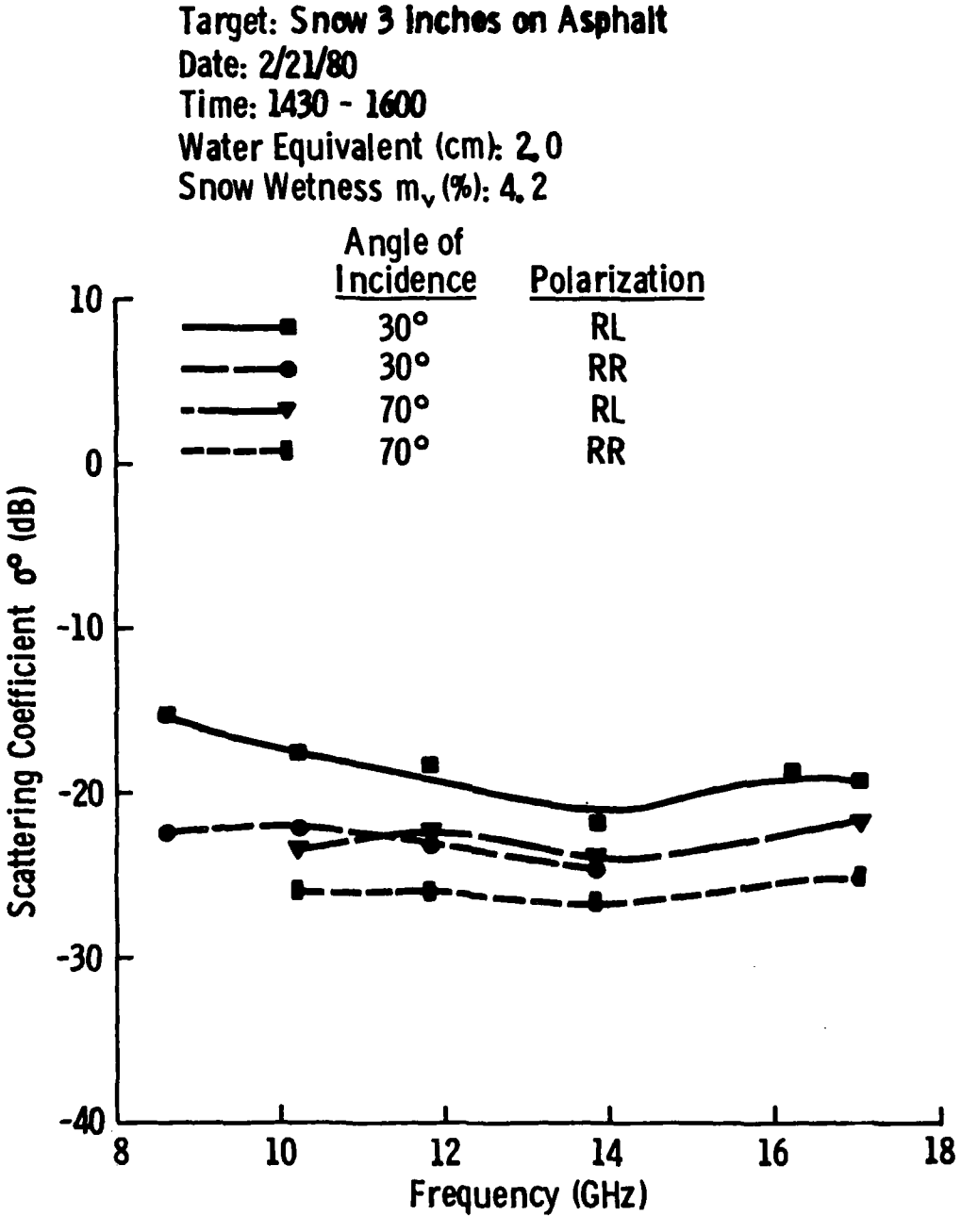

Figure 3-16 Spectral response of σ^{o} of snow 3 inches on asphalt.

Figure 3-17 View of Test Site No. 3 with a trace of snow on 2/17/80.

DATE: 2/17/80

TIME: 1010-1340

TARGET: Asphalt

See Figure 3-17

TYPE OF SET: Snow trace

LOCATION : High School Parking Lot
Steamboat Springs, CO
Test Site #3

Layer Number (From Ground)	Depth (cm) (To Layer Top)	Density $\rho(g/cm^3)$	Water Equivalent W(cm)	Grain Size (mm)
Overall	0-1	--	0-1	NA
9				
8				
7				
6				
5				
4				
3				
2				
1	0-1	--	--	

TARGET CONDITIONS

Height (cm): NA

Soil Moisture (0-5 cm): NA

Temperature °C: 1.3
(Ground)

WEATHER OBSERVATIONS

Air Temperature °C: 0.8

Relative Humidity: 96%

General:

Light snow during data set, no accumulation

SNOW WETNESS m_v

Wet but not measurable due to sample size

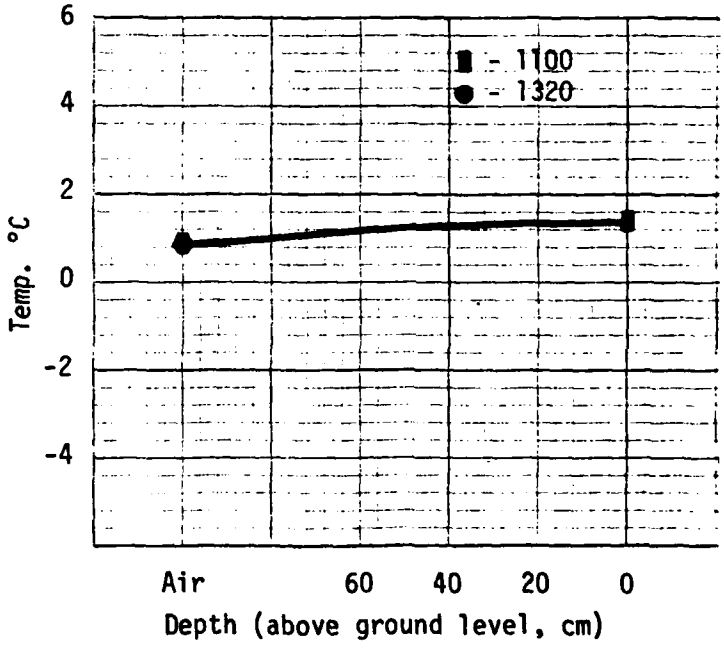

TABLE 3-7

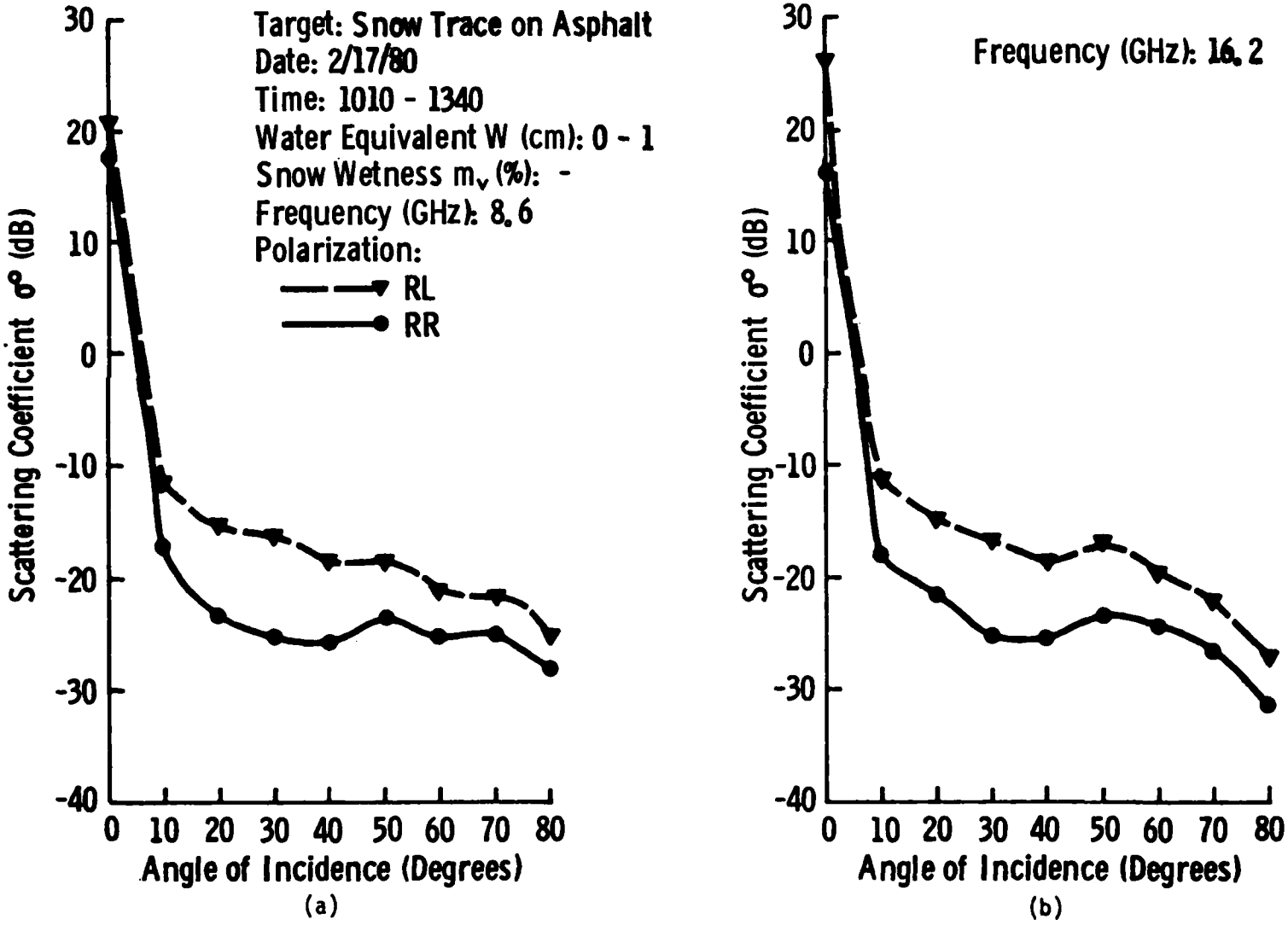

Figure 3-18 Angular response of σ^o of snow-trace on asphalt.

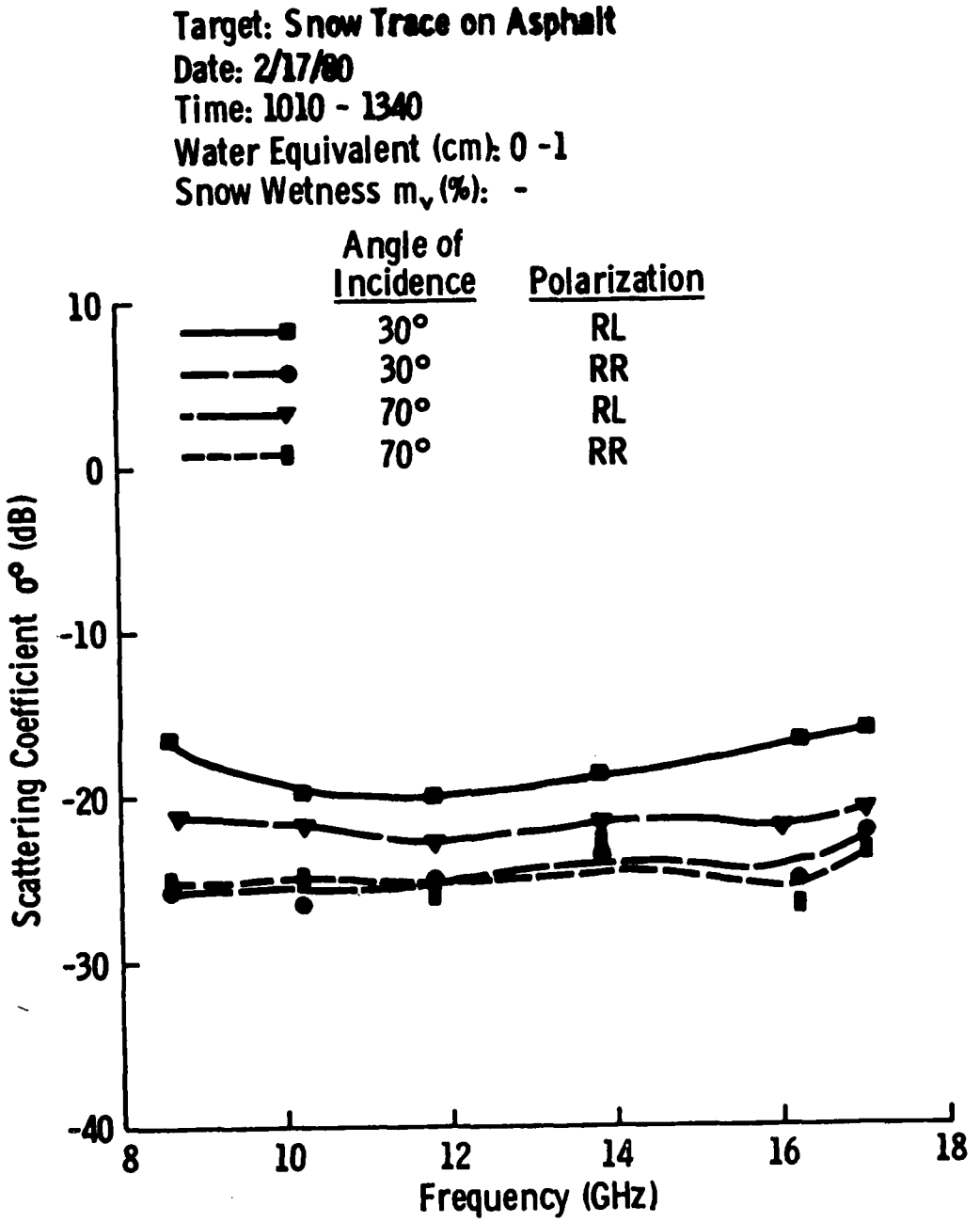

Figure 3-19 Spectral response of σ^{o} of snow-trace on asphalt.

3.2.2.2 Concrete

As a result of the uncooperative weather conditions and because no large concrete areas were available near Steamboat Springs, Colorado, the measurements of snow over concrete with circular polarization were not obtained. In lieu of these measurements, analyses in Section 3.3 will show the levels that would be expected from snow-covered concrete. The levels were determined from linear and circular measurements of bare (non-snow-covered) targets and from linear polarization measurements of snow-covered concrete.

3.2.3 Ice and Snow

In this target category, two data sets were obtained.

Lake-ice was observed at Shadow Mountain Lake, located in the Arapaho National Forest in Colorado (Figure 3-1d). The MAS system overlooked the lake from the Green Ridge Road. Figure 3-20 shows the overall area. The open-water area is outside the MAS observation range as shown in the diagram of Figure 3-21. Because of the distance to the lake from the road, it was not possible to obtain 0° (nadir) data and the 10° data, although given, may be biased by the edge of the shore. Figures 3-22 and 3-23 present the angular and spectral responses of σ^o and the ground-truth data are given in Table 3-8.

Since the resolution cell of the MAS radar is small with respect to a parking lot and since both cars and snowpiles are not area-extensive targets, the concept of σ^o is not really valid. Using the standard method (for the MAS systems) of data-taking does not yield a valid result. For this reason, a snowpile was built in the Steamboat Springs High School parking lot (Figure 3-24) and the radar was operated in a scan mode across the snowpile and a car.

The scans were obtained by setting the MAS system to a specific angle, polarization and frequency combination and then moving in azimuth across the targets and parking lot while recording the received power. These values were converted also to radar cross-section (RCS) σ. Figures 3-25 a, b, and c give examples of the scan data for 10.2 GHz and RL polarization at three angles of incidence: 0°, 10°, and 70°. Received power is plotted on the vertical axis while the horizontal axis is in relative distance along the ground.

Figure 3-20 Overall view of Test Site No. 4 showing the snow-covered lake-ice on 2/27/80 with open water seen in the background.

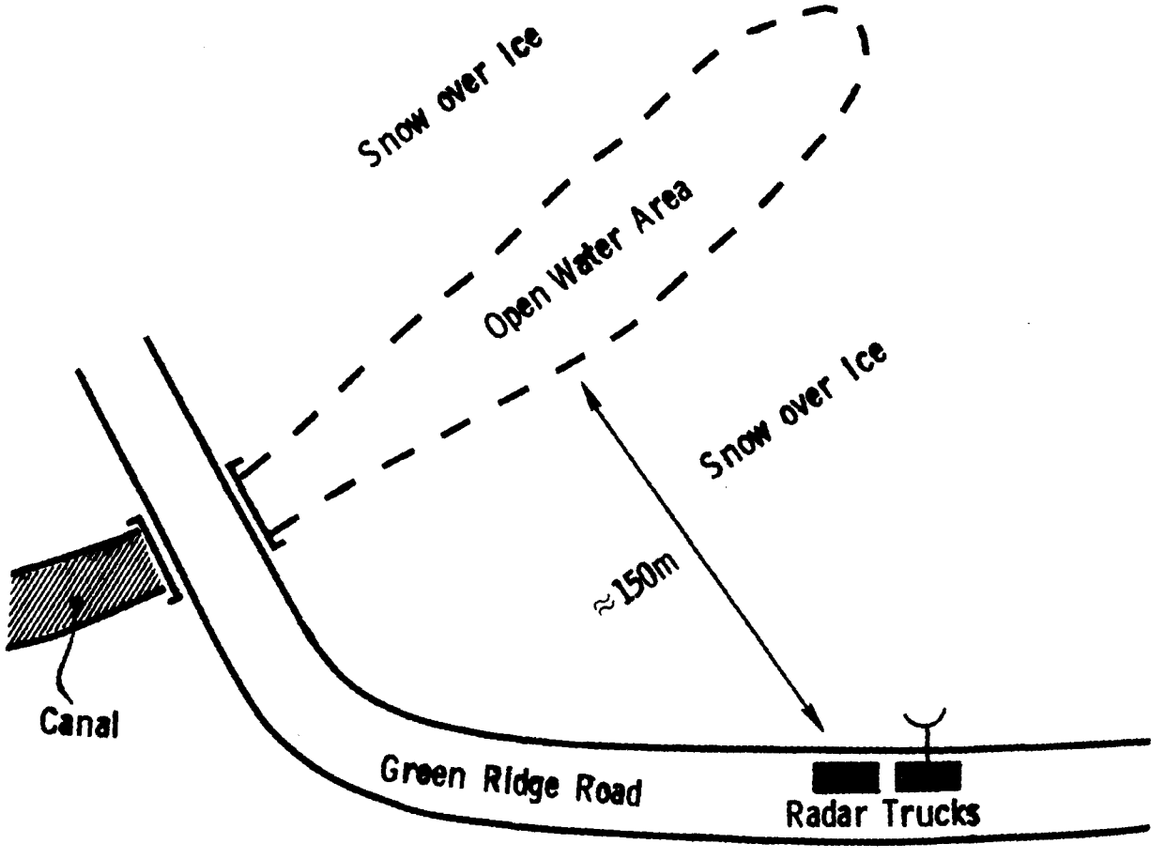

Figure 3-21 Shadow Mountain Lake Test Site.

DATE: 2/27/80

TIME: 0900-1300

TARGET: Lake Ice

TYPE OF SET: Ice

LOCATION: Shadow Mountain Dam
Grand Lake, CO
Test Site #4

Ice thickness approximately 40 cm.

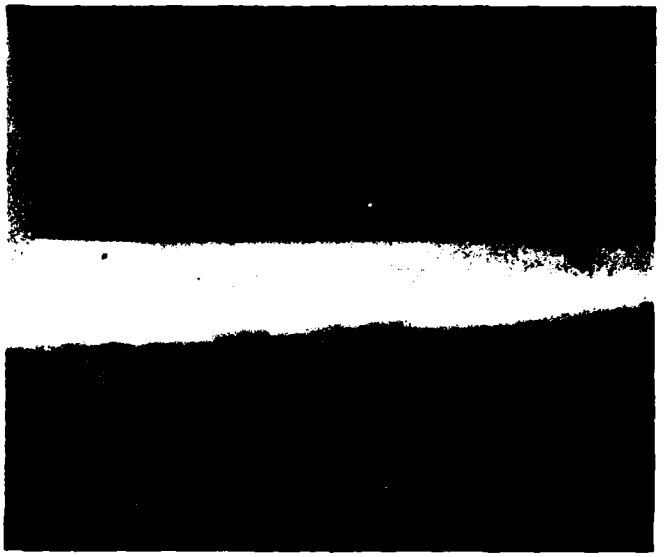

Layer Number (From Ground)	Depth (cm) (To Layer Top)	Density ρ(g/cm^3)	Water Equivalent W(cm)	Grain Size (mm)
Overall	20	--	5.5	NA
9				
8				
7				
6				
5				
4				
3				
2	20	.25	3.75	--
1	5	.35	1.75	--

TARGET CONDITIONS

Height (cm): NA

Soil Moisture (0-5 cm): NA

Temperature °C: Not Measured (Ice Surface)

WEATHER OBSERVATIONS

Air Temperature °C: →

Relative Humidity: Not Measured

General:

Clear, warming through the data set

SNOW WETNESS m_v

0-2 cm: 0.34%

5-10 cm:

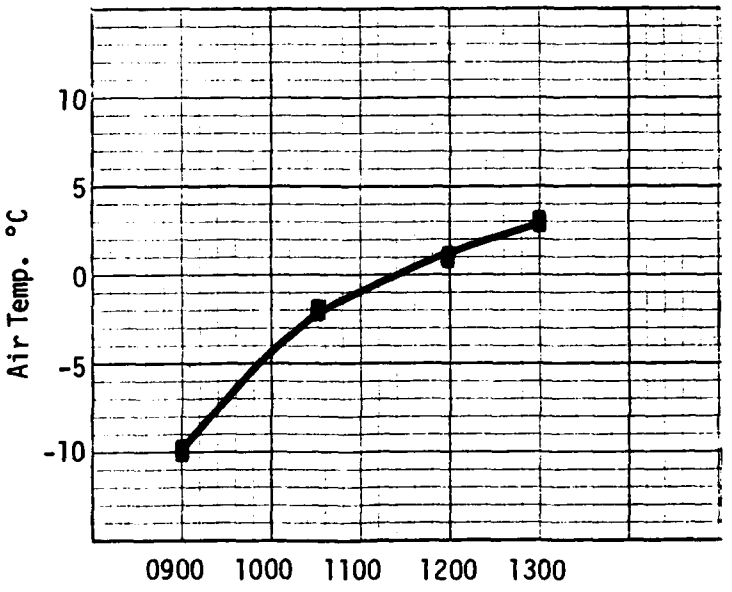

TABLE 3-8

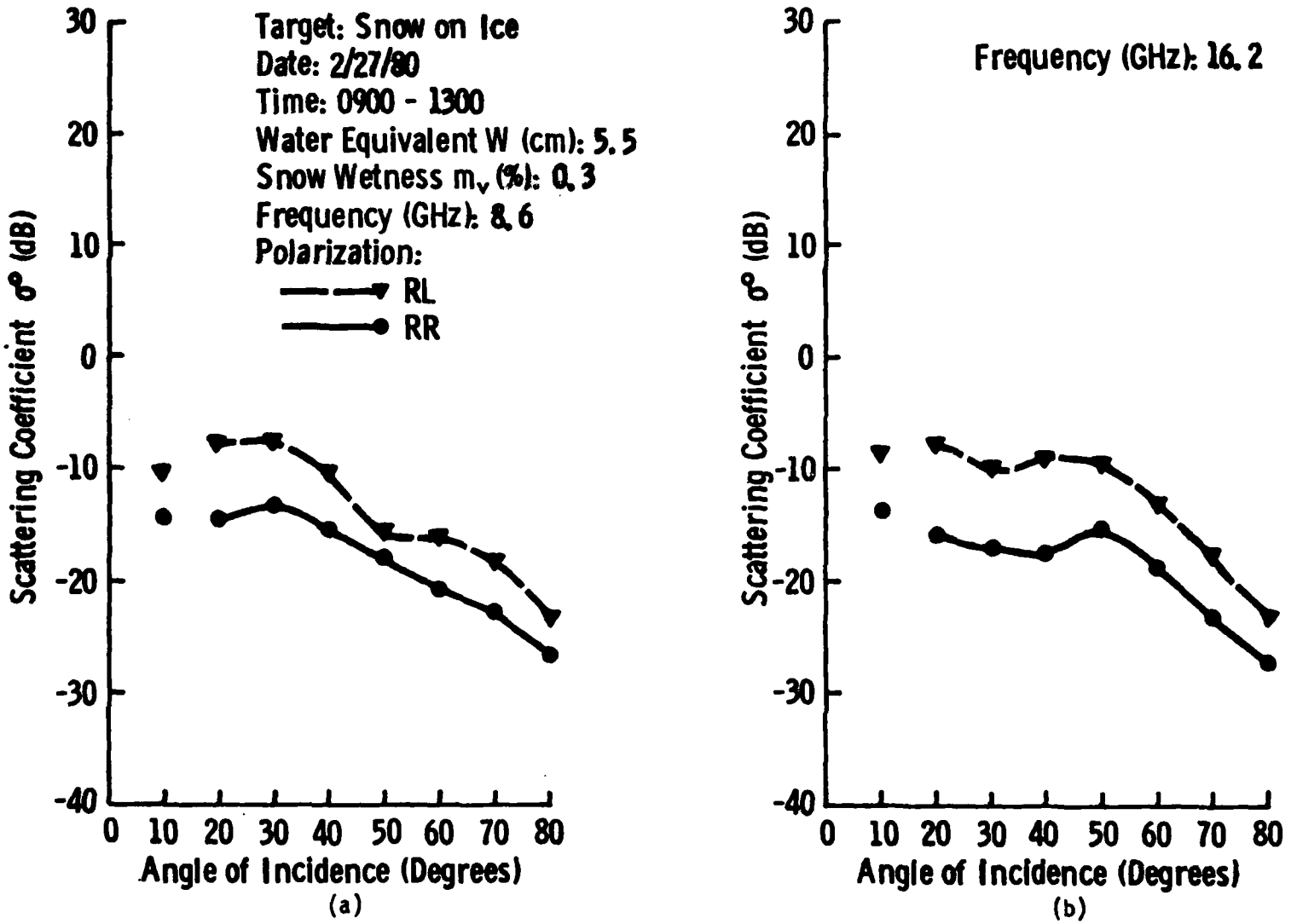

Figure 3-22 Angular response of σ° of snow on ice.

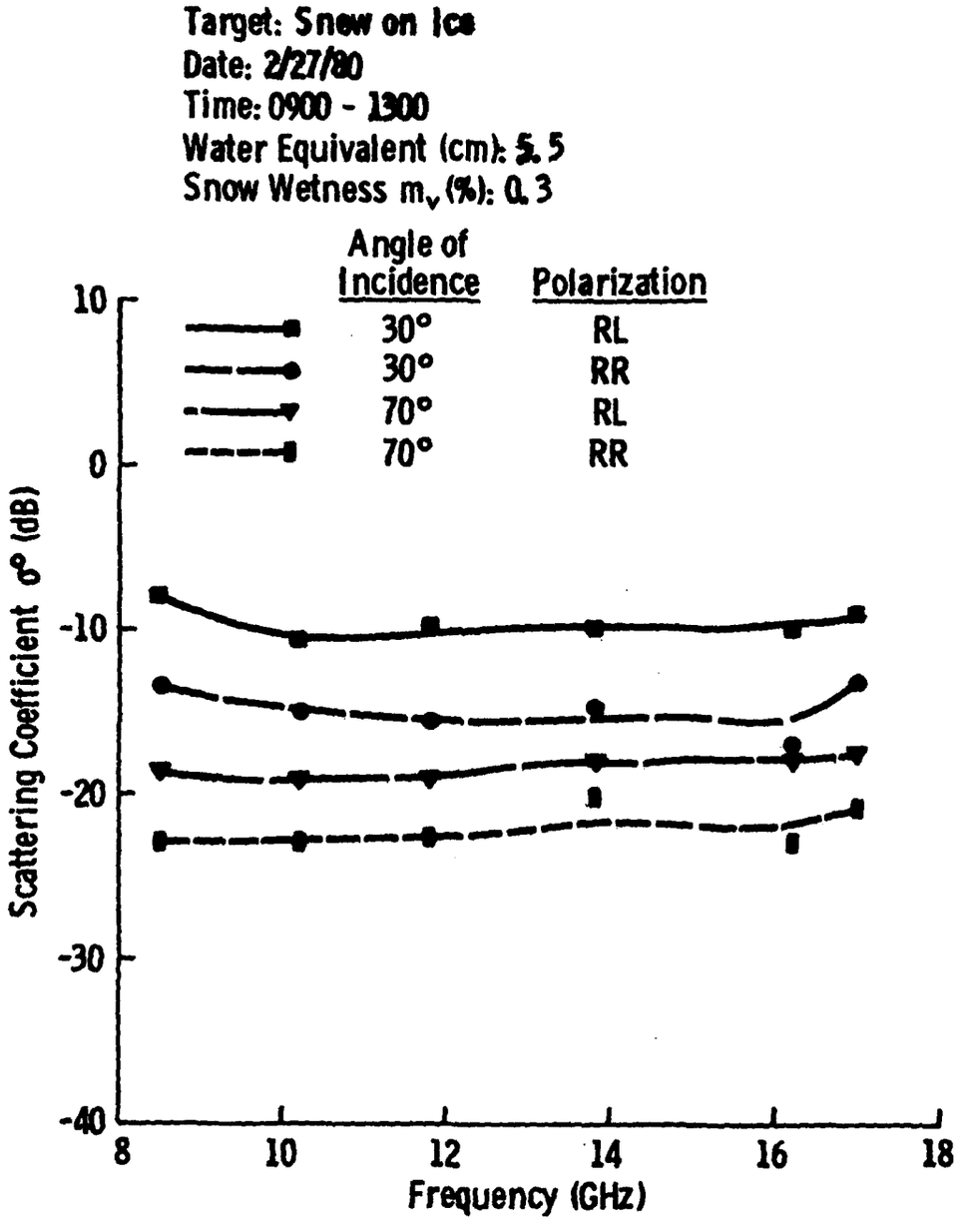

Figure 3-23 Spectral response of σ^0 of snow on ice.

Figure 3-24 View of the snowpile and the car observed on 2/17/80.

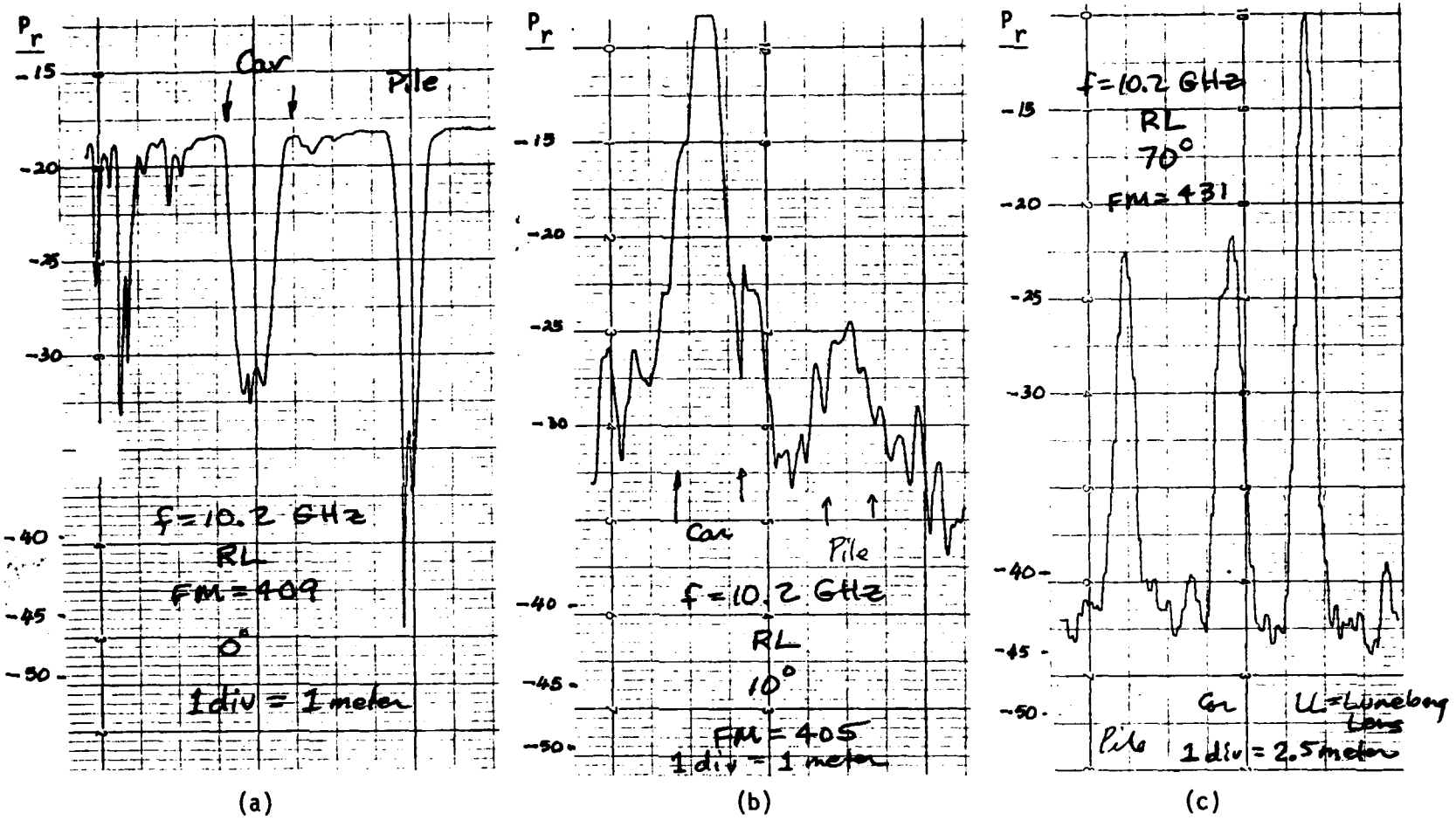

Figure 3-25 Variation in received power P_r for the scan data at 10.2 GHz, RL polarization at three angles of incidence: (a) 0° (nadir), (b) 10°, and (c) 70°.

FM is the modulation rate used for determining the range to the target.

The results of all the scans in both relative received power and σ units are given in Appendix B.

At nadir, Figure 3-25a shows that the asphalt backscatter is higher in level than that of the car because of the convex curvature of the car-roof. At the higher angles of incidence (Figure 3-25b and c), the backscatter from the smooth asphalt surface is substantially lower than that obtained from the car or the snowpile. The Luneber Lens (LL) also was placed along the scan-line to provide a reference radar cross-section at 30° and 70°

If the peak values of the backscatter from the car and snowpile are converted to numbers using the standard calibration routine, the angular and spectral responses may be found. Figures 3-26 and 3-27 illustrate these responses.

3.3 Analyses of Snowcover Effects

3.3.1 Linear and Circular Polarization Backscatter Relationship

The understanding of the relationship between linear and circular polarization backscatter coefficients is valuable for several reasons. First, it would allow usage of the much larger volume of linear polarization data to be applied to circular polarization data bases. Secondly, it would improve our basic understanding of the backscatter mechanism, although this effort will require additional work.

Linear polarization data were obtained for Sandia Laboratories [4,5] in 1978. Figures 3-28 to 3-30 illustrate the backscatter coefficient data for linear and circular polarizations at two frequencies for three targets: concrete, asphalt, and short grass. From these curves, the indication is that for very smooth surfaces, concrete and asphalt at 8.6 GHz, the differences between circular and linear are small, while for the rougher surfaces, circular is generally a few dB below the linear data. This observation, however, will be shown to be a minor consideration for the case of snowcover on concrete.

Figure 3-31 illustrates the repeatability for system measurements between the first report [1] and data presented in this report. The σ° agreement is seen to be very good.

DATE: 2/17/80

TIME: 1400-1600

TARGET: Snowpile

LOCATION: High School Parking Lot
Steamboat Springs, CO
Test Site #3

The snowpile was made from wet snow. It was approximately 0.9 m high and 1.2 m in diameter. For other pertinent ground-truth data, see Table 3-7.

TABLE 3-9

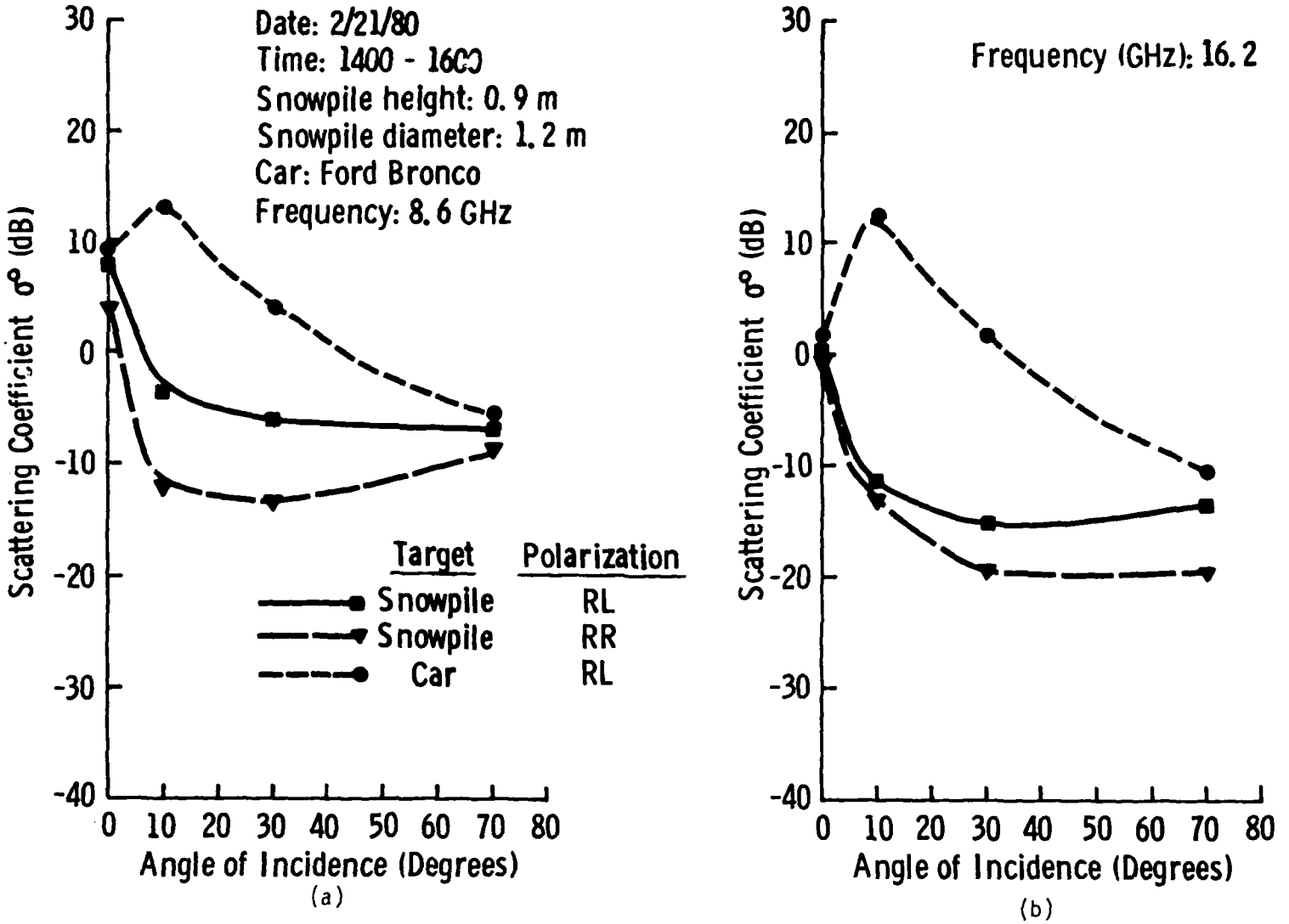

Figure 3-26 Angular response of σ° of snowpile and car on asphalt.

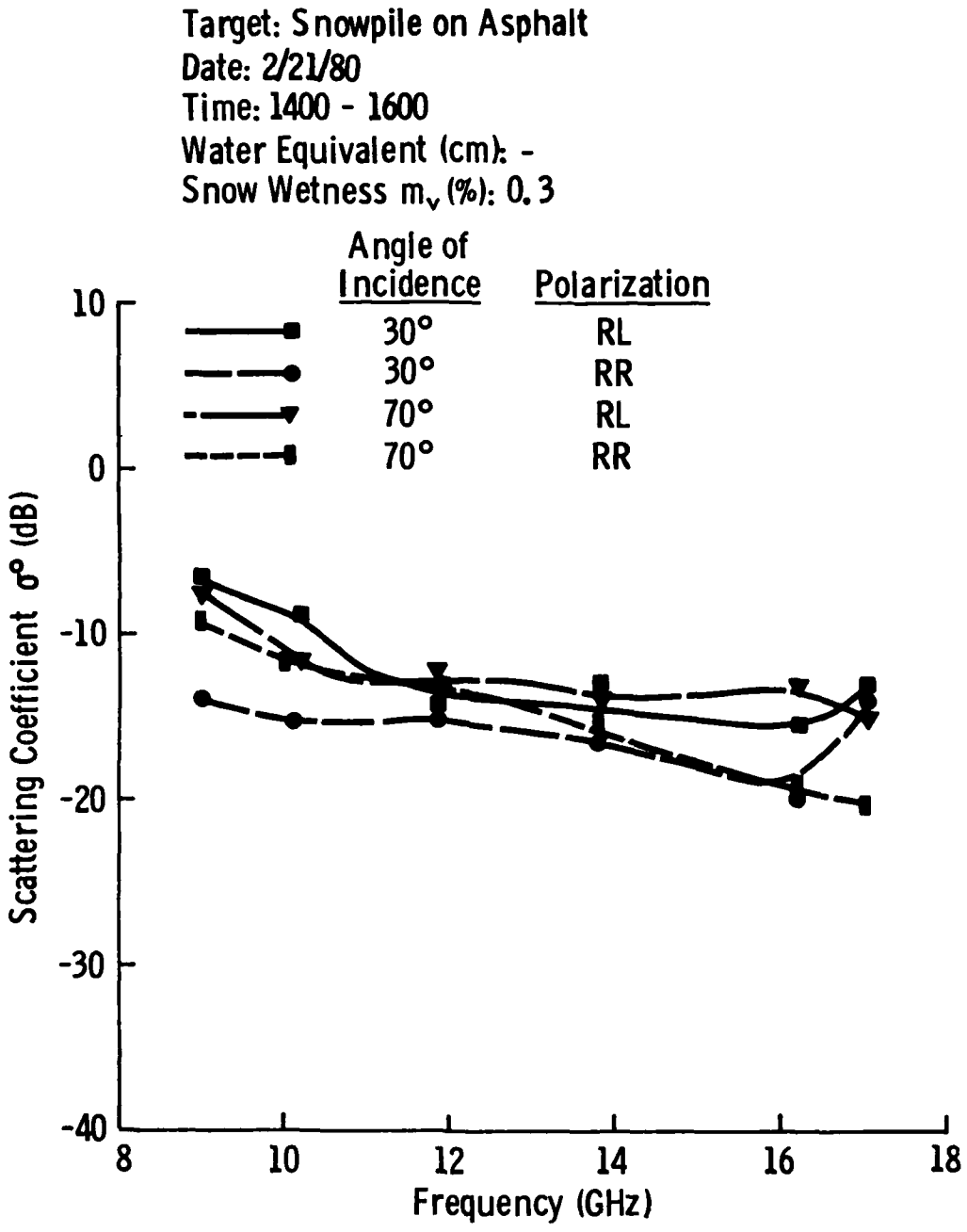

Figure 3-27 Spectral response of σ^{o} of snowpile on asphalt.

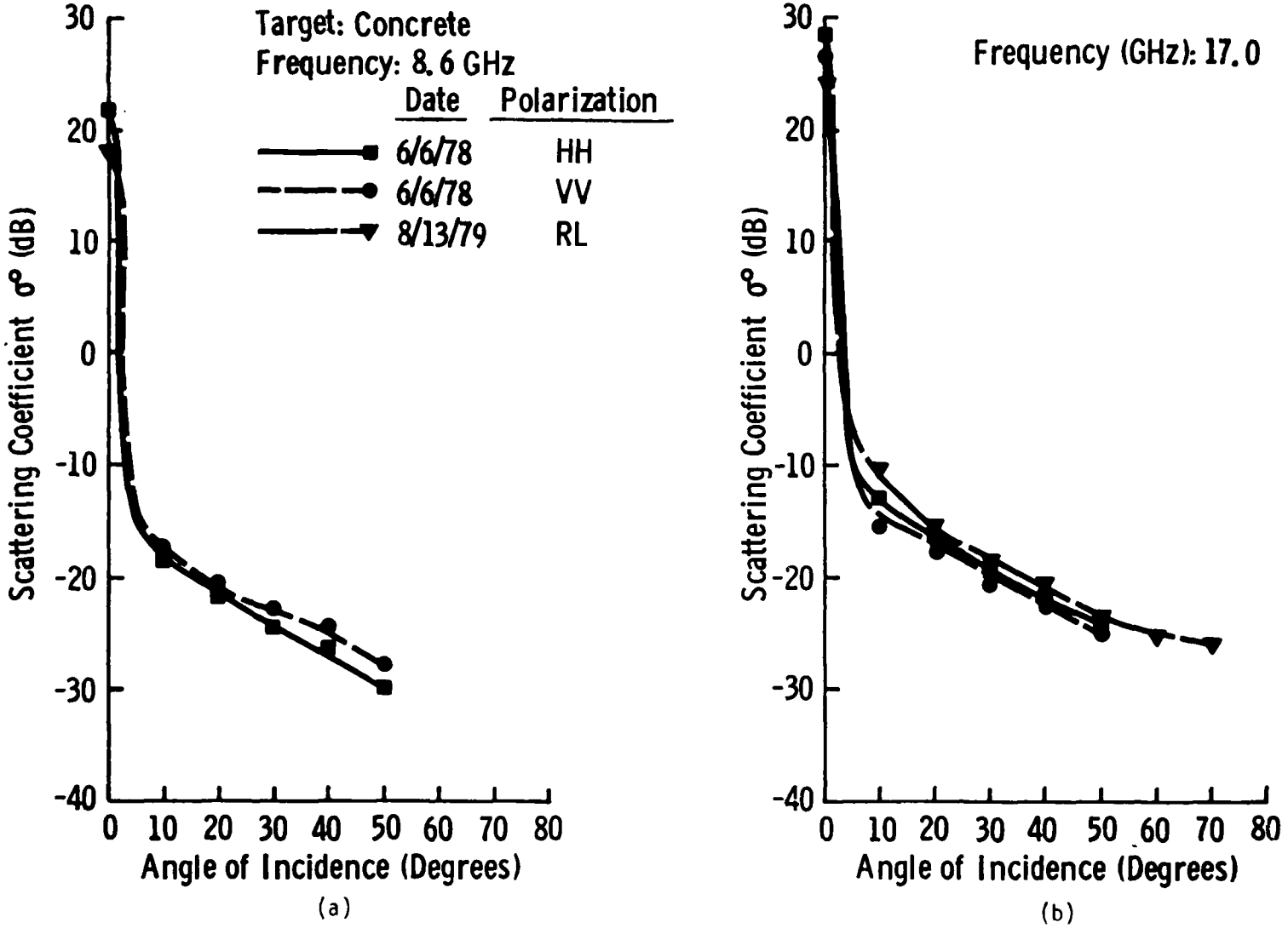

Figure 3-28 Linear and circular σ^{o} comparison on dry concrete.

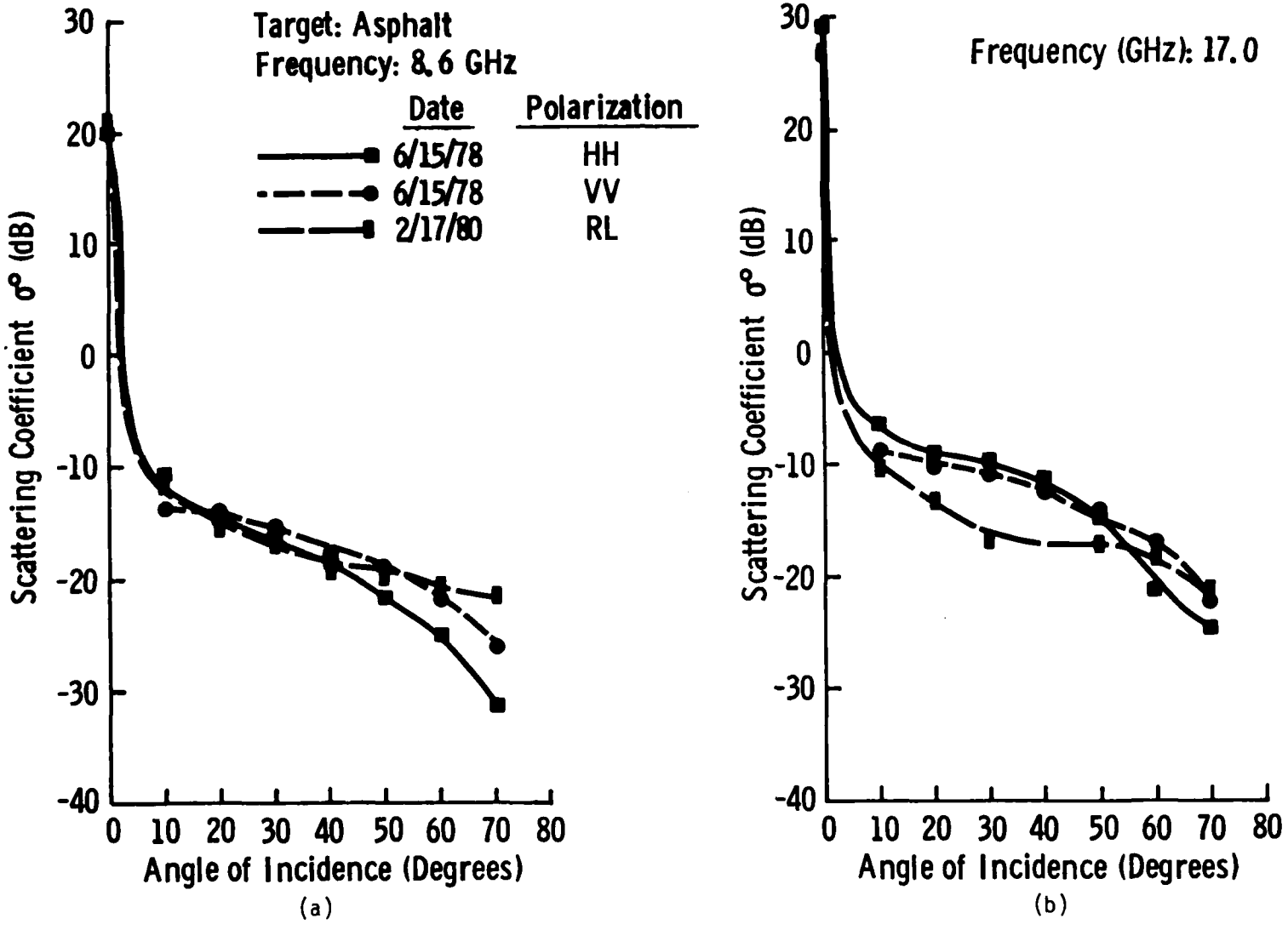

Figure 3-29 Linear and circular σ^{o} comparison on asphalt.

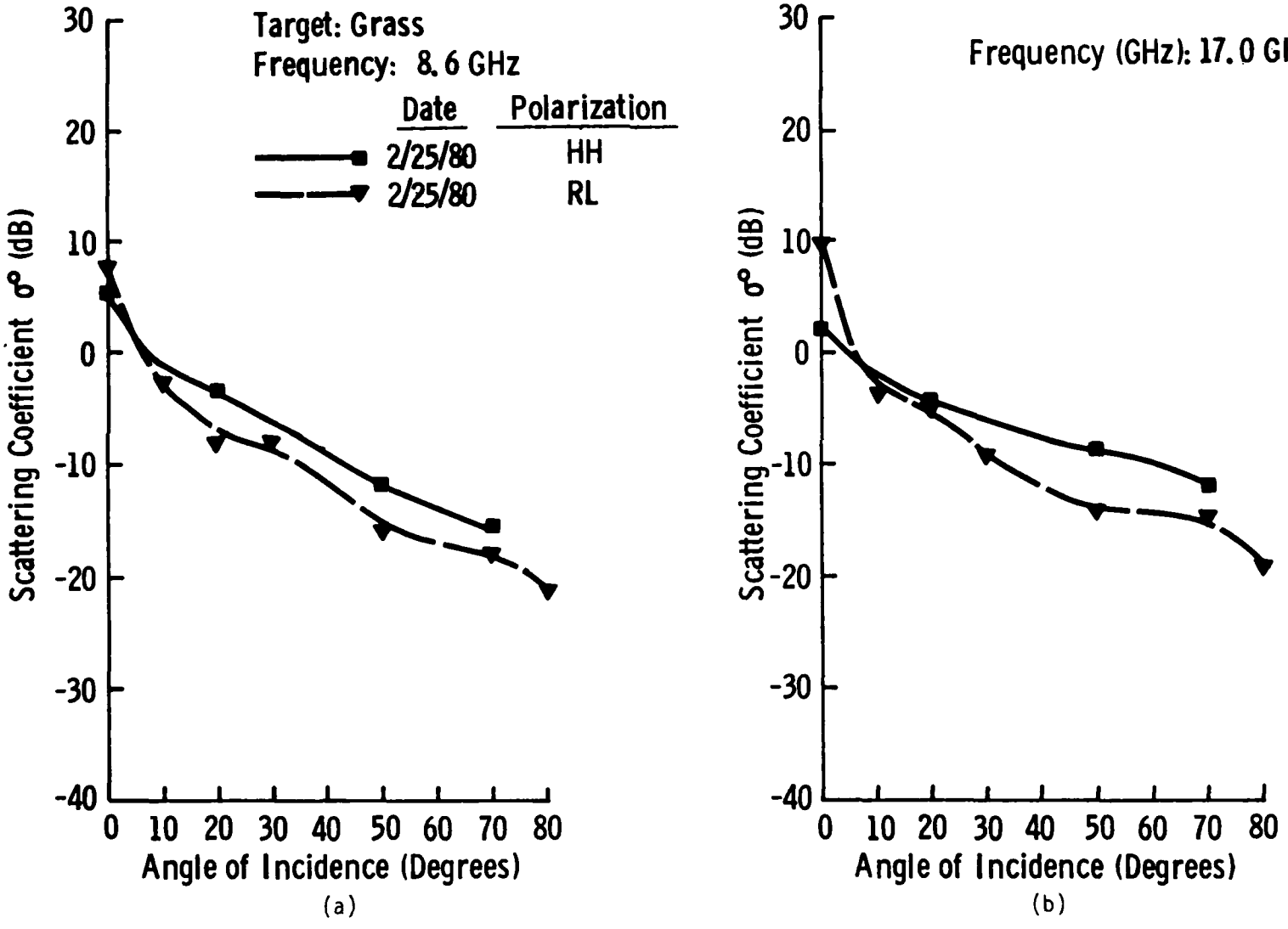

Figure 3-30 Linear and circular polarization σ° comparison on bare grass.

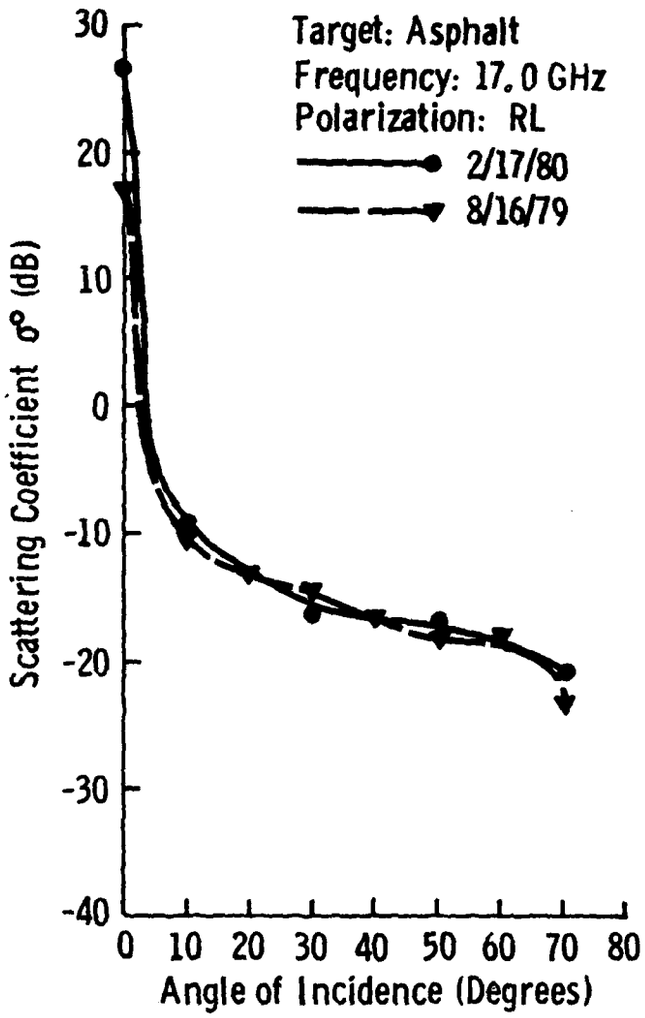

Figure 3-31 Comparison of data reported in reference [1] with the data obtained for this report.

3.3.2 Effects of Snow on the Backscatter Response of Grass

From the three data sets obtained on snow-covered grass, the smoothed angular responses of σ^o with RL polarization are shown in Figure 3-33 at two frequencies. These results indicate that, depending upon snow conditions, the backscatter coefficient may be either higher or lower than the grass in the absence of snow.

The two dominant snow parameters affecting the microwave backscatter properties are water equivalent and snow wetness [6,7]. The effect of increasing snowcover (water equivalent) at angles away from nadir is to increase the backscatter [7]. The effect of snow wetness is to decrease the backscatter at angles away from nadir. The behavior near nadir to changes in either water equivalent or wetness is not as well-understood but may be dominated by the contribution from the underlying terrain.

Observing Figure 3-32, one notes that the data obtained on 2/14/80 is on fairly dry snow, m_v = 1.4% in the surface layer, while the internal snowpack was dry. In this case, the effects of W and m_v appear almost to cancel with the σ^o curve being slightly above the bare-grass case. Two days later, on 2/16/80, the complete snowpack was wet and the surface was very wet (m_v = 5.2%). The σ^o response at angles of incidence above 10° is seen to be much lower than the bare grass. This effect results from the radar response being dominated by the smooth, wet snow surface. The attenuation for snow of this wetness is very large and therefore only the surface layers affect the σ^o response. If dry snow had been observed, its σ^o response would have been higher than the curves of 2/14/80.

3.3.3 Effects of Snow on the Backscatter Response of Asphalt and Concrete

The four data-sets obtained over asphalt are illustrated in smoothed form in Figure 3-33 at two frequencies. Again, the parameters W and m_v are the dominant snow effects. These curves, in comparison with those of Figure 3-32, seem very different; however, the differences may be explained by reviewing the general situation of snow over terrain.

The backscatter coefficient for snow-covered terrain may have contributions from both snow and the underlying terrain. The snow has two effects:

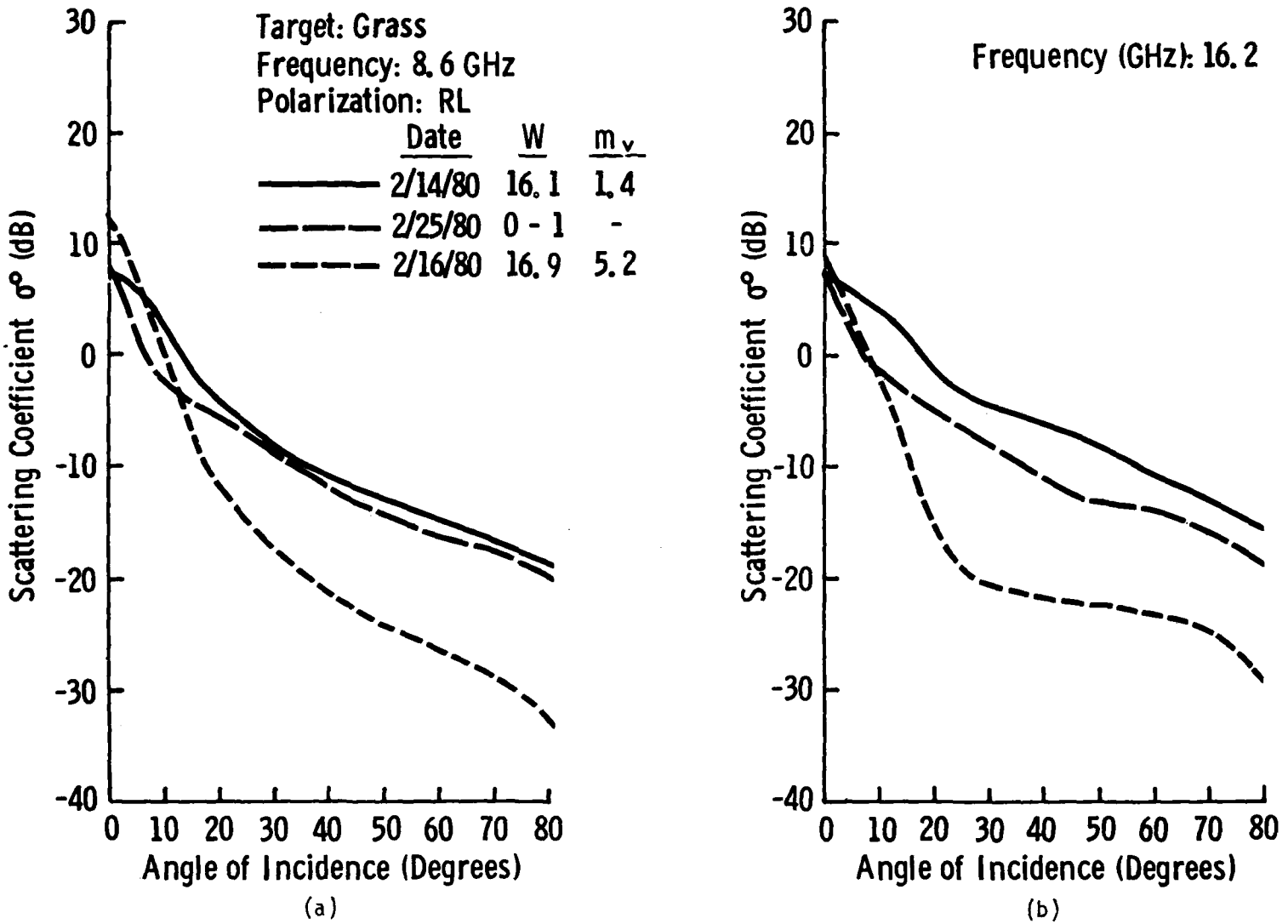

Figure 3-32 Effects of snow on the backscatter from grass.

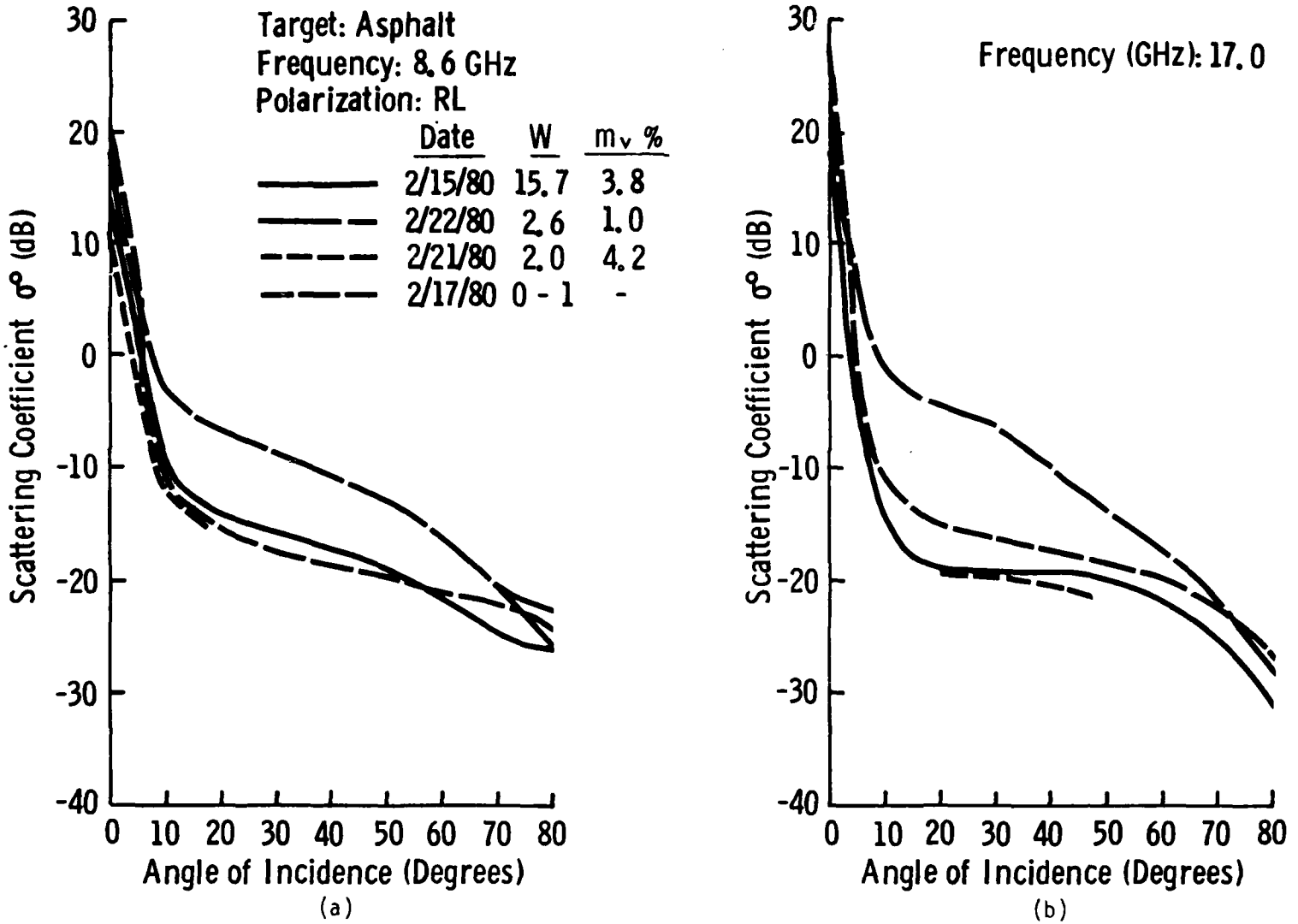

Figure 3-33 Effects of snow on the backscatter from asphalt.

(1) The snow has an attenuating effect upon the radar backscatter from the terrain, and

(2) the snow also contributes directly to the backscatter.

As a result of (1), since the backscatter coefficient for grass is greater than that of asphalt, for equivalent conditions the backscatter from snow-covered grass is affected more by the grass than the backscatter from snow-covered asphalt is affected by the asphalt.

As little as W = 2.6 cm of snow on 2/22/80 is observed to raise σ^o significantly over the trace-of-snow case, even though there was some snow wetness. Both of the other dates (2/15/80 and 2/21/80) on very wet snow (4.2 and 3.8%) show similar responses for drastically dissimilar values of W (15.7 versus 2.0 cm) indicating that the snow is dominating the backscatter at high wetness values and therefore the penetration depth must be less than W = 2.0 cm for these wetness levels.

The effects of snow on both asphalt and concrete on linearly polarized backscatter coefficients have been measured previously [4,5]. Figures 3-34 and 3-35 present wet and dry snow responses along with bare asphalt and concrete. In Figure 3-34, similar behavior to Figure 3-33 on asphalt is observed. The snow is seen to have a much greater effect on the backscatter from the "smoother" concrete surface. When the curves for snow on asphalt and concrete are combined in Figure 3-36, it is noted that, for these smooth targets, the backscatter with snowcover is approximately the same regardless of the target. This fact indicates that the snow is the dominant scatter mechanism and that for water equivalents greater than about W = 2 cm, the backscatter from snow-covered concrete and snow-covered asphalt is approximately the same. Similar trends also would be expected for circularly polarized data, therefore the levels for snow-covered asphalt given in Figure 3-33 will be comparable to the levels that would be observed on concrete.

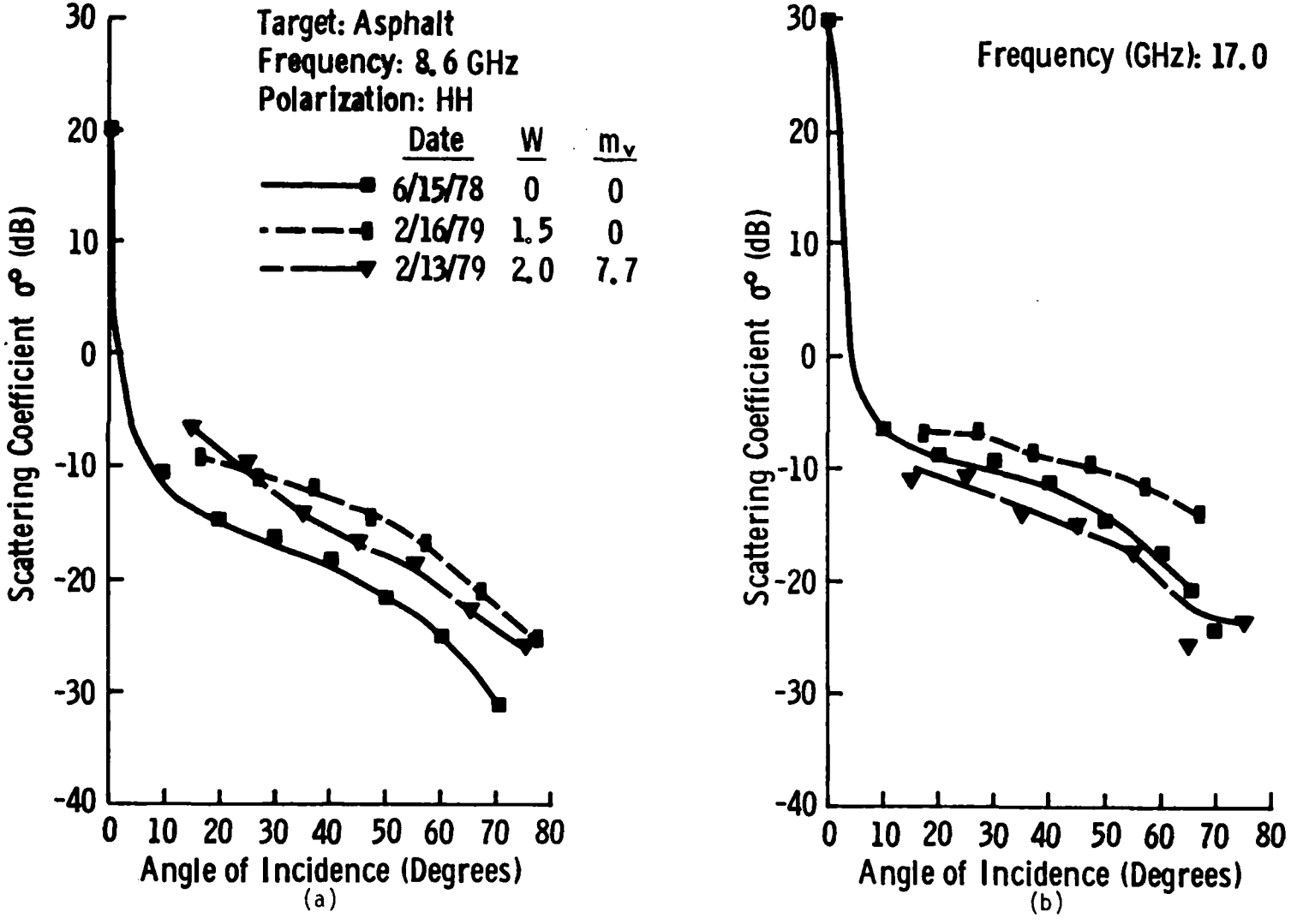

Figure 3-34 Effects of snow on the linear polarization backscatter from asphalt.

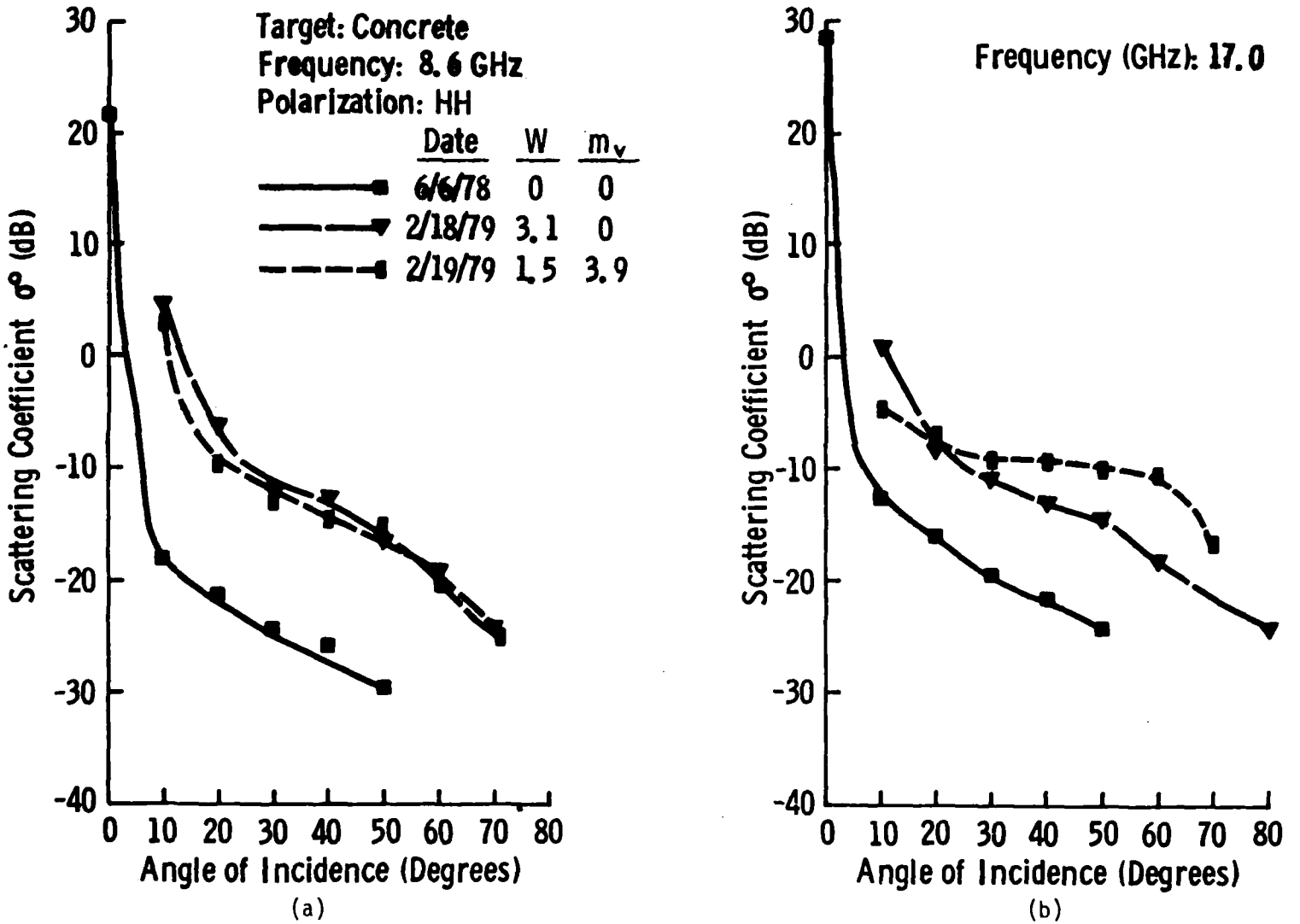

Figure 3-35 Effects of snow on the linear polarization backscatter from concrete.

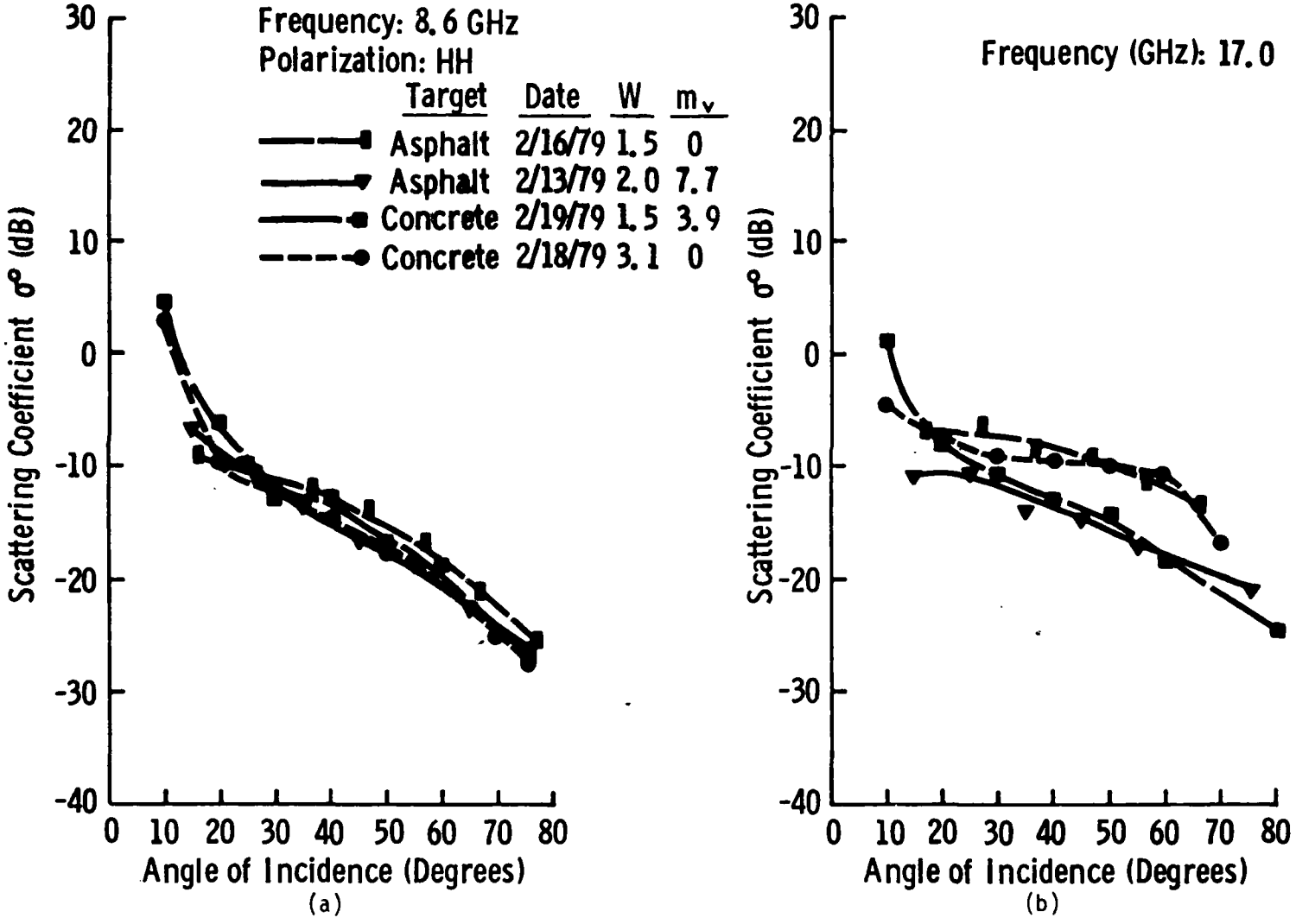

Figure 3-36 Backscatter from snow using linear polarization.

3.3.4 Ice and Snow

The data set over lake-ice (Figure 3-22) was taken with a 20-centimeter snowcover. No other circularly polarized data are available on snow-covered lake-ice (smooth ice), therefore, a comparison with the HH-polarized results of Onstott [8] is shown in Figure 3-37. These data sets on bare and snow-covered ice were obtained in the arctic. It is observed that the levels of σ^o of the snow-covered ice are within about 3 dB of each other. The exact behavior of the snow-covered ice may have been affected slightly by a low-level salinity, since this lake was close to the ocean. Noting the much lower level for the non-snow-covered ice indicates, as for the road-like surfaces, that the contribution of the backscatter from the snow probably is the dominant factor.

Pack-ice data, as previously stated, was not obtained. In lieu of this data, the closest target found was a sea-ice pressure-ridge. This ridge was 0.9 m high and consisted of 10-cm-thick blocks of ice (Onstott [8]). Figure 3-38 presents the σ^o data for this target.

The parking-lot data (Figure 3-26) is replotted with the addition of the asphalt background in Figure 3-39. The values of σ^o calculated for the car and the snowpile can then be compared with the level of the parking lot. The interpretation of this information requires knowledge of the sensor's resolution cell and the purpose of the measurement. If the resolution cell is large, then integrated effects of cars, snowpiles and asphalt will be observed. Spatial averaging of the areas of each target multiplied by their respective σ^o values would then give an effective "σ^o" for the whole parking lot. On the other hand, if the resolution cell is small, then direct comparisons may be made (Figure 3-39).

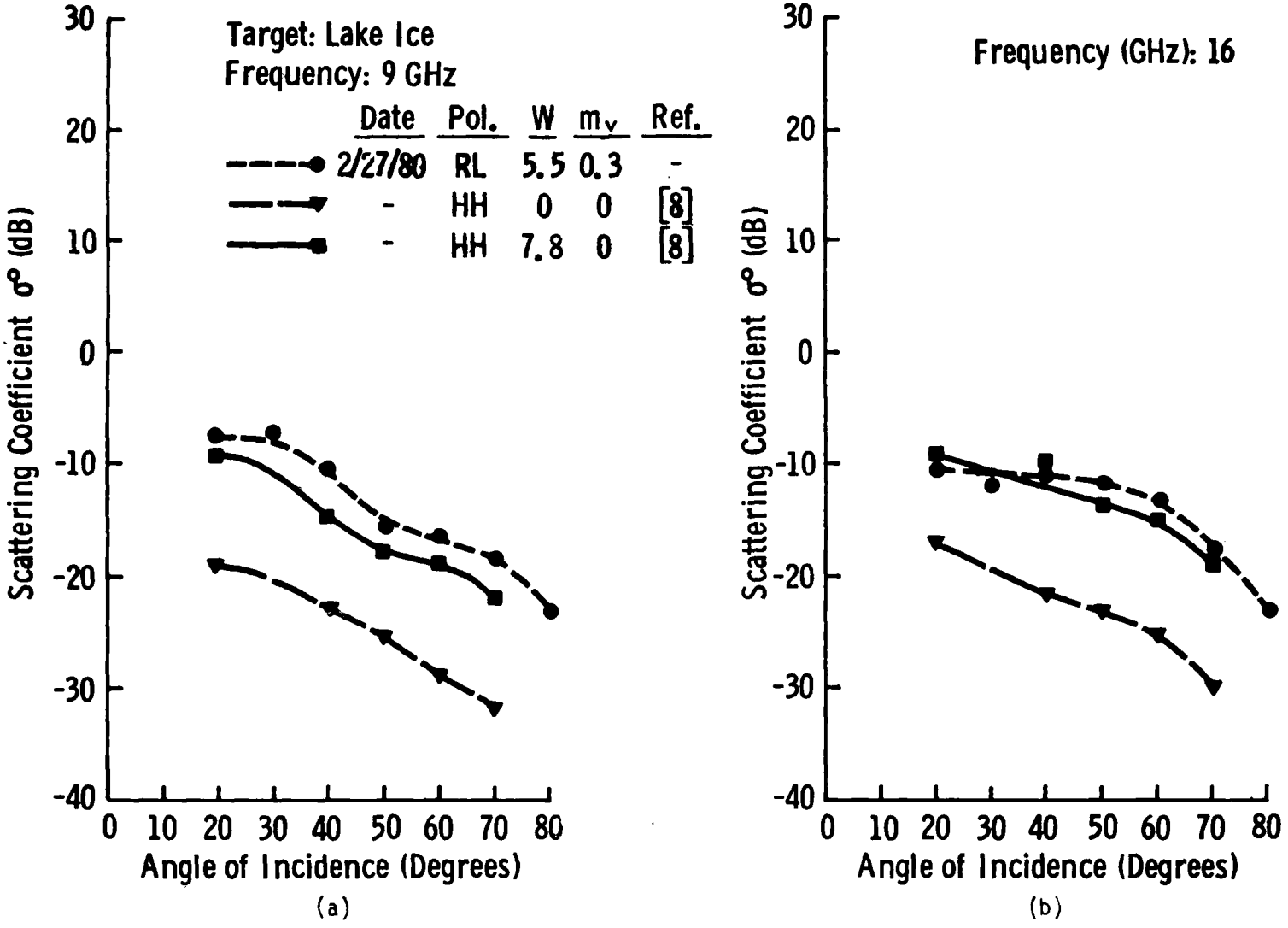

Figure 3-37 Backscatter from smooth ice for linear and circular polarization. Linear polarization data from Onstott [8].

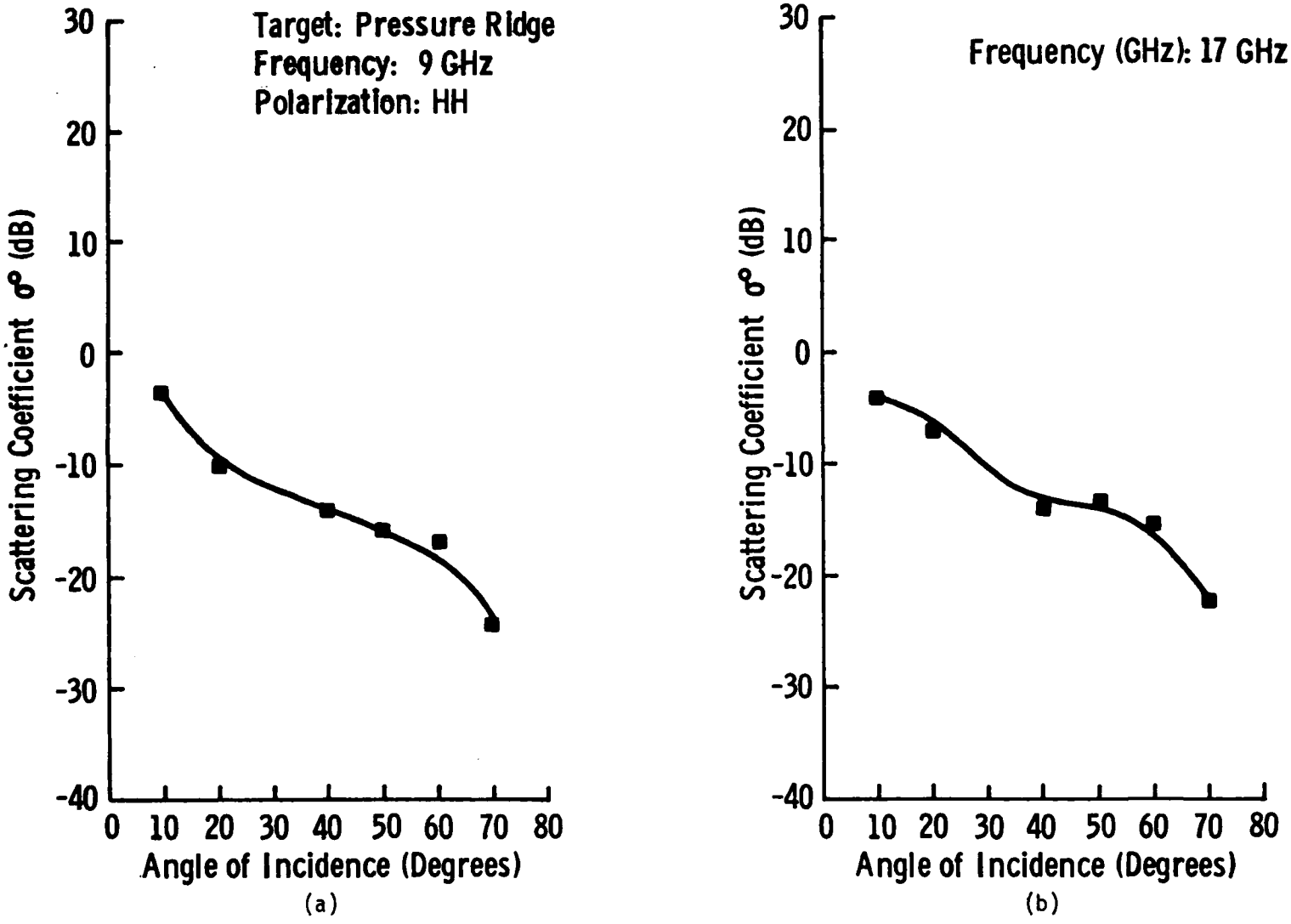

Figure 3-38 Backscatter coefficient of a sea-ice pressure ridge from Onstott [8].

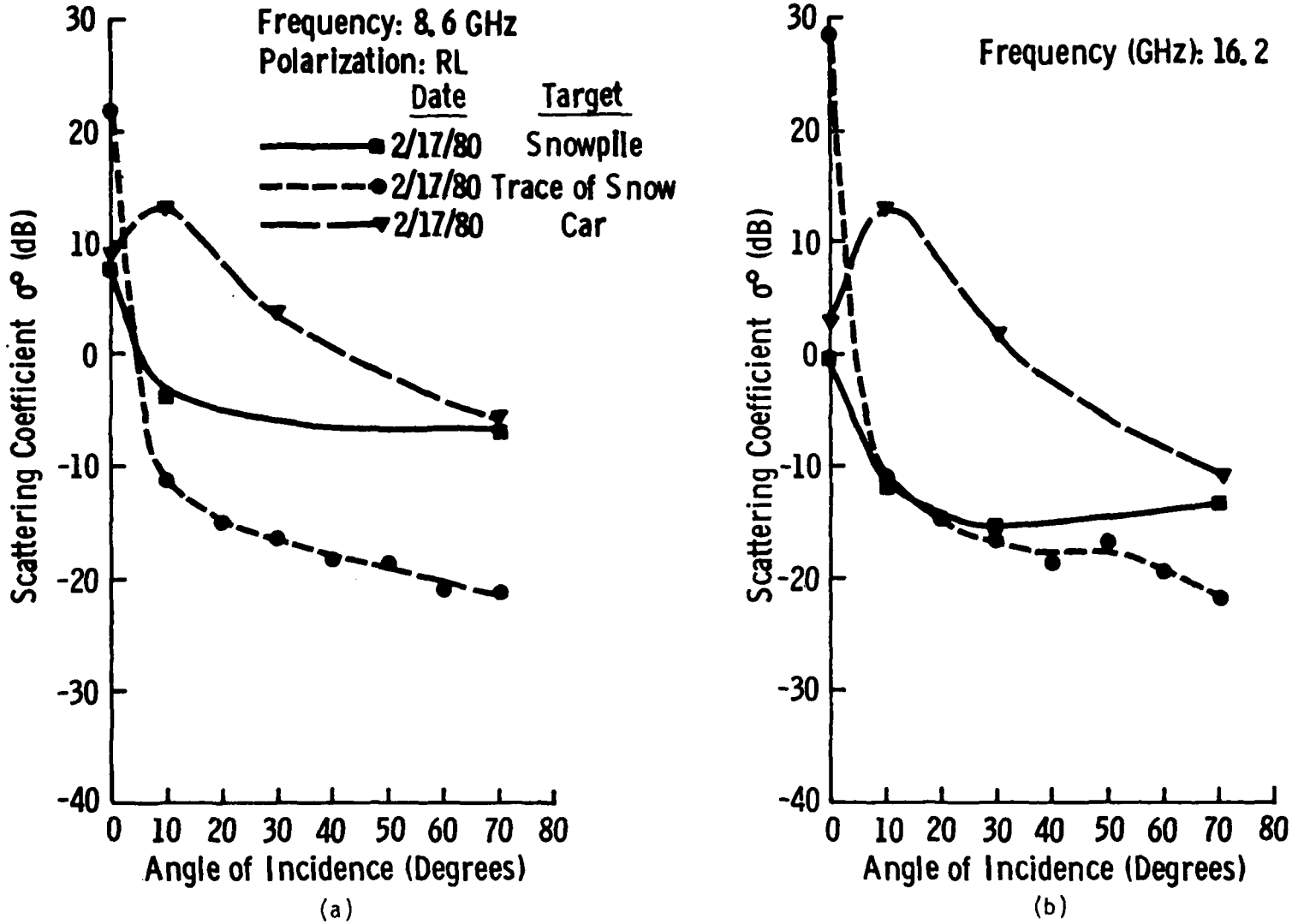

Figure 3-39 Backscatter from a snowpile, a car, and an asphalt parking lot.

4.0 RECOMMENDATIONS

Based on the experience gained from the present study, the following recommendations are proposed:

Circular Polarization: For the few cases where the same target was measured by the same system for linearly polarized (HH or VV) and circularly polarized (RL) antenna configurations, the results show that the magnitude of σ^o is comparable, although not exactly the same, for all three like-polarizations. Specifically, for concrete (Figure 3-28), the σ^o curves corresponding to the three polarizations essentially are indistinguishable one from the other. Although some differences in level are apparent between σ^o of the different polarizations for asphalt (Figure 3-29) and grass (Figure 3-30), the volume of the data are not a sufficient volume from which to draw general conclusions. For cross-polarization, HV and RR (or LL), there is even less data available for comparison. Since linearly polarized data is much more available than circularly polarized data, it may be possible to use the available linearly polarized data bases for estimating the circularly polarized scattering coefficient of terrain types if a procedure can be established to relate σ^o(RL) and σ^o(RR) to σ^o(HH), σ^o(VV) and σ^o(HV). To this end, a two-task program is proposed:

(a) Using surface- and volume-scattering theoretical models, to develop relationships between the circularly polarized scattering coefficients and their linearly polarized counterparts.

(b) To design and conduct careful experiments to measure σ^o(RL), σ^o(RR), σ^o(HH), σ^o(VV) and σ^o(HV) using the same system for three classes of terrain types: (1) smooth surfaces, such as concrete and asphalt; (2) rough surfaces, such as plowed ground; and (3) volume scattering media, such as snow and trees.

Using the data generated under Task (b), the validity of the models of Task (a) may be evaluated and the process, it is hoped, will lead to the desired relationships.

Backscatter from Trees: The measured σ^o value of a tree canopy represents the backscattered power integrated over the effective volume of the canopy that contributes most of the return. Thus, it is difficult to ascertain (a) the relative significance of the contributions by the various "layers" of the canopy and (b) the degree of penetration into the canopy volume. Without this type of information, it is difficult to formulate realistic theoretical models for the backscatter from tree canopies. It is therefore recommended that careful measurements be made using a high range resolution system such as a short-pulse radar or a wide-bandwidth FM-CW radar. By increasing the modulation bandwidth of the MAS 8-18 system to 4 GHz, for example, a range resolution of the order of 15 cm may be obtained in practice (compared to a theoretical range-resolution of 7.5 cm). A record of the spectrum analyzer display corresponds to the power return as a function of range. Such a record provides information on the relative backscatter by scattering range layers between the treetops and the underlying soil surface, with a range resolution of approximately 15 cm. Detailed measurements of this type, coupled with the standard measurements of σ^o (which employ spatial and frequency averaging to reduce signal-fading) would lead to a better understanding of the backscatter differences between different types and/or conditions of trees and to the formulation of theoretical models based on a more sound foundation.

Backscatter from Snow: Based on the experimental observations made in connection with this and other investigations [5-7] of the radar backscatter from snow-covered terrain, it may be concluded that the three major parameters governing σ^o are (a) the snow water equivalent (which is related to the snow density and depth), (b) snow wetness profile and (c) the backscattering behavior of the terrain with no snow-cover. In lieu of acquiring large volumes of data to cover a wide range of parameters (a) and (b) for each terrain-type of interest, it is proposed that the models developed by the University of Kansas [6,7] (although for linear polarization configurations) be used to generate families of σ^o versus θ curves (at frequencies of interest) corresponding to various combinations of snow depth and wetness. Such an approach

is not an exact substitute for direct measurements of σ^o; it is felt that the backscatter contribution of the snow layers and the attenuation of the underlying ground contribution by the snow layer may be estimated with acceptable accuracy from previous measurement programs [5-7] to provide approximate, but useful, estimates of σ^o for snow-covered terrain types of interest.

REFERENCES

[1] Wilson, E. A., D. R. Brunfeldt, F. T. Ulaby and J. C. Holtzman, "Circularly Polarized Measurements of Radar Backscatter from Terrain," RSL Technical Report 393-1, University of Kansas Center for Research, Inc., Lawrence, Kansas, February 1980.

[2] Stiles, W. H. and F. T. Ulaby, "Microwave Remote Sensing of Snowpacks," RSL Technical Report 340-3, University of Kansas Center for Research, Inc., Lawrence, Kansas, October 1979.

[3] Leaf, C. F., "Free Water Content of Snowpack in Subalpine Areas," Proc. of the Western Snow Conference, 1966.

[4] Stiles, W. H. and F. T. Ulaby, "Backscatter Response of Roads and Roadside Surfaces," RSL Technical Report 377-1, University of Kansas Center for Research, Inc., Lawrence, Kansas, July 1978.

[5] Ulaby, F. T. and W. H. Stiles, "Backscatter Response of Snow-Covered Roads and Roadside Surfaces," RSL Technical Report 377-2, University of Kansas Center for Research, Inc., Lawrence, Kansas, May 1979.

[6] Stiles, William H. and Fawwaz T. Ulaby, "The Active and Passive Microwave Response to Snow Parameters: 1. Wetness," Journal of Geophysical Research, Vol. 85, No. C2, pp. 1037-1044, February 20, 1980.

[7] Ulaby, Fawwaz T. and William H. Stiles, "The Active and Passive Microwave Response to Snow Parameters: 2. Water Equivalent of Dry Snow," Journal of Geophysical Research, Vol. 80, No. C2, pp. 1045-1049, February 20, 1980.

[8] Onstott, Robert G., G. J. Dome, C. V. Delker, J. E. Patel and R. K. Moore, "Radar Backscatter Study of Sea Ice," RSL Technical Report 331-14, University of Kansas Center for Research, Inc., Lawrence, Kansas, December 1979.

APPENDIX A

RADAR BACKSCATTER COEFFICIENT σ^{o} DATA

BACKSCATTER COEFFICIENT σ^{o}(dB)

TARGET: Snow ≥ 6 Inch on Grass
DATE: 2/14/80
TIME: 1245-1535
SITE: No. 1

FREQ.	POL.	0°	10°	20°	30°	40°	50°	60°	70°	80°
8.6 GHz	RR	0.63	- 5.45	-11.35	-13.59	-16.25	-16.19	-19.01	-19.7	-21.04
	RL	7.46	2.58	- 6.15	- 8.37	-11.06	-13.27	-15.05	-16.63	-18.71
	LL	1.51	- 3.86	-10.13	-12.25	-14.93	-15.42	-17.77	-18.11	-20.20
10.2 GHz	RR	0.70	- 6.25	-10.88	-12.51	-13.68	-15.62	-17.14	-16.98	-19.49
	RL	6.04	1.39	- 5.75	- 8.24	-11.48	-12.61	-14.78	-15.95	-18.48
	LL	- 0.90	- 6.20	-10.97	-12.58	-14.86	-16.44	-18.8	-18.25	-20.36
11.8 GHz	RR	1.32	- 3.72	- 9.77	-10.61	-13.23	-14.37	-16.14	-16.82	-18.56
	RL	6.49	1.16	- 5.42	- 6.88	-11.19	-11.40	-13.51	-15.03	-17.83
	LL	0.76	- 6.60	-11.45	-11.53	-15.15	-16.39	-17.51	-17.98	-20.08
13.8 GHz	RR	1.31	- 2.20	- 7.20	- 9.97	-10.51	-12.45	-14.68	-14.23	-16.21
	RL	6.61	2.81	- 5.46	- 8.08	- 8.61	-11.14	-12.78	-14.62	-16.76
	LL	0.28	- 4.61	-10.01	-12.12	-13.66	-14.77	-16.4	-16.28	-18.12
16.2 GHz	RR	- 2.08	- 2.75	-10.25	-12.08	-12.20	-14.88	-15.09	-16.34	-18.51
	RL	6.77	4.22	- 3.49	- 5.26	- 5.64	- 9.28	-11.69	-12.79	-16.00
	LL	4.32	1.11	- 4.78	- 6.40	- 6.82	- 8.77	-10.24	-11.44	-13.74
17.0 GHz	RR	- 1.01	- 2.01	- 7.11	- 9.55	-11.09	-12.49	-12.66	-13.82	-15.90
	RL	6.30	3.23	- 2.92	- 5.06	- 8.09	- 8.10	-10.28	-12.30	-15.30
	LL	0.06	- 1.57	- 6.45	- 8.51	- 8.47	-11.17	-12.34	-13.00	-14.98

BACKSCATTER COEFFICIENT σ^{o}(dB)

TARGET: Snow ≥ 6 Inch (wet) on Grass
DATE: 2/16/80
TIME: 1400-1630
SITE: No. 1

FREQ.	POL.	0°	10°	20°	30°	40°	50°	60°	70°	80°
8.6 GHz	RR	5.2	- 7.1		-24.7		-28.5		-33.2	-37.0
	RL	13.3	- 0.2		-17.2		-24.1		-28.8	-32.9
10.2 GHz	RR	2.1	- 6.6		-28.0		-30.6		-34.7	-38.7
	RL	11.1	1.2		-23.8		-26.6		-28.8	-33.8
11.8 GHz	RR	0.8	- 7.3		-29.2		-31.1		-34.5	-38.1
	RL	9.1	1.3		-25.2		-27.1		-28.5	-32.7
13.8 GHz	RR	- 0.4	- 5.2		-27.3		-27.8		-31.0	-35.0
	RL	8.0	- 0.5		-23.6		-23.4		-26.2	-31.1
16.2 GHz	RR	- 3.6	-11.8		-27.5		-29.3		-32.5	-36.0
	RL	7.7	- 1.6		-21.7		-22.1		-25.9	-29.9
17.0 GHz	RR	- 1.9	- 9.6		-26.2		-27.0		-29.8	-34.2
	RL	8.0	- 1.6		-21.2		-22.5		-24.3	-29.3

BACKSCATTER COEFFICIENT σ^{o}(dB)

TARGET: Snow Trace on Grass
DATE: 2/25/80
TIME: 1730-1930
SITE: No. 1

FREQ.	POL.	0°	10°	20°	30°	40°	50°	60°	70°	80°
8.6 GHz	RR	5.1	- 8.19	-10.61	-11.96		-17.69		-20.57	-23.47
	RL	8.6	- 2.29	- 7.81	- 7.24		-15.64		-17.25	-20.72
10.2 GHz	RR	- 1.3	-11.63	-11.80	-15.99		-19.89		-20.13	-24.55
	RL	7.9	- 6.84	- 5.68	- 9.25		-17.29		-18.14	-20.84
11.8 GHz	RR	- 1.5	-11.22	-10.29	-13.90		-18.63		-20.28	-24.70
	RL	5.9	- 4.73	- 6.89	- 9.60		-15.90		-16.25	-20.07
13.8 GHz	RR	1.2	- 8.92	- 9.34	-14.25		-16.66		-17.94	-22.71
	RL	7.3	- 3.21	- 7.28	-10.25		-11.95		-15.20	-20.15
16.2 GHz	RR	- 2.4	-12.18	-11.12	-15.82		-19.26		-19.88	-25.67
	RL	7.4	- 3.31	- 3.53	- 7.82		-15.15		-14.86	-20.08
17.0 GHz	RR	1.5	- 9.04	- 8.70	-12.54		-16.85		-16.38	-21.74
	RL	9.7	- 3.87	- 4.14	- 9.00		-14.41		-14.46	-19.30

BACKSCATTER COEFFICIENT σ^{o}(dB)

TARGET: Snow ≥ 6 Inch on Asphalt
DATE: 2/15/80
TIME: 1315-1600
SITE: No. 2

FREQ.	POL.	0°	10°	20°	30°	40°	50°	60°	70°	80°
8.6 GHz	RR	1.6		-22.5	-28.0		-31.2		-35.9	-42.3
	RL	13.7		-14.3	-15.6		-19.0		-25.6	-25.9
10.2 GHz	RR	7.0		-23.8	-23.2		-26.9		-33.6	-39.6
	RL	16.0		-17.5	-17.5		-20.2		-29.1	-33.7
11.8 GHz	RR	10.1		-24.5	-23.8		-26.4		-32.5	-39.9
	RL	18.7		-20.1	-18.1		-20.5		-27.8	-36.3
13.8 GHz	RR	8.9		-24.0	-26.0		-26.5		-31.1	-37.8
	RL	17.1		-20.1	-21.1		-21.8		-25.5	-34.0
16.2 GHz	RR	7.2		-24.7	--		--		--	--
	RL	18.4		-19.4	-20.2		-19.9		-24.5	--
17.0 GHz	RR	8.2		-24.1	-24.6		-26.1		-30.9	-37.3
	RL	18.8		-19.8	-18.7		-19.6		-25.0	-31.0

BACKSCATTER COEFFICIENT σ^{o}(dB)

TARGET: Snow: 6-Inch on Asphalt
DATE: 2/22/80
TIME: 0945-1400
SITE: No. 2

FREQ.	POL.	0°	10°	20°	30°	40°	50°	60°	70°	80°
8.6 GHz	RR	12.89	- 7.65	-11.36	-12.74	-13.38	-15.67	-17.29	-23.87	-26.05
	RL	17.95	- 3.11	- 6.94	- 8.85	-10.07	-12.88	-15.31	-21.83	-22.71
10.2 GHz	RR	10.85	- 8.94	-13.59	-14.51	-14.32	-18.14	-20.44	-24.48	-28.40
	RL	19.48	- 1.39	- 9.21	-10.60	-10.91	-14.95	-15.75	-21.04	-24.89
11.8 GHz	RR	10.6	- 9.78	-12.74	-14.91	-15.08	-18.64	-21.25	-24.38	-30.11
	RL	20.95	- 4.31	- 6.54	- 9.83	-12.09	-15.10	-17.4	-21.96	-26.89
13.8 GHz	RR	12.56	- 6.46	- 7.92	- 8.85	-11.65	-17.54	-19.02	-23.00	-28.91
	RL	21.67	- 0.21	- 4.69	- 6.14	- 9.77	-14.69	-16.21	-21.39	-27.62
16.2 GHz	RR	10.56	- 7.76	-10.8	-12.75	-15.45	-19.01	-22.31	-26.06	-33.39
	RL	22.76	- 0.84	- 5.16	- 3.96	- 8.71	-14.24	-15.96	-21.57	-27.91
17.0 GHz	RR	12.40	- 6.38	- 9.72	-10.31	-12.47	-18.23	-19.58	-23.60	-30.13
	RL	22.44	- 1.63	- 4.40	- 5.78	- 7.23	-14.65	-17.24	-20.29	-27.00

BACKSCATTER COEFFICIENT σ^{o}(dB)

TARGET: Snow 3-Inch on Asphalt
DATE: 2/21/80
TIME: 1430-1600
SITE: No. 2

FREQ.	POL.	0°	10°	20°	30°	40°	50°	60°	70°	80°
8.6 GHz	RR	1.3		-22.4			--			
	RL	10.3		-15.3			--			
10.2 GHz	RR	- 4.2		-22.1			-25.8			
	RL	--		-17.5			-23.1			
11.8 GHz	RR	- 3.2		-23.0			-26.0			
	RL	4.5		-18.2			-22.3			
13.8 GHz	RR	-11.3		-24.4			-26.6			
	RL	- 7.9		-21.9			-23.3			
16.2 GHz	RR	--		--			--			
	RL	--		-18.6			--			
17.0 GHz	RR	--		--			-24.9			
	RL	--		-19.2			-21.6			

AD-A092 077 KANSAS UNIV/CENTER FOR RESEARCH INC LAWRENCE REMOTE --ETC F/G 17/9
CIRCULARLY POLARIZED MEASUREMENTS OF RADAR BACKSCATTER FROM TER--ETC(U)
JUL 80 W H STILES, F T ULABY, E A WILSON DAAK70-78-C-0121
UNCLASSIFIED CRINC/RSL-TR-393-2 ETL-0234 NL

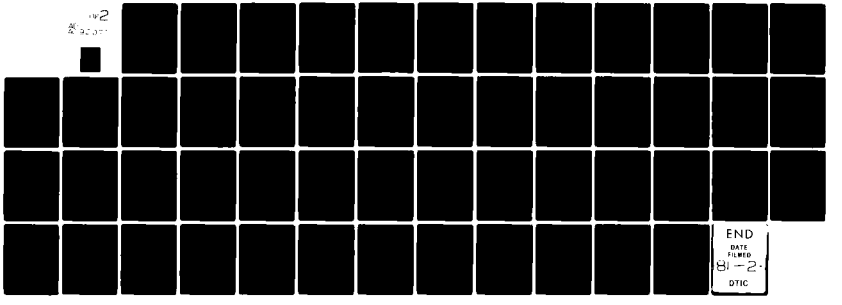

END
DATE FILMED
81-2
DTIC

BACKSCATTER COEFFICIENT σ^{o}(dB)

TARGET: Snow Trace on Asphalt
DATE: 2/17/80
TIME: 1010-1340
SITE: No. 3

FREQ.	POL.	0°	10°	20°	30°	40°	50°	60°	70°	80°
8.6 GHz	RR	18.62	-17.33	-23.47	-25.25	-25.89	-23.61	-25.49	-25.12	-28.24
	RL	21.75	-11.41	-15.03	-16.38	-18.46	-18.53	-21.13	-21.30	-25.09
10.2 GHz	RR	14.84	-20.52	-24.20	-26.40	-26.25	-24.15	-25.86	-24.91	-29.3
	RL	18.75	-14.22	-18.33	-19.92	-20.76	-19.28	-21.49	-21.61	-26.66
11.8 GHz	RR	15.63	-20.27	-24.67	-25.10	-26.09	-24.41	-27.26	-25.76	-30.44
	RL	20.99	-15.34	-17.68	-19.82	-22.11	-19.98	-22.6	-23.16	-28.76
13.8 GHz	RR	19.00	-14.74	-19.78	-23.15	-23.15	-20.14	-22.51	-22.65	-27.63
	RL	23.04	- 9.78	-15.63	-18.66	-19.35	-16.93	-18.87	-21.32	-26.20
16.2 GHz	RR	17.70	-18.09	-21.51	-25.20	-25.28	-23.42	-24.34	-26.54	-31.5
	RL	27.78	-11.21	-14.48	-16.62	-18.51	-16.74	-19.53	-21.91	-27.03
17.0 GHz	RR	19.41	-15.29	-19.93	-22.18	-22.74	-21.2	-22.36	-23.94	-29.84
	RL	26.35	- 9.71	-13.16	-16.47	-19.75	-16.93	-18.74	-21.13	-27.33

BACKSCATTER COEFFICIENT σ^{o}(dB)

TARGET: Snow on Ice
DATE: 2/27/80
TIME: 0900-1300
SITE: No. 4

FREQ.	POL.	0°	10°	20°	30°	40°	50°	60°	70°	80°
8.6 GHz	RR		-14.4	-14.9	-13.21	-15.44	-18.03	-20.85	-22.73	-26.91
	RL		-10.4	- 7.6	- 7.53	-10.4	-16.07	-16.29	-18.39	-23.54
10.2 GHz	RR		-15.0	-15.5	-14.76	-16.02	-17.66	-19.81	-22.48	-26.69
	RL		-10.6	-10.2	-10.52	-12.01	-13.97	-15.99	-19.2	-24.35
11.8 GHz	RR		-12.4	-16.4	-15.51	-15.63	-18.13	-19.72	-22.51	-26.65
	RL		- 8.0	-10.8	- 9.57	-11.57	-13.77	-15.42	-18.83	-24.85
13.8 GHz	RR		-13.1	-14.7	-14.39	-13.58	-14.04	-17.03	-20.16	-24.17
	RL		- 7.8	- 9.0	- 9.8	- 9.95	-11.16	-14.5	-17.58	-23.32
16.2 GHz	RR		-13.6	-16.0	-17.10	-17.69	-15.46	-19.08	-23.22	-27.12
	RL		- 8.5	- 8.1	- 9.98	- 9.04	- 9.45	-13.28	-17.76	-23.49
17.0 GHz	RR		-11.9	-14.0	-13.25	-13.43	-13.28	-16.47	-20.8	-24.95
	RL		- 7.6	- 9.2	- 8.67	- 8.22	- 9.81	-13.85	-17.36	-22.97

BACKSCATTER COEFFICIENT σ^{o}(dB)

TARGET: Snowpile and Car on Asphalt
DATE: 2/17/80
TIME: 1400-1600
SITE: No. 3

FREQ.	POL.	Snowpile 0°	Snowpile 10°	Snowpile 30°	Snowpile 70°	Car 0°	Car 10°	Car 30°	Car 70°
8.6 GHz	RR	3.6	-12.5	-13.7	- 9.0	--	- 2.6	- 1.8	- 9.8
	RL	7.8	- 3.9	- 6.4	- 7.1	8.8	13.0	- 3.7	- 5.7
10.2 GHz	RR	-2.2	- 8.7	-15.3	-11.4	--	3.4	3.9	- 9.7
	RL	1.3	- 6.0	- 8.6	- 9.2	5.8	12.7	1.9	- 8.4
11.8 GHz	RR	2.6	-12.8	-14.3	-13.2	--	5.7	- 1.2	- 9.7
	RL	-2.0	- 6.0	-14.4	-12.1	5.0	13.7	1.0	- 7.5
13.8 GHz	RR	-1.0	-10.2	-16.1	-15.7	--	8.3	- 0.9	- 9.7
	RL	0.0	- 6.0	-12.9	-13.7	3.0	13.6	0.7	- 7.6
16.2 GHz	RR	-0.3	-13.2	-19.7	-19.8	--	4.3	- 4.2	-14.6
	RL	-0.2	-11.7	-15.5	-13.4	2.8	13.4	1.7	-10.7
17.0 GHz	RR	-3.6	-11.2	-13.6	-20.1	--	7.6	- 1.6	-20.3
	RL	0.4	- 2.7	-13.9	-15.1	1.4.	11.3	5.0	-12.8

APPENDIX B

RADAR SNOWPILE SCAN MEASUREMENTS

The scan measurements were conducted at Test Site #3 (Steamboat Springs High School parking lot). Two scales are given for each scan. The relative values of received power are given along with the calculations of radar cross-section σ. The radar cross-section σ is related to the radar backscatter coefficient by:

$$\sigma = \sigma^{o} A_{ill}$$

where A_{ill} is the illuminated area.

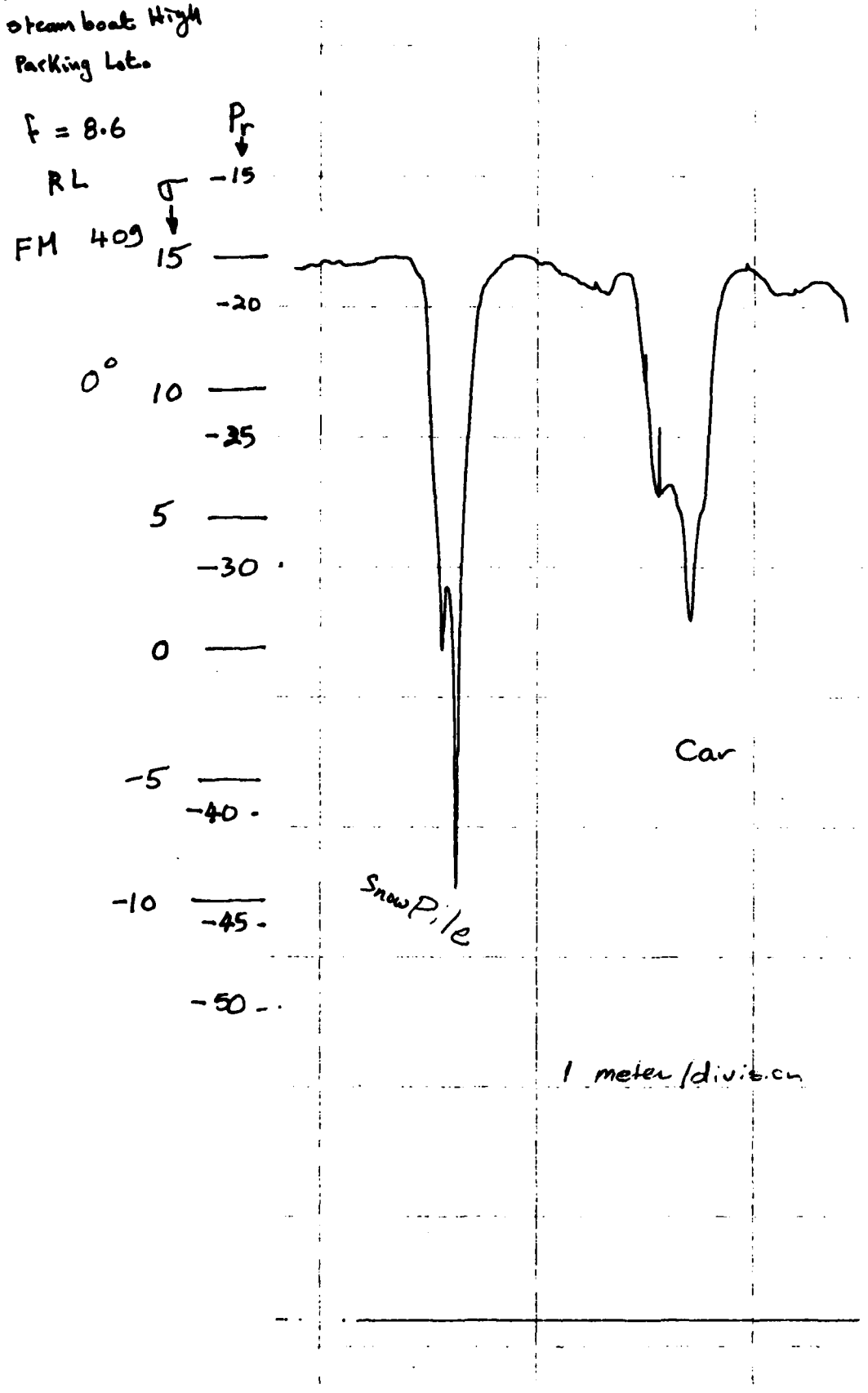
Date : 2/17/80
Steamboat High
Parking Lot
f = 8.6
RL
FM 409
P_r
σ
-15
15
-20
0°
10
-25
5
-30
0
-5
-40
-10
-45
-50
Snow Pile
Car
1 meter/division

Date: 2/17/80

Steamboat High Parking Lot.

F = 8.6

RR

FM = 409

0°

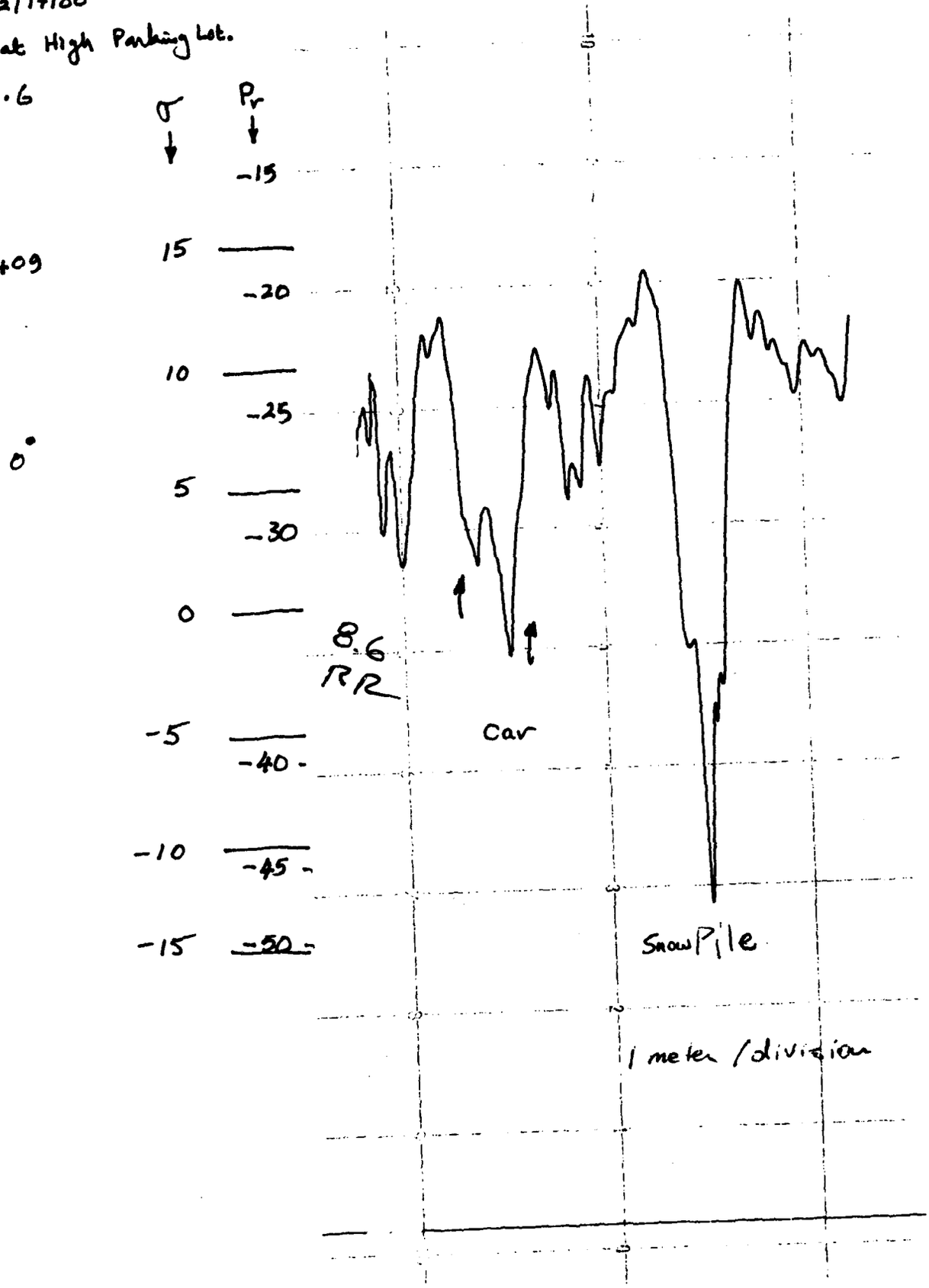

Date: 2/17/80

Steamboat High Parking Lot

$f = 10.2$

RL

FM = 409

0°

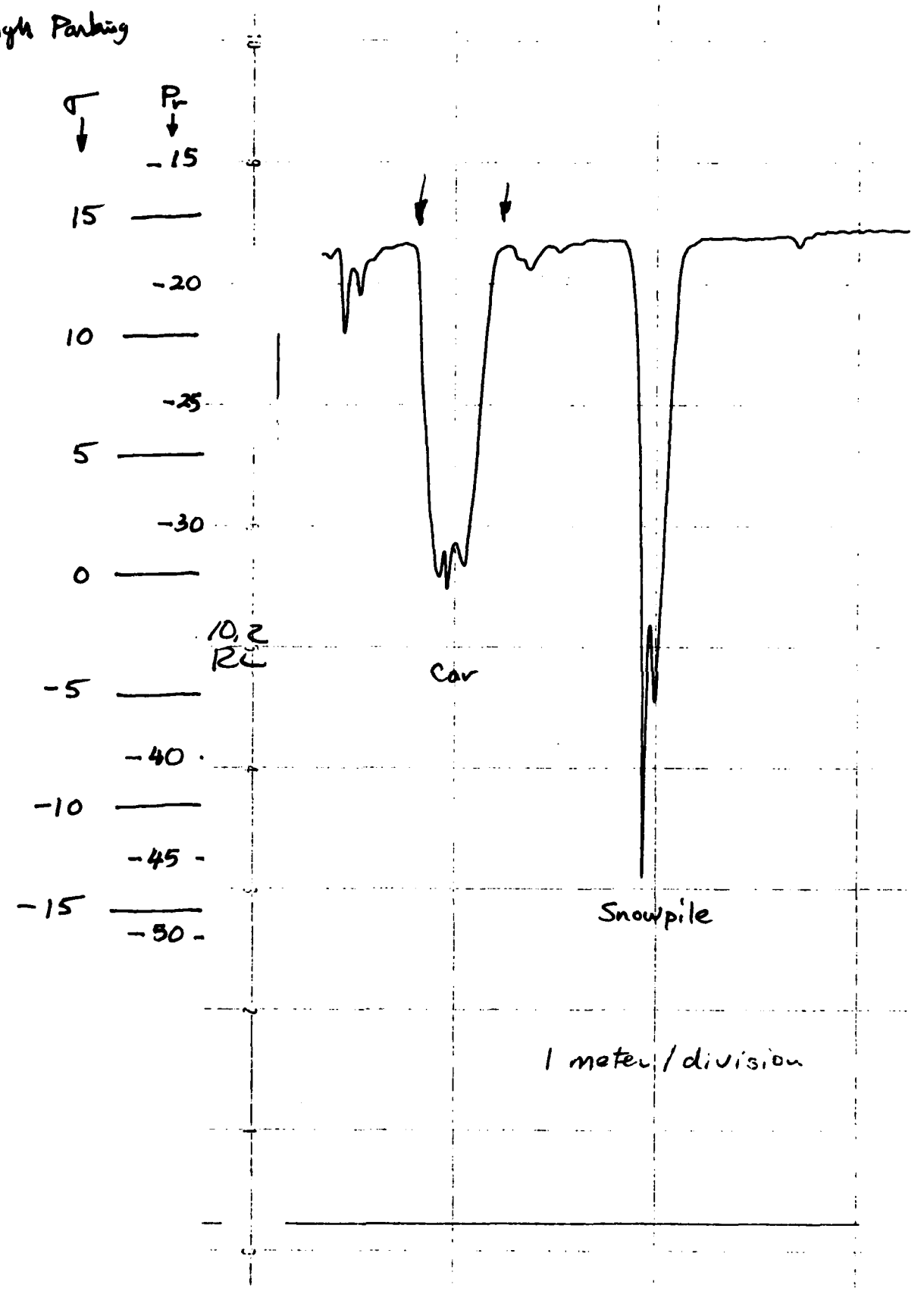

Date : 2/17/80

Steamboat Hight Parking Lot

$f = 10.2$

R R

FM = 409

0°

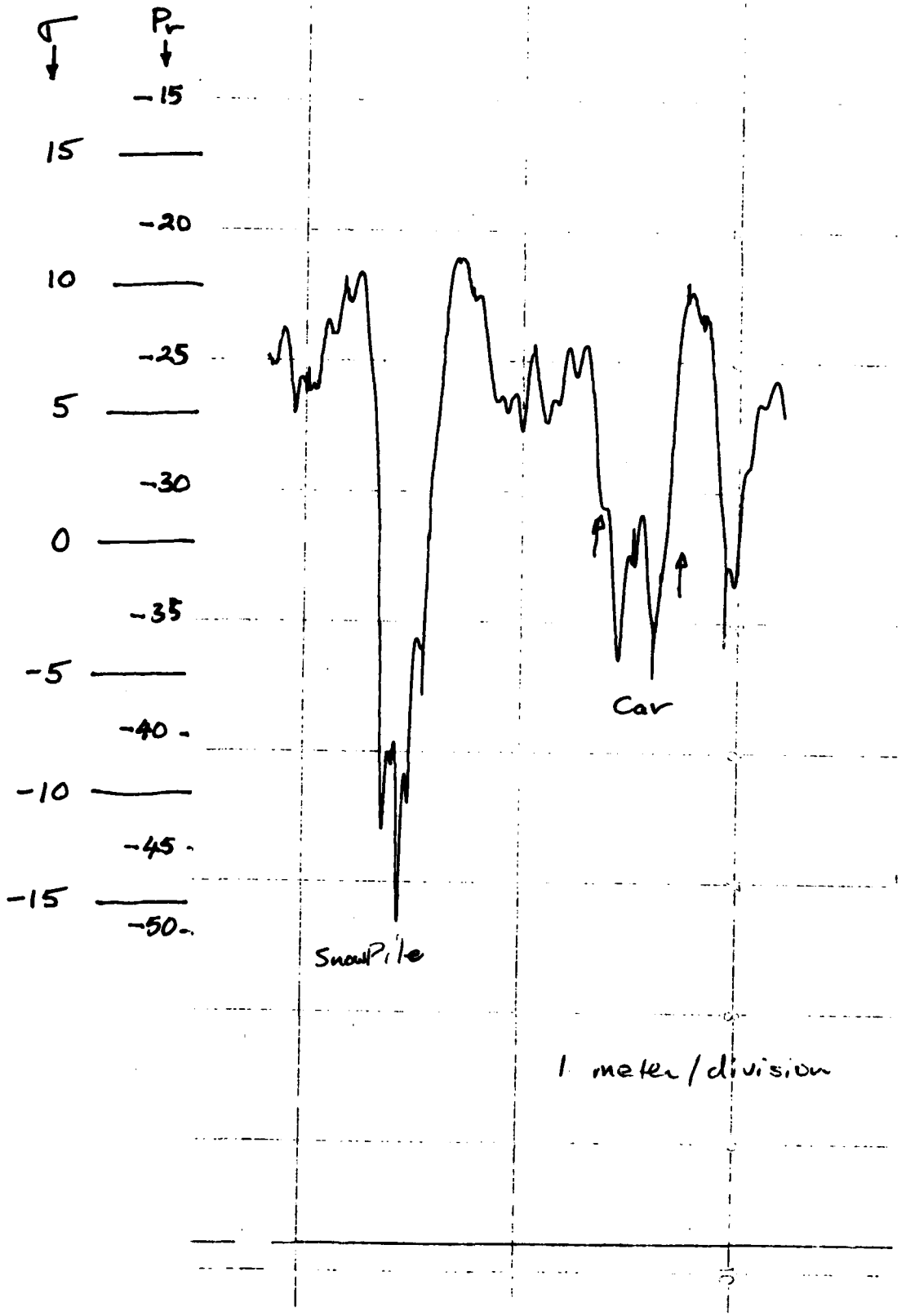

Date: 2/17/80

Steam boat High Parking Lot

F = 11.8

RL

FM = 409

0°

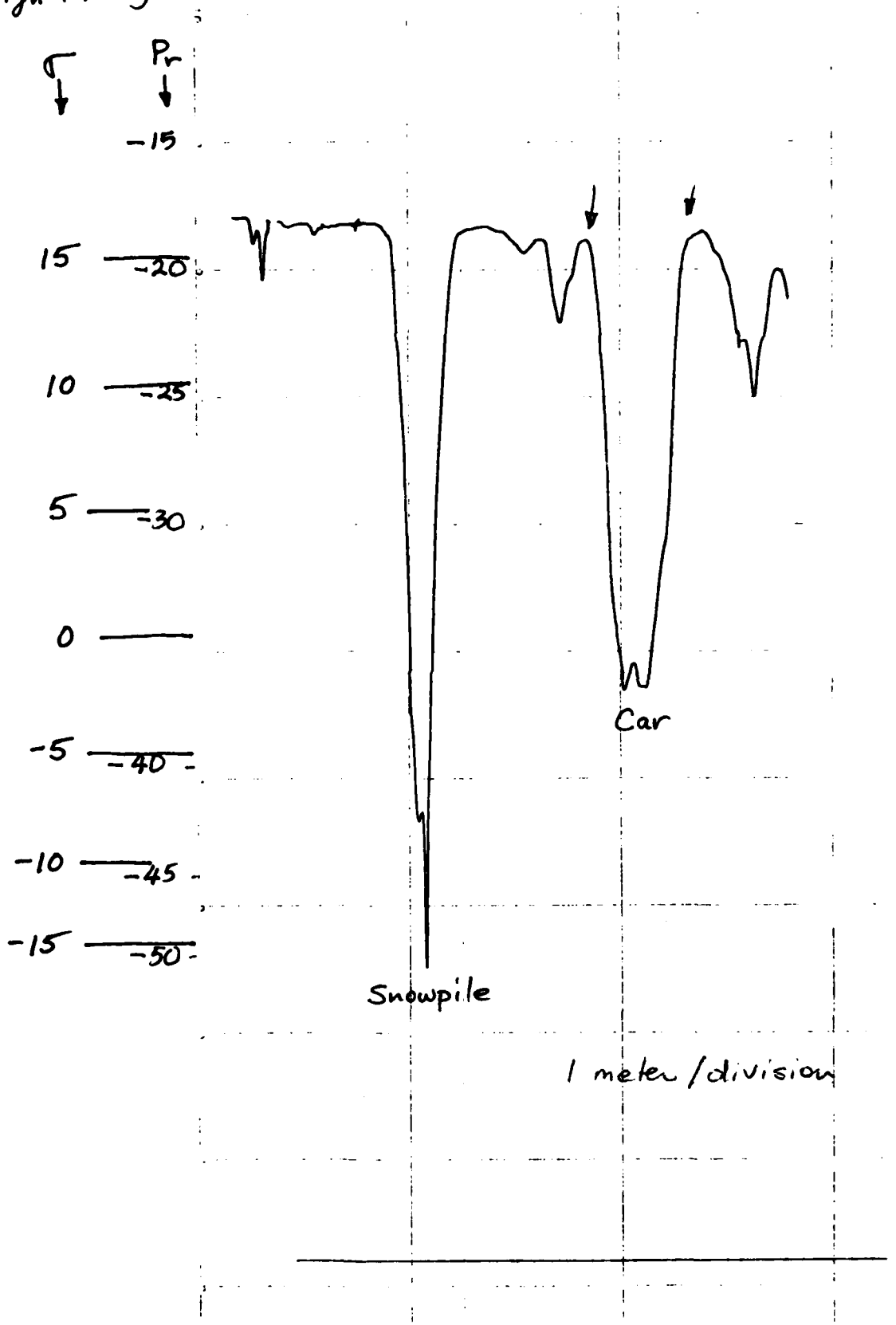

Date : 2/17/80
Steamboat High Parking Lot

F = 11.8

RR

FM = 409

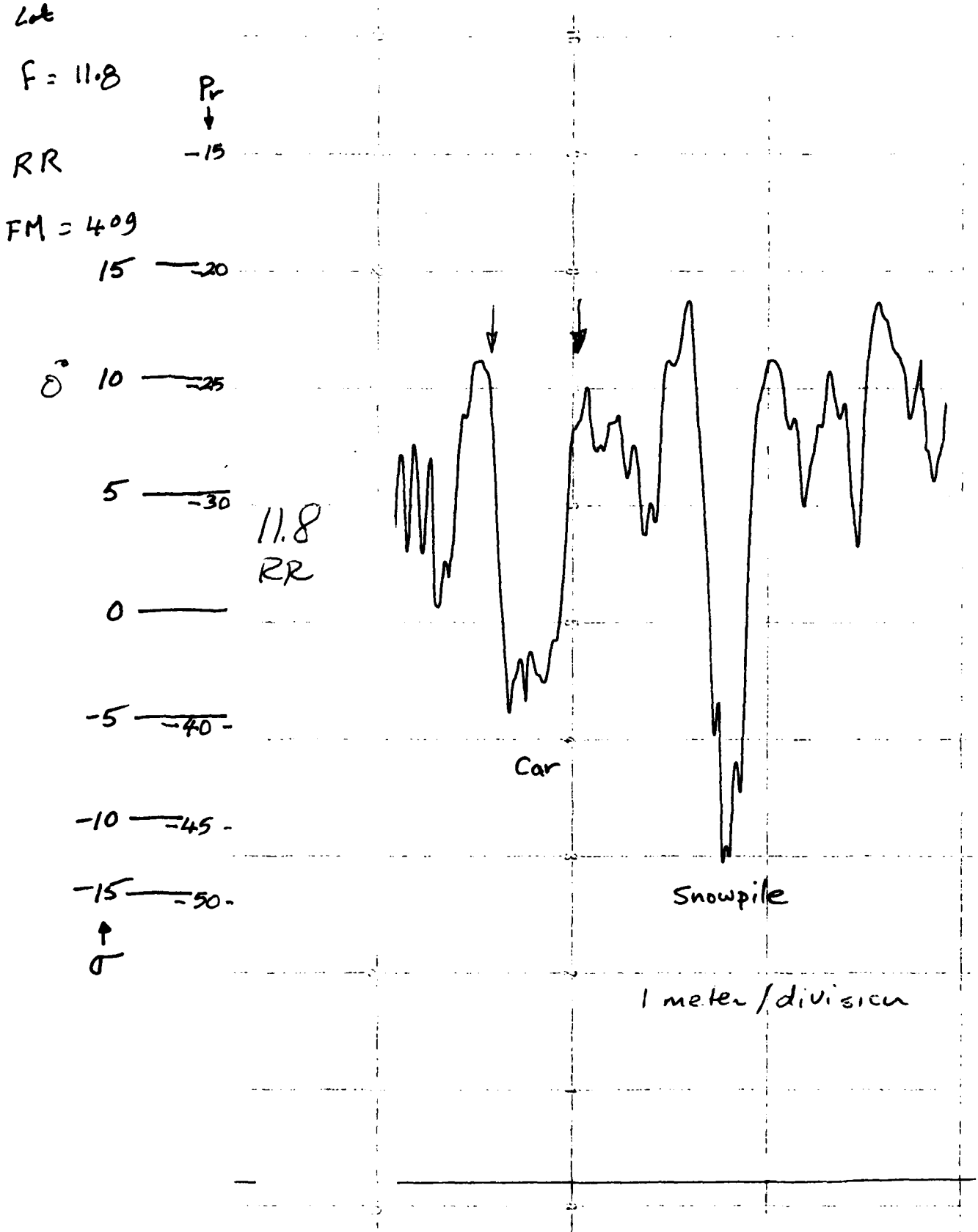

Date: 2/17/80
Stream bank High Parking Lot

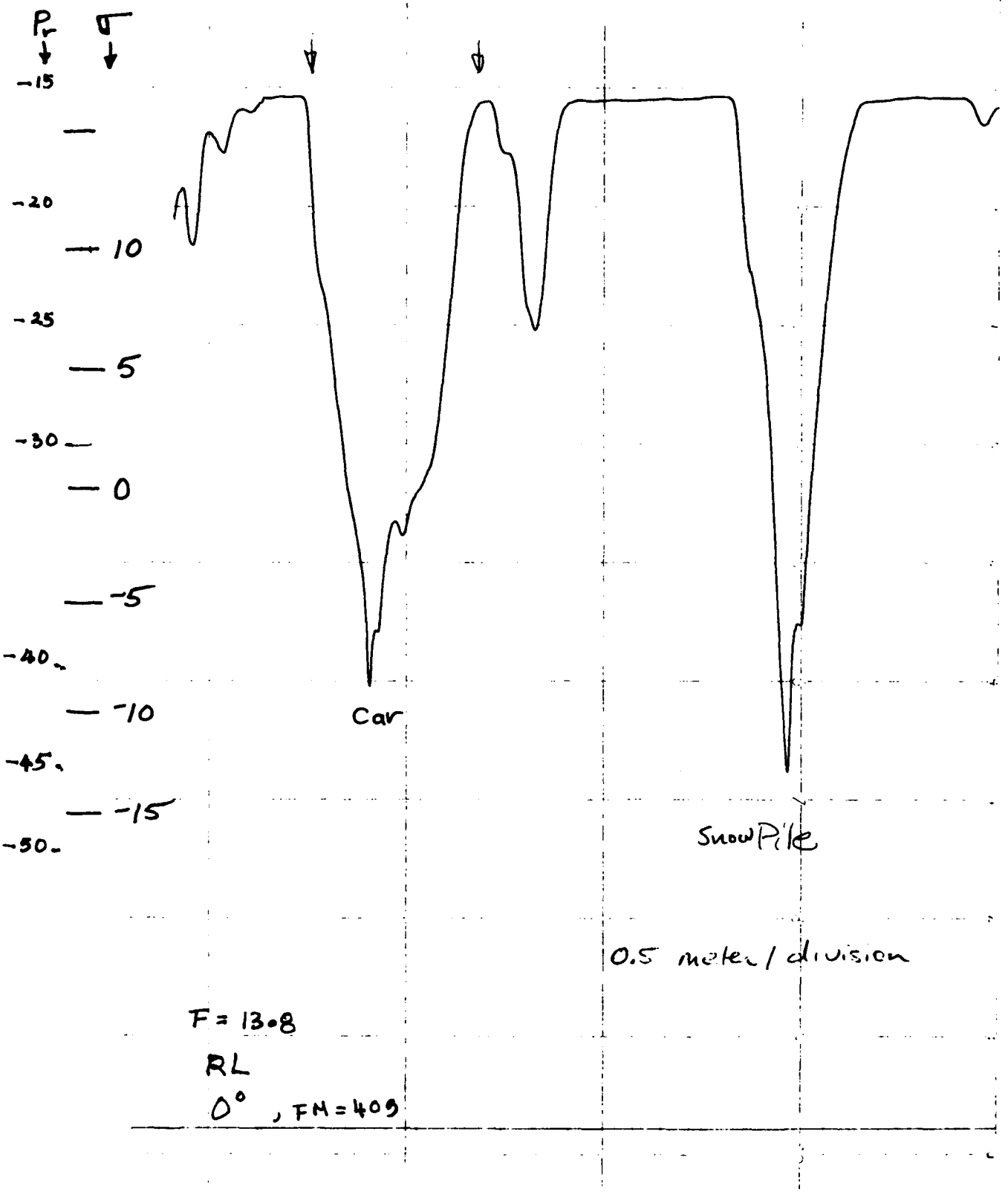

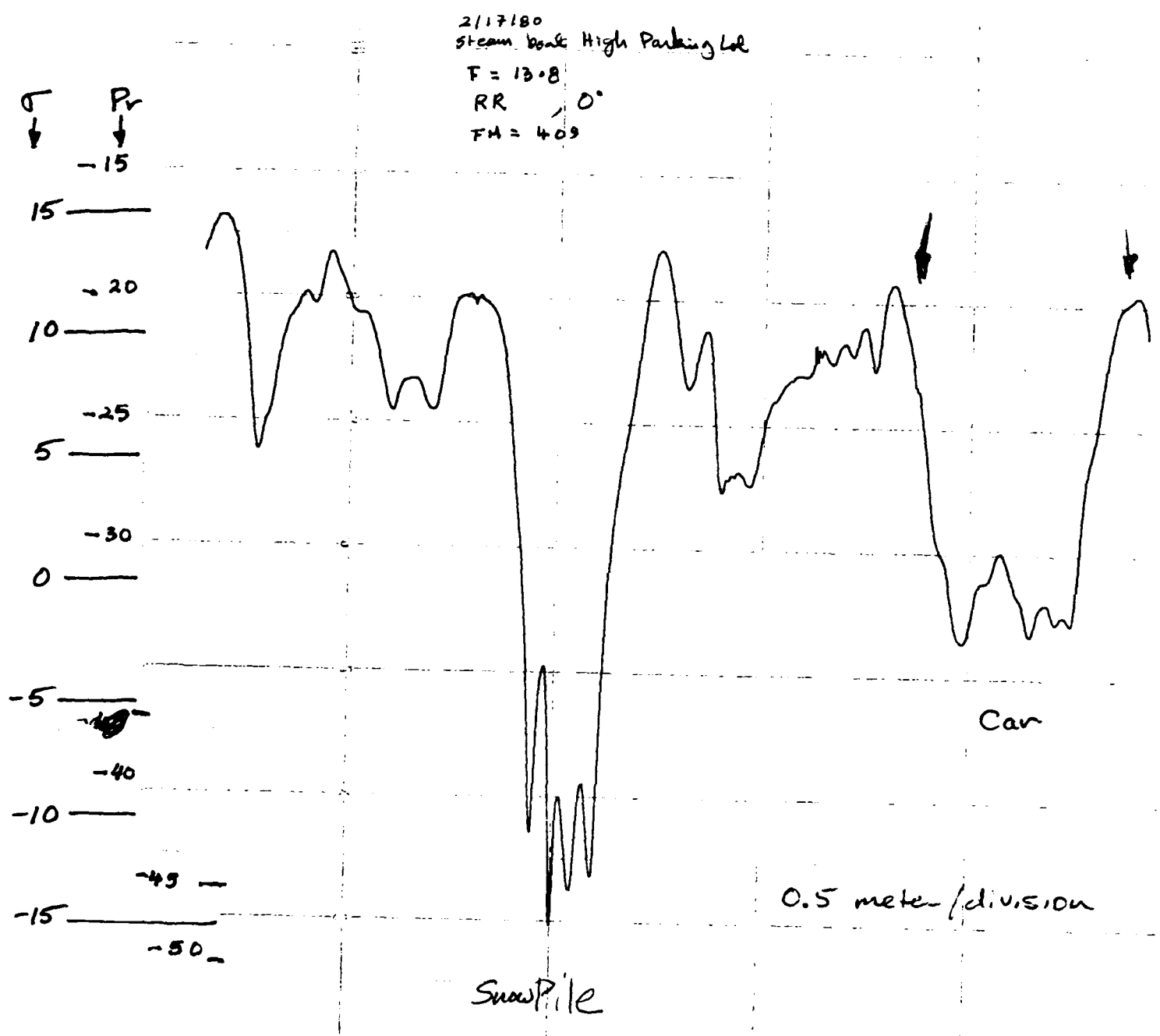
2/17/80
Steam Boat High Parking Lot
F = 13.8
RR 0°
FH = 409
T
Pr
-15
15
-20
10
-25
5
-30
0
-5
-40
-10
-45
-15
-50
Car
0.5 meter/division
Snow Pile

Date 6 2/17/80
Steamboat High Parking Lot

F = 16.2

RL ,0°

FM = 409

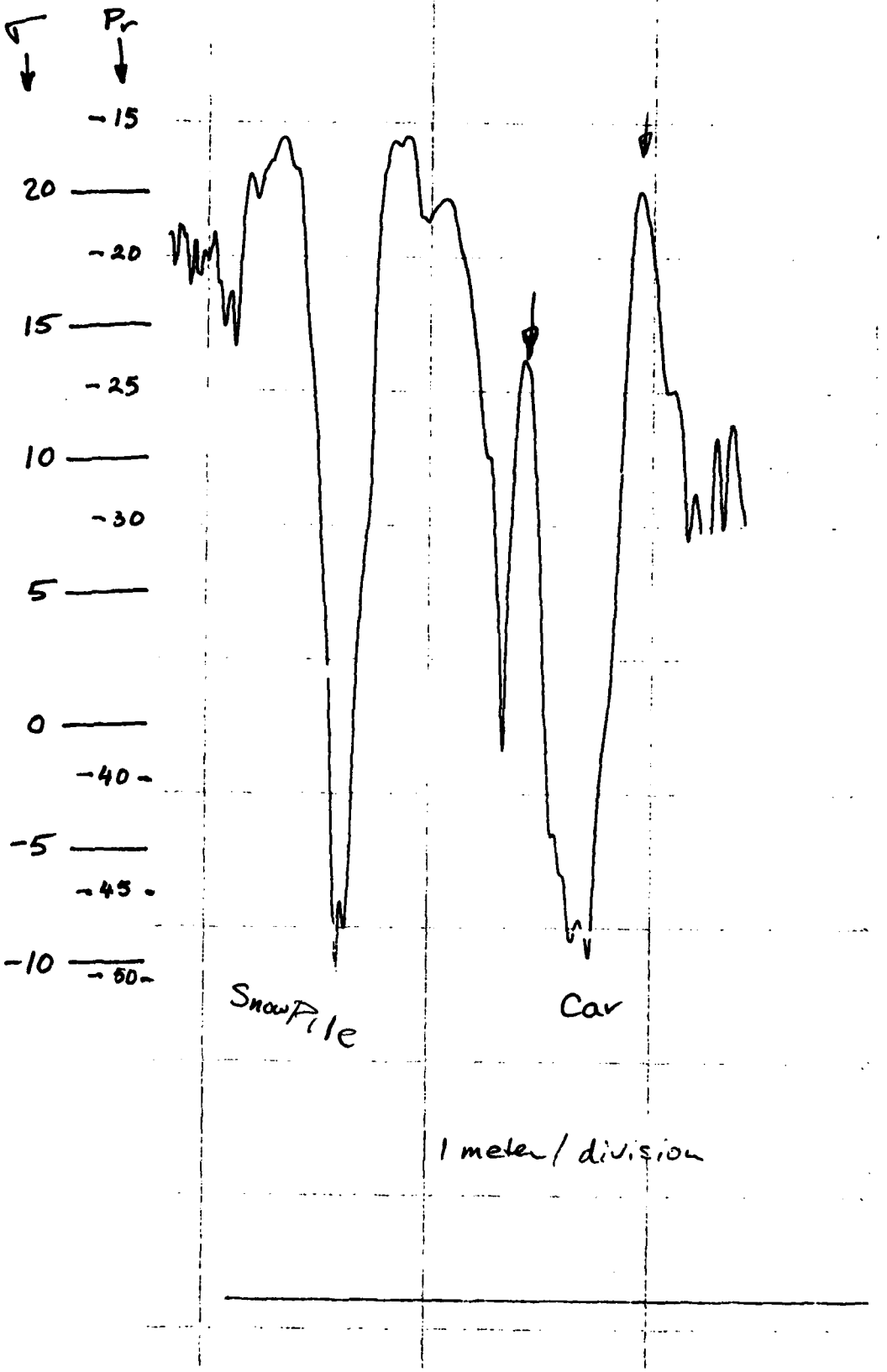

Date: 2/17/80
Steamboat High Parking Lot

F = 16.2

RR , 0°

FM=409

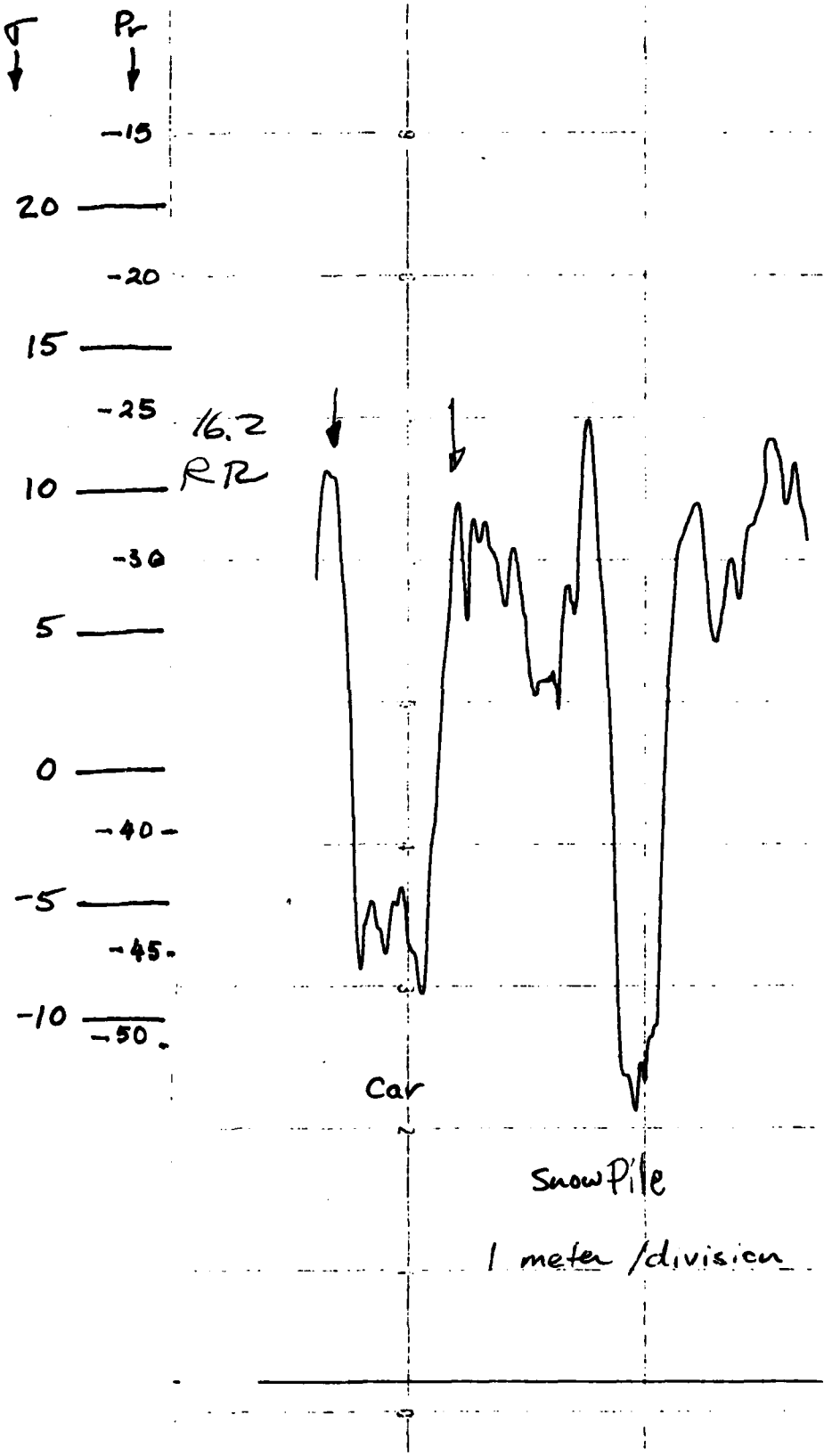

Date: 2/17/80
Steamboat High Parking Lot

F = 17.0

RL , 0°

FM=409

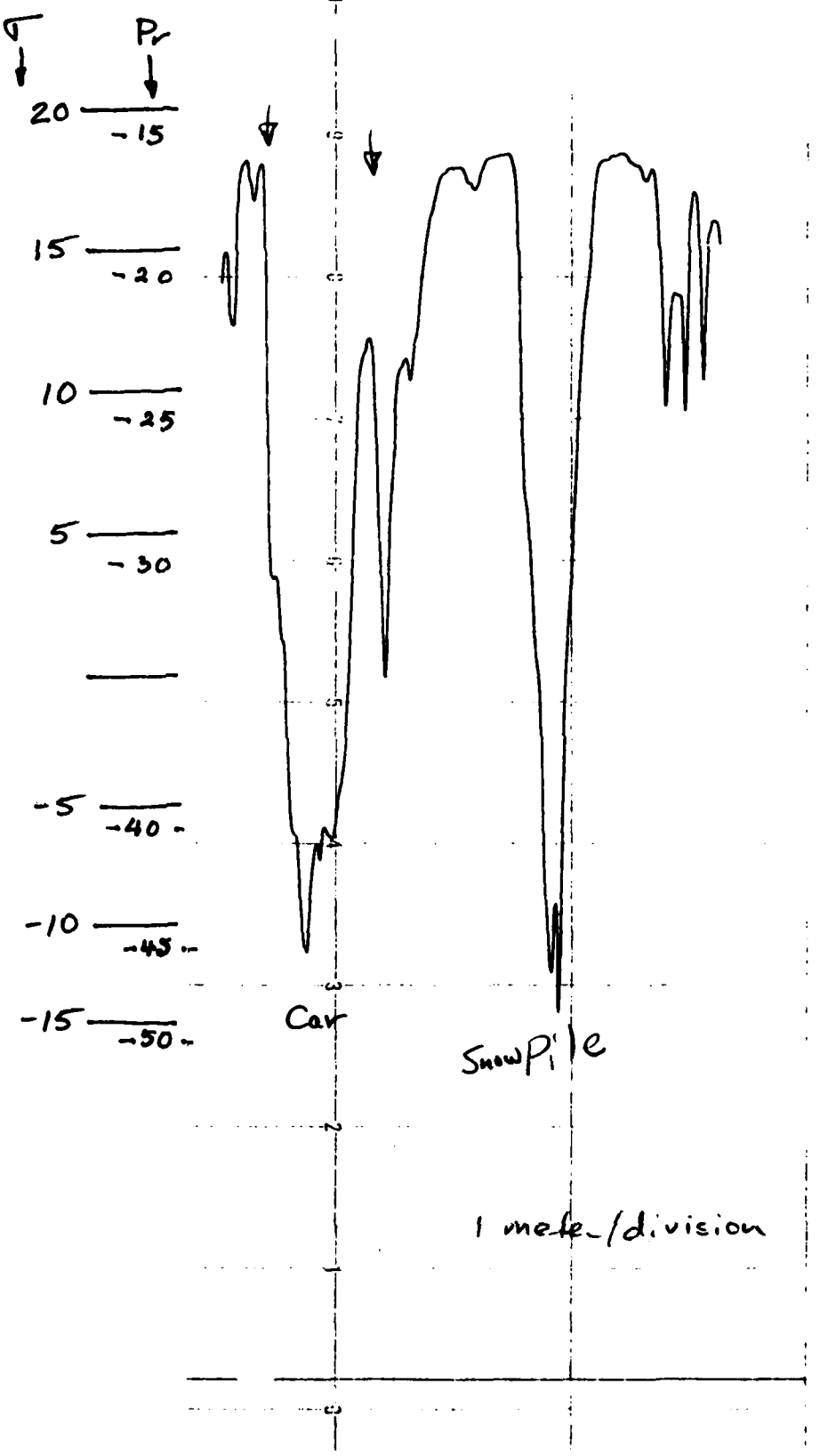

Date: 2/17/90
Steam boat High Parking Lot

F = 17.0

RR , 0°

FM = 409

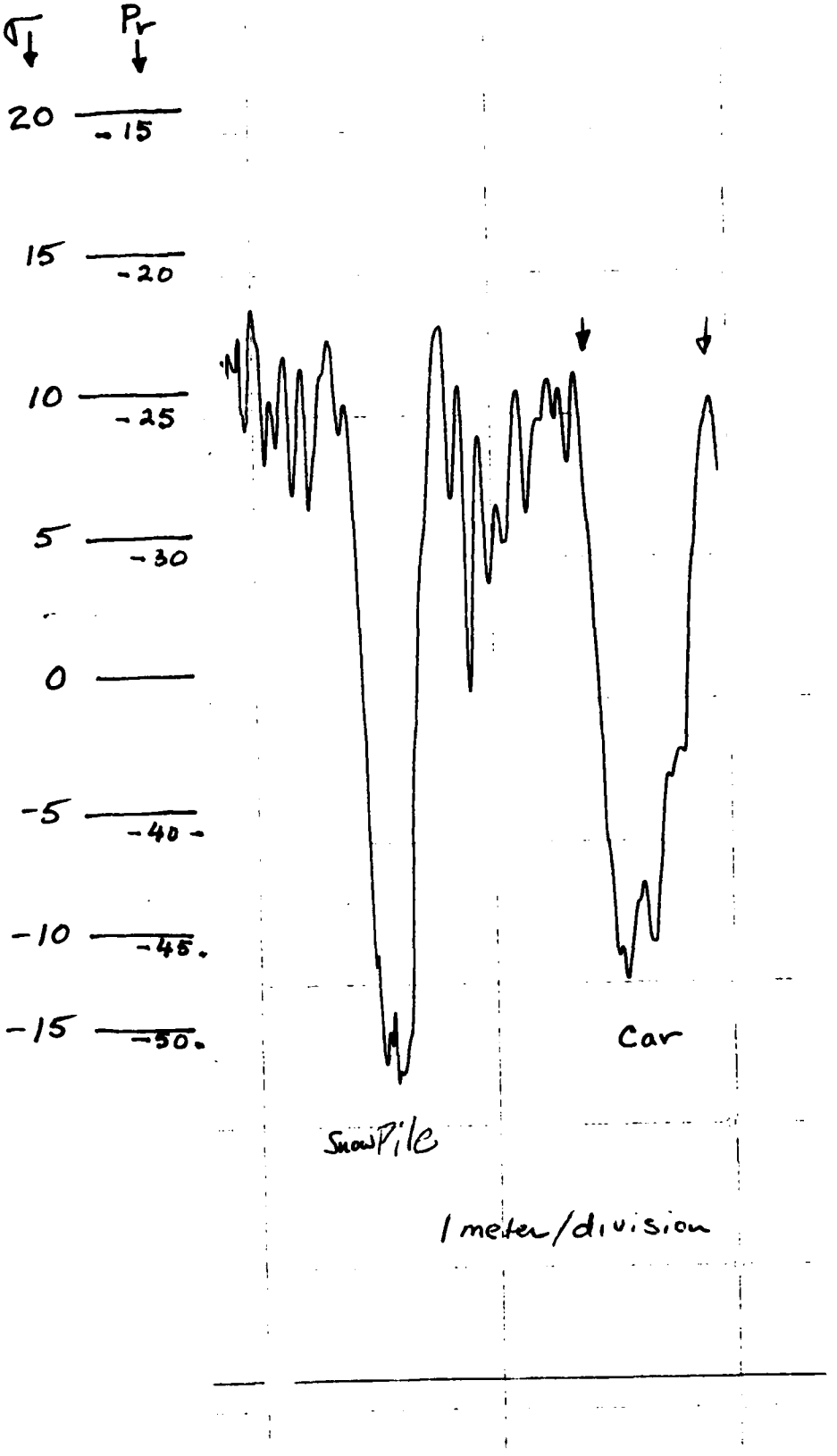

Date 8/17/80
Steamboat High Parking Lot

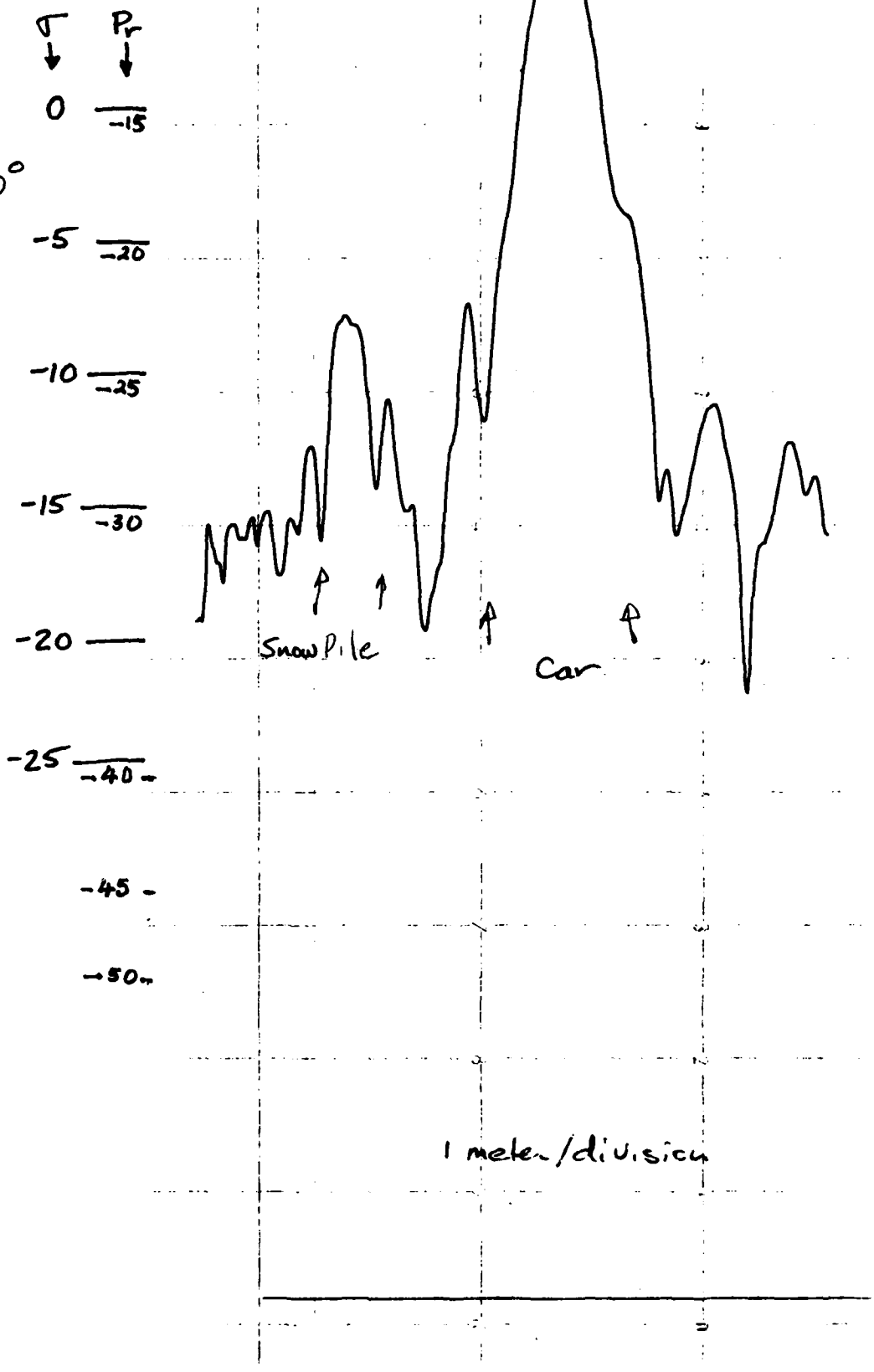

F = 8.6

RL , 10°

FM = 405

Date: 2/17/80
Steamboat High Parking Lot

F = 8.6

RR , 10°

FM = 405

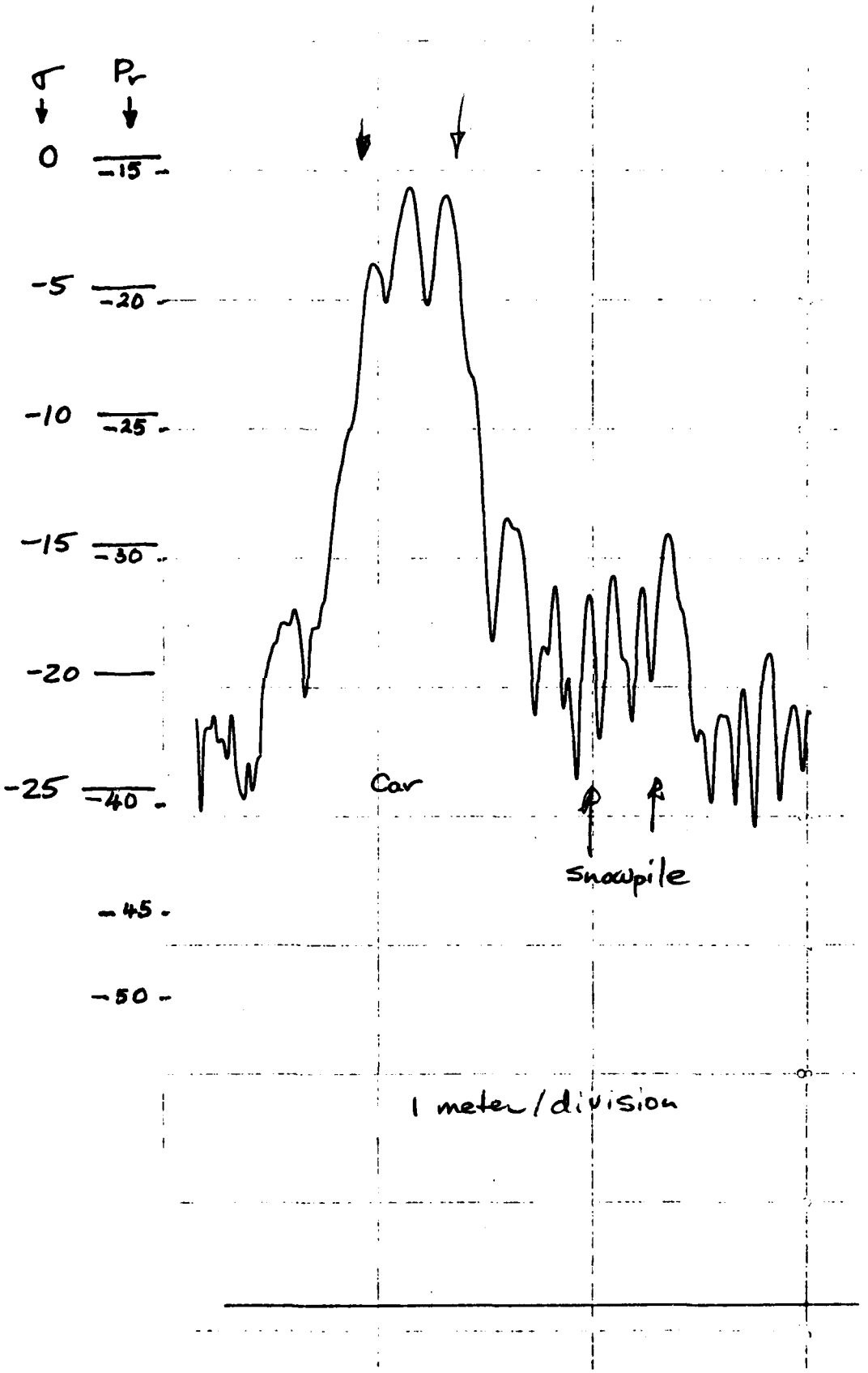

Data: 2/17/80

Steamboat High Parking Lot

F = 10.2

RL , 10°

FM = 405

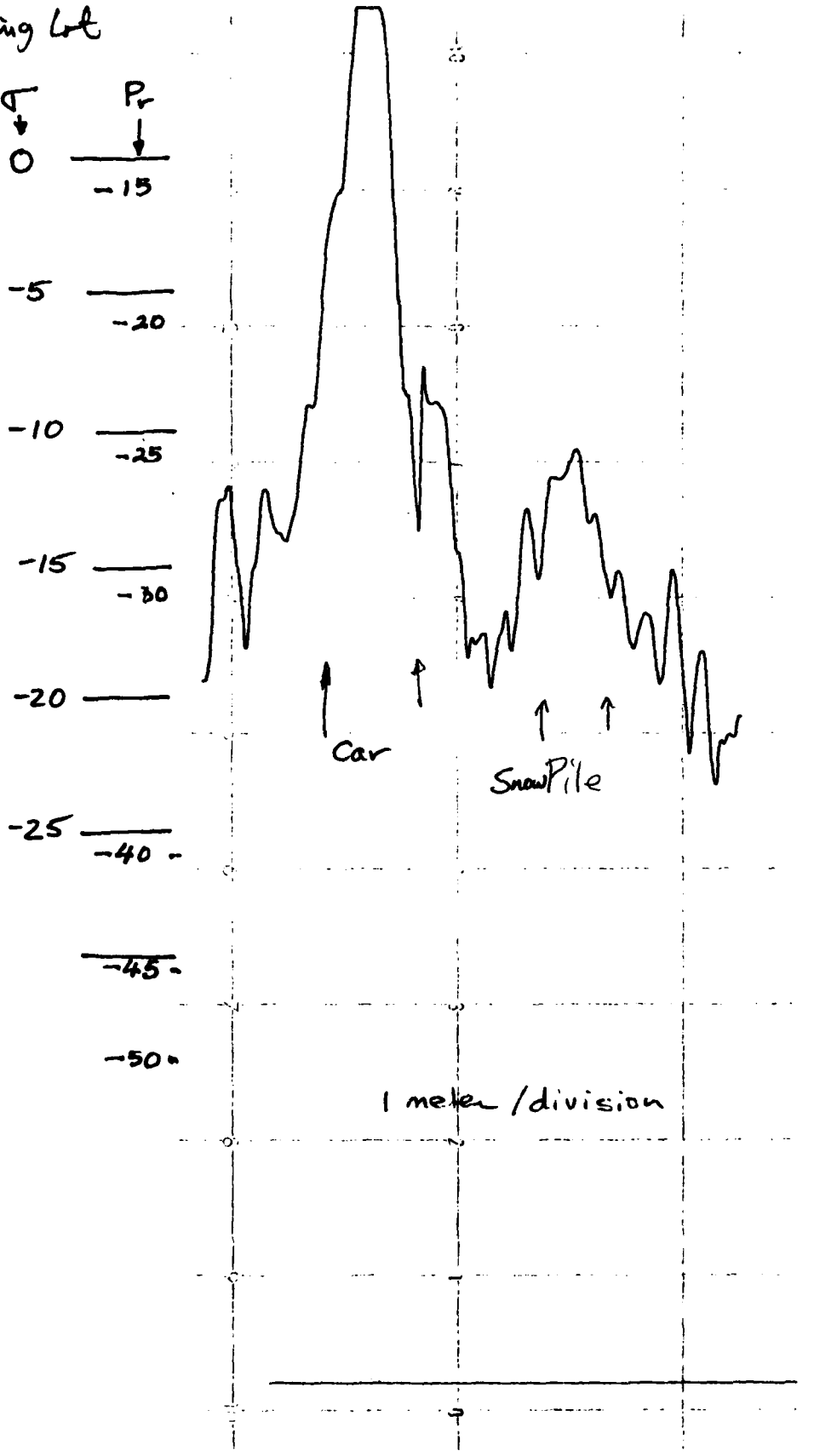

Date: 2/17/80
Steamboat High Parking Lot

F = 10.2

RR , 10°

FM = 405

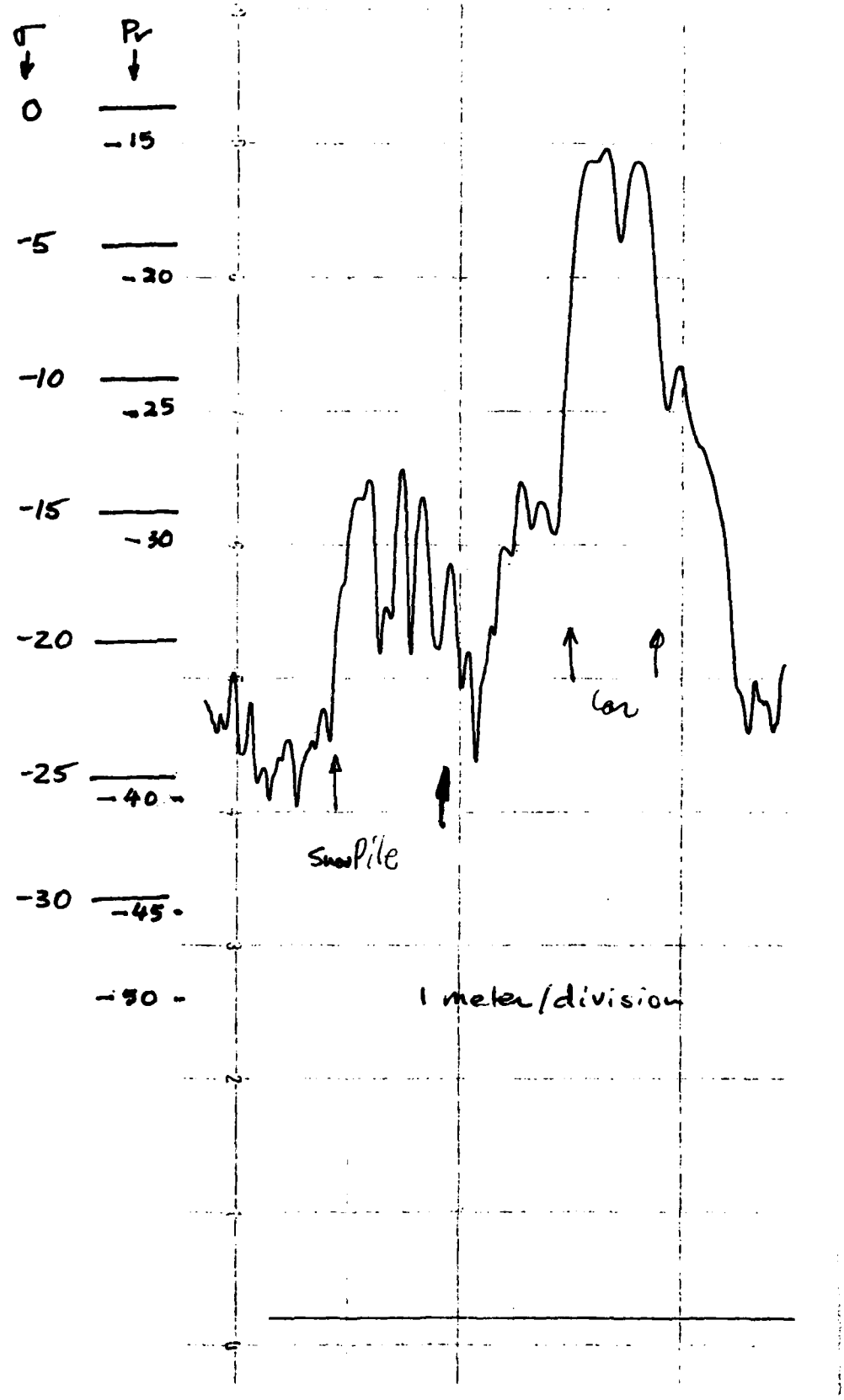

Date: 2/17/80
Steamboat High Parking Lot

F = 11.8

RL

10°

FM = 405

τ	Pr
0	-15
-5	-20
-10	-25
-15	-30
-20	
-25	-40
	-45
-30	
	-50

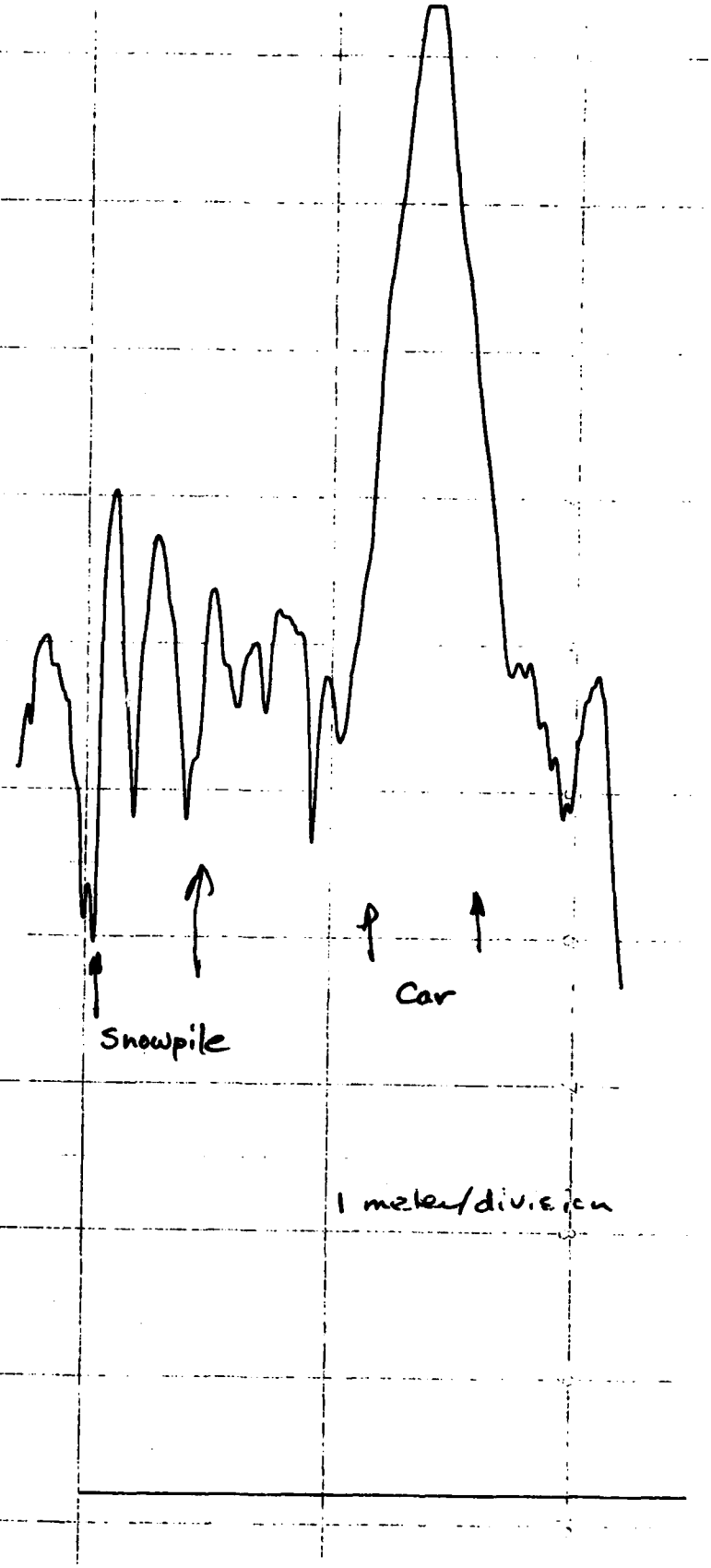

Date: 2/17/80

Steamboat High Parking lot.

F = 11.8

RR, 10°

FM = 405

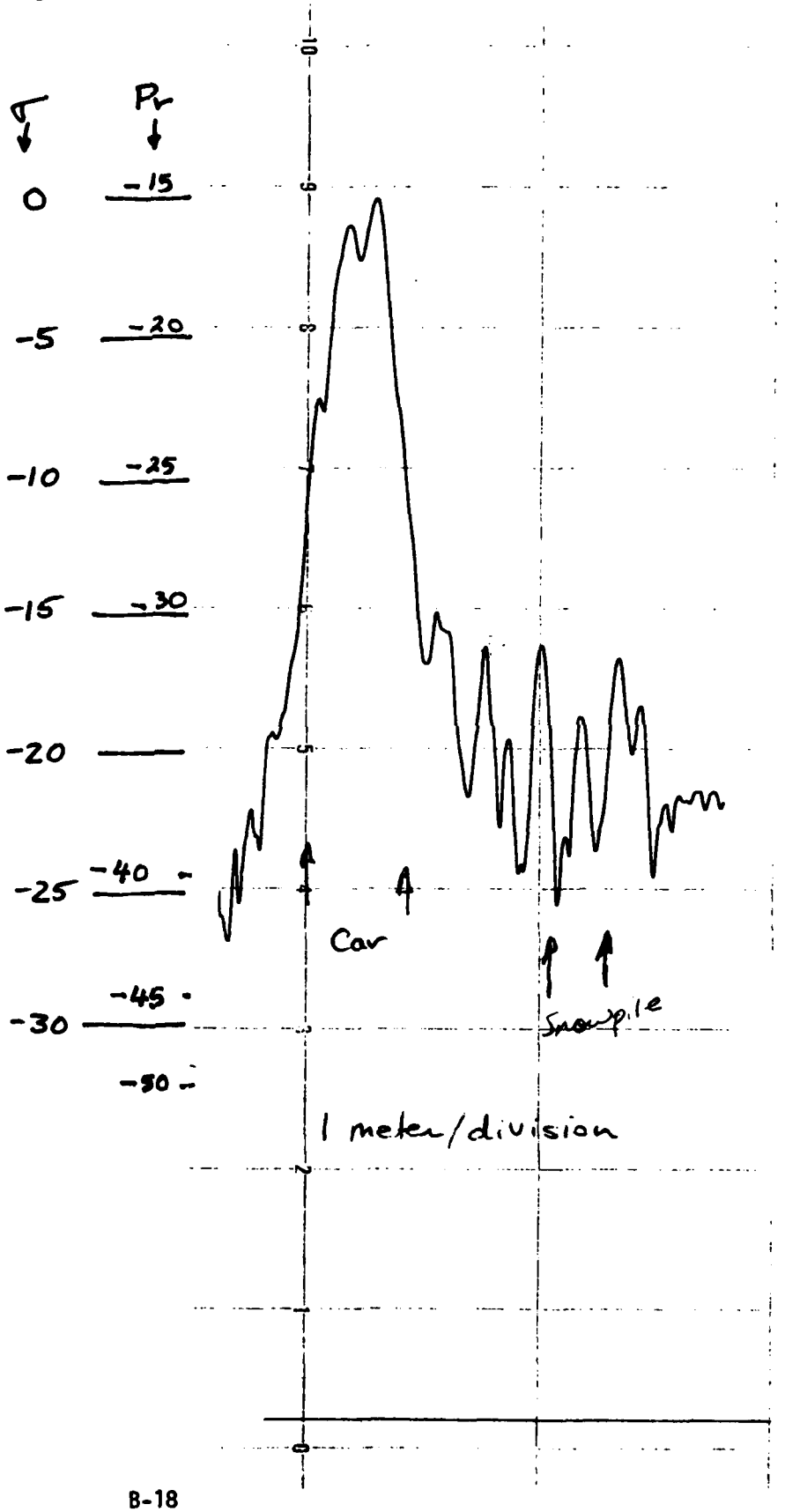

Date: 2/17/80
Steamboat High Parking Lot

F = 13.8

RL , 10°

FH = 405

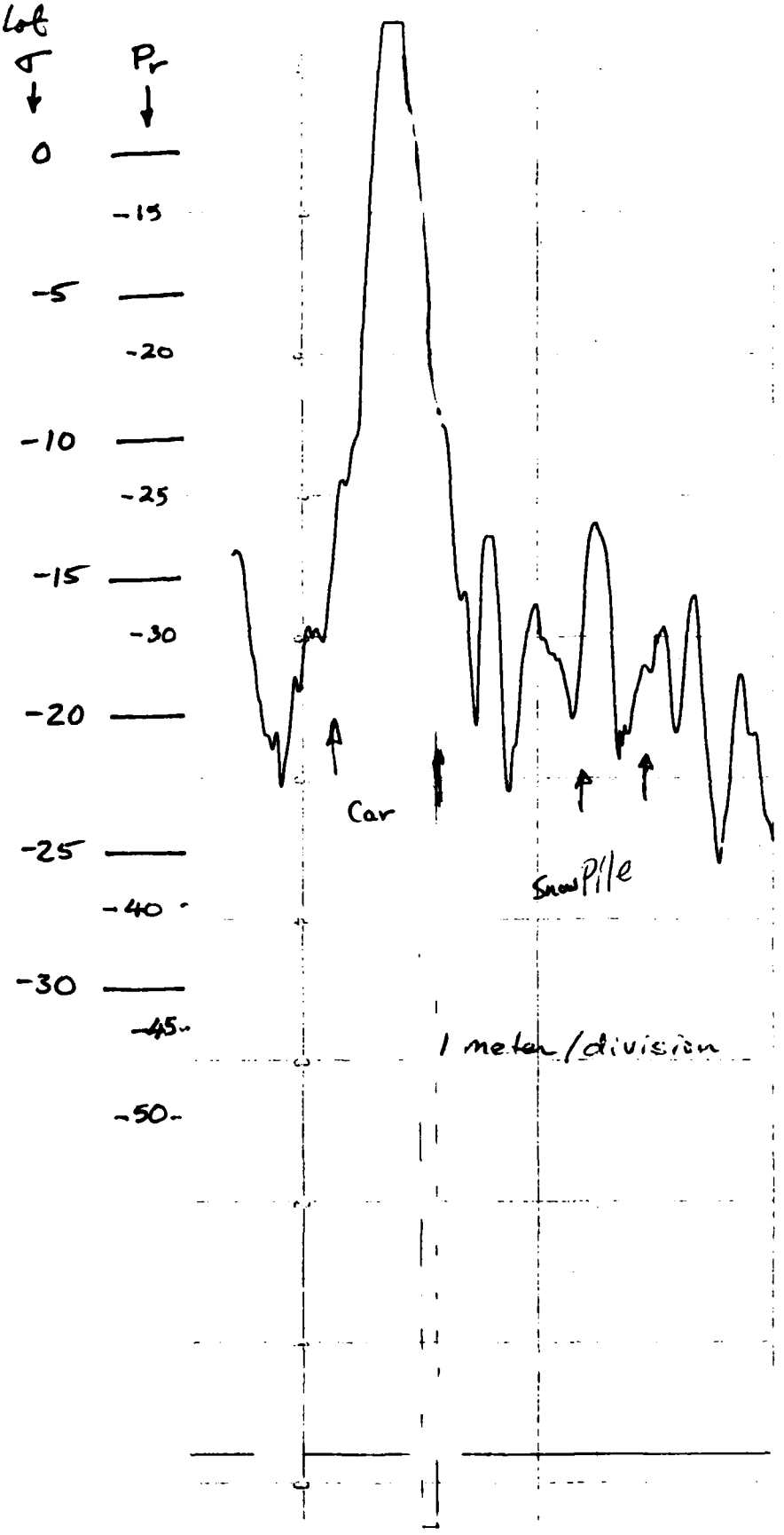

Date 2/17/80
Steamboat Alps Parking Lot

F = 13.8

RR , 10°

FH=405

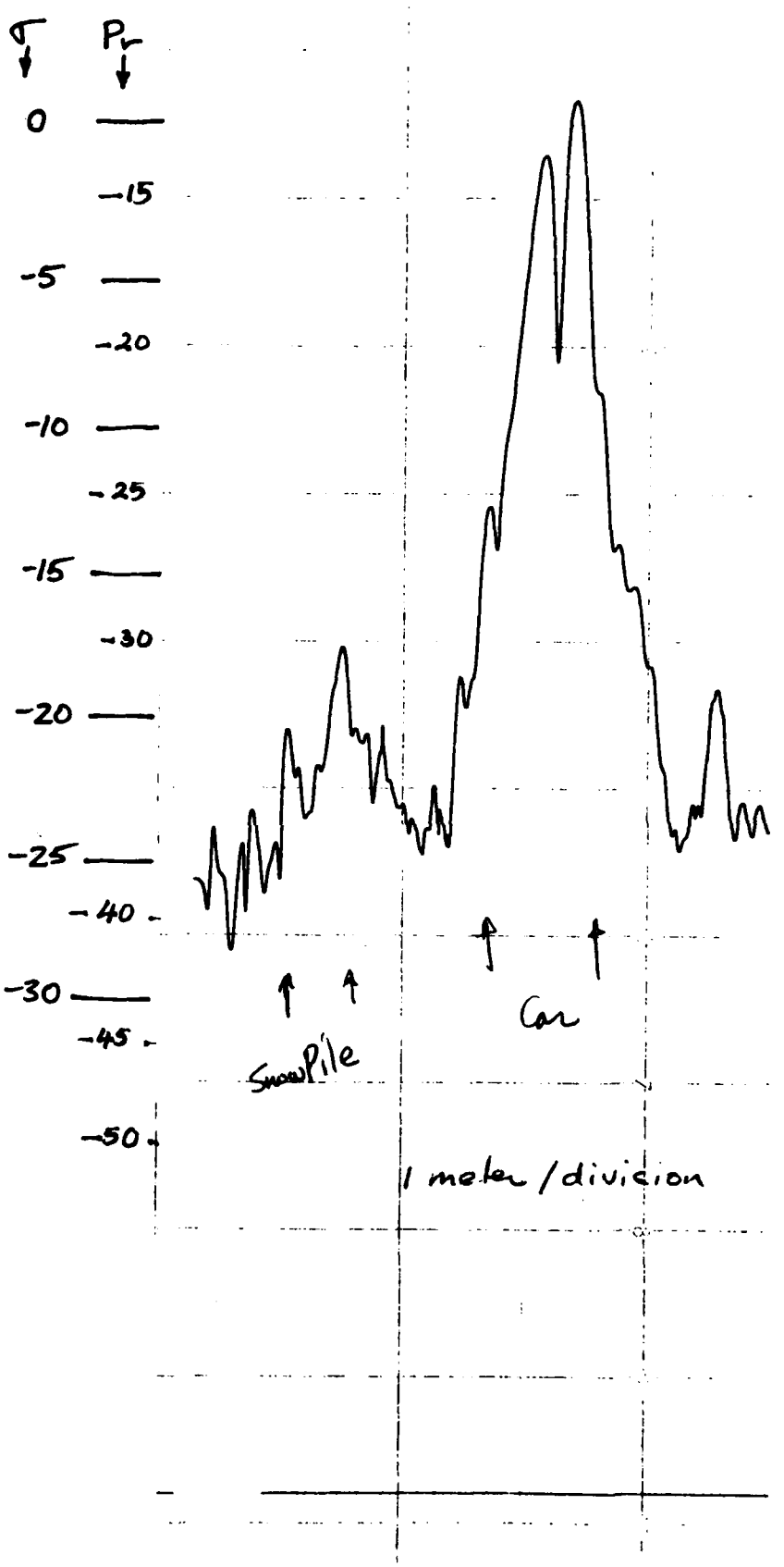

Date: 2/17/80
Steamboat High Parking Lot

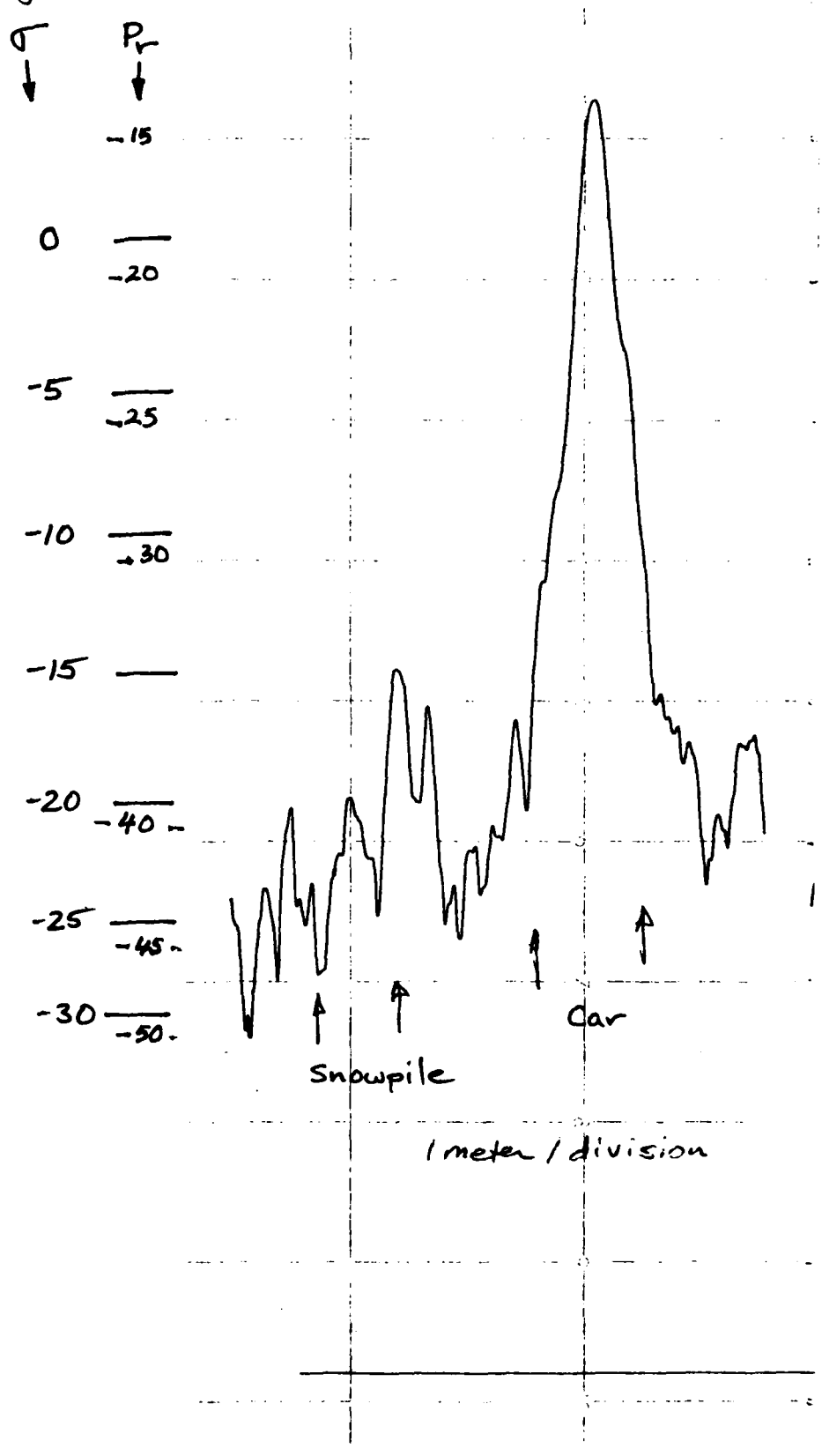

F = 16.2

RL, 10°

FH = 405

Date: 2/17/80
Steamboat High Parking Lot

F = 16.2

RR, 10°

FM = 405

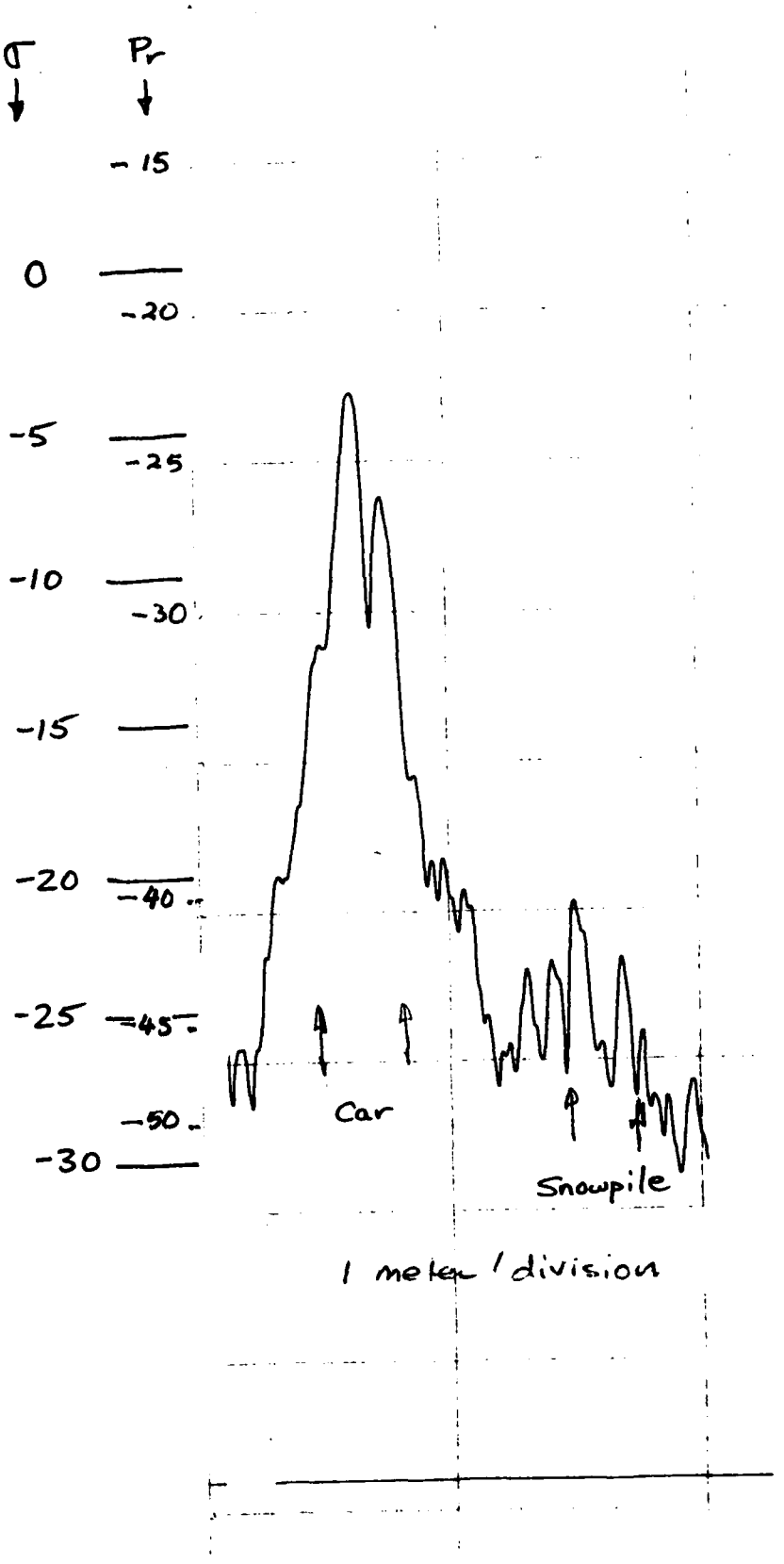

Date: 2/17/80
Steamboat High Parking Lot

F = 17.0

RL , 10°

FM = 405

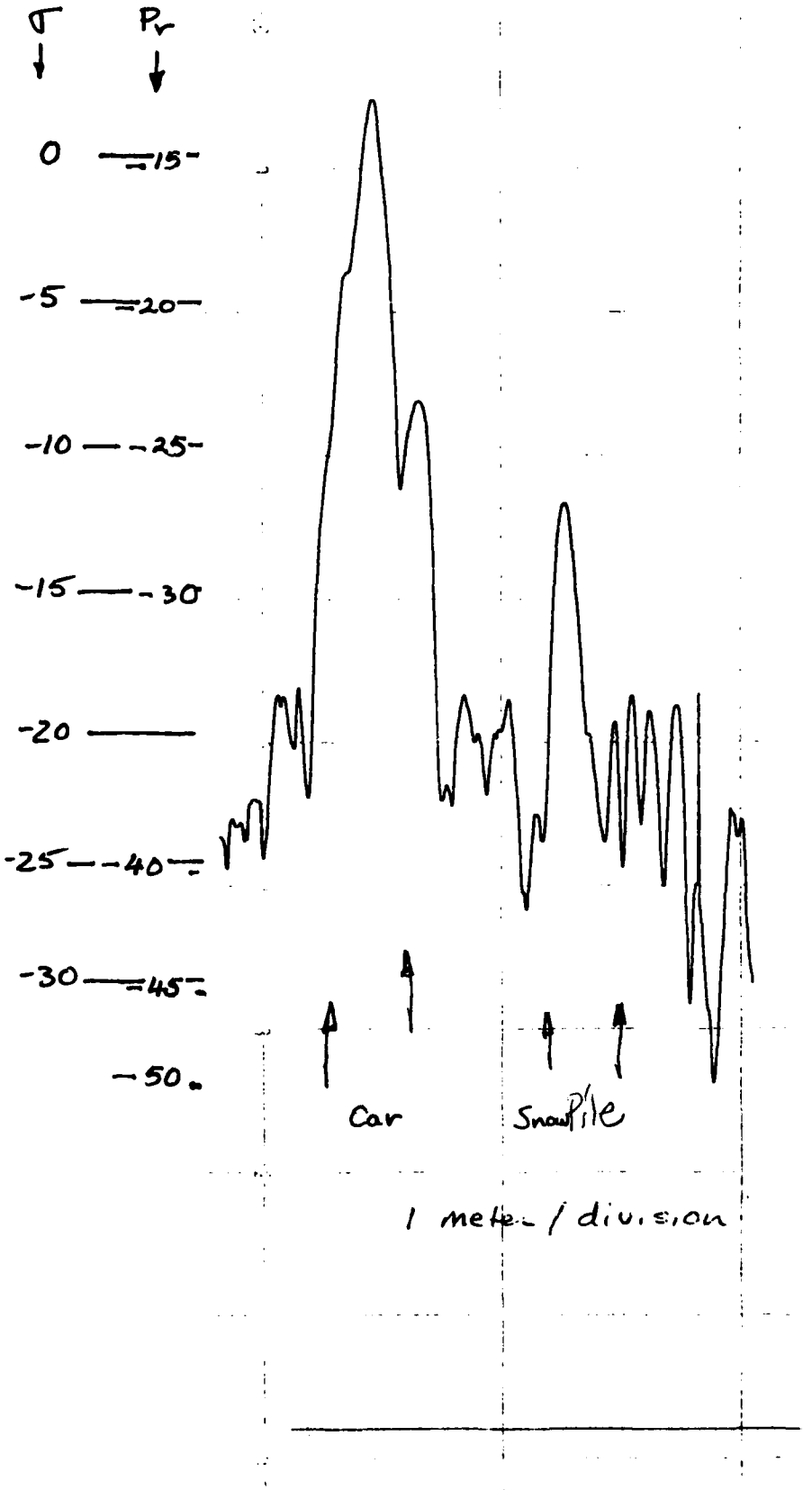

Date: 2/17/80

Steamboat High Parking Lot

T = 17.0

RR, 10°

FM = 405

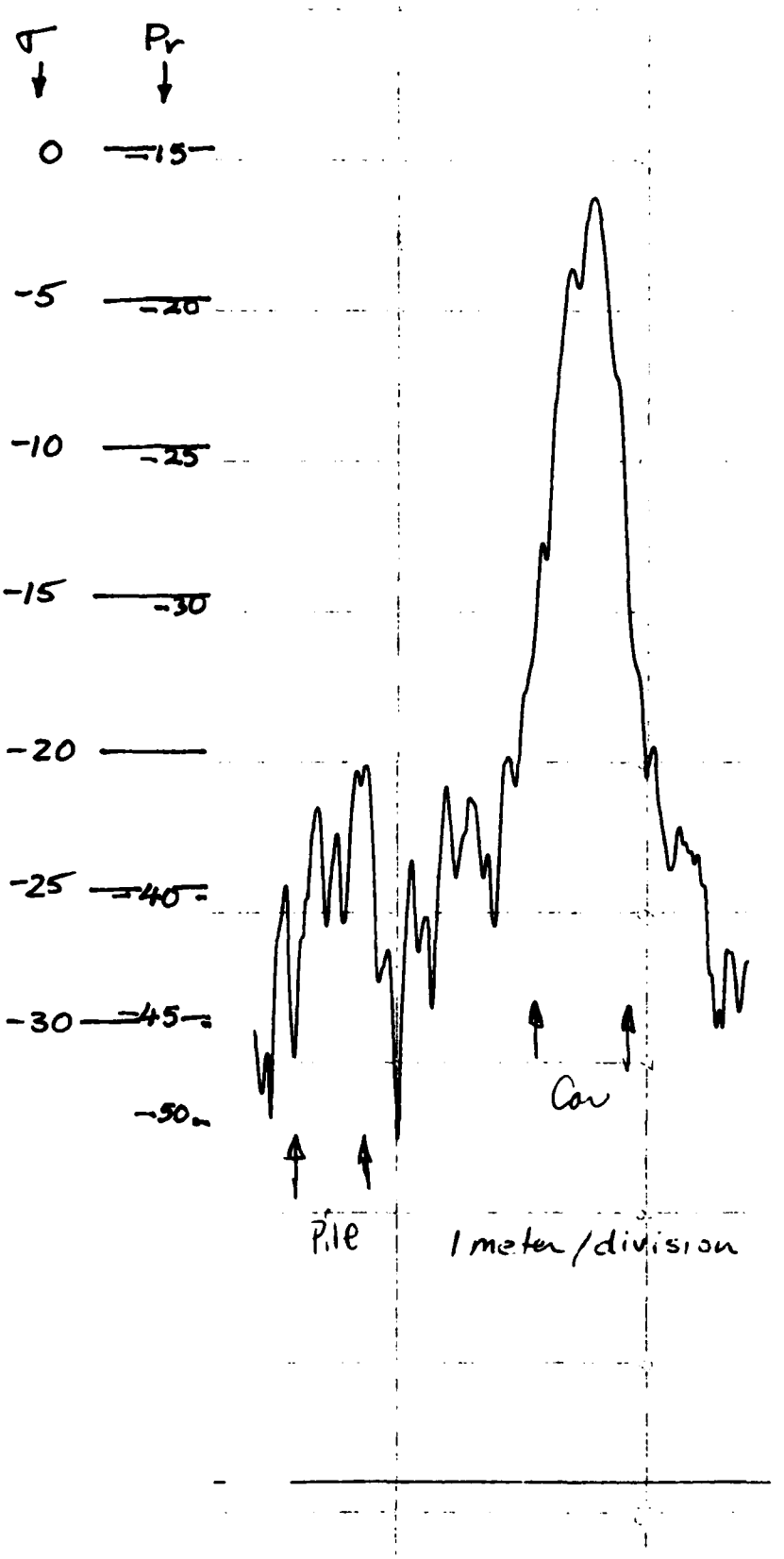

Date: 2/17/80
Steamboat High Parking Lot.

F = 8.6

RL

30°

FM = 371

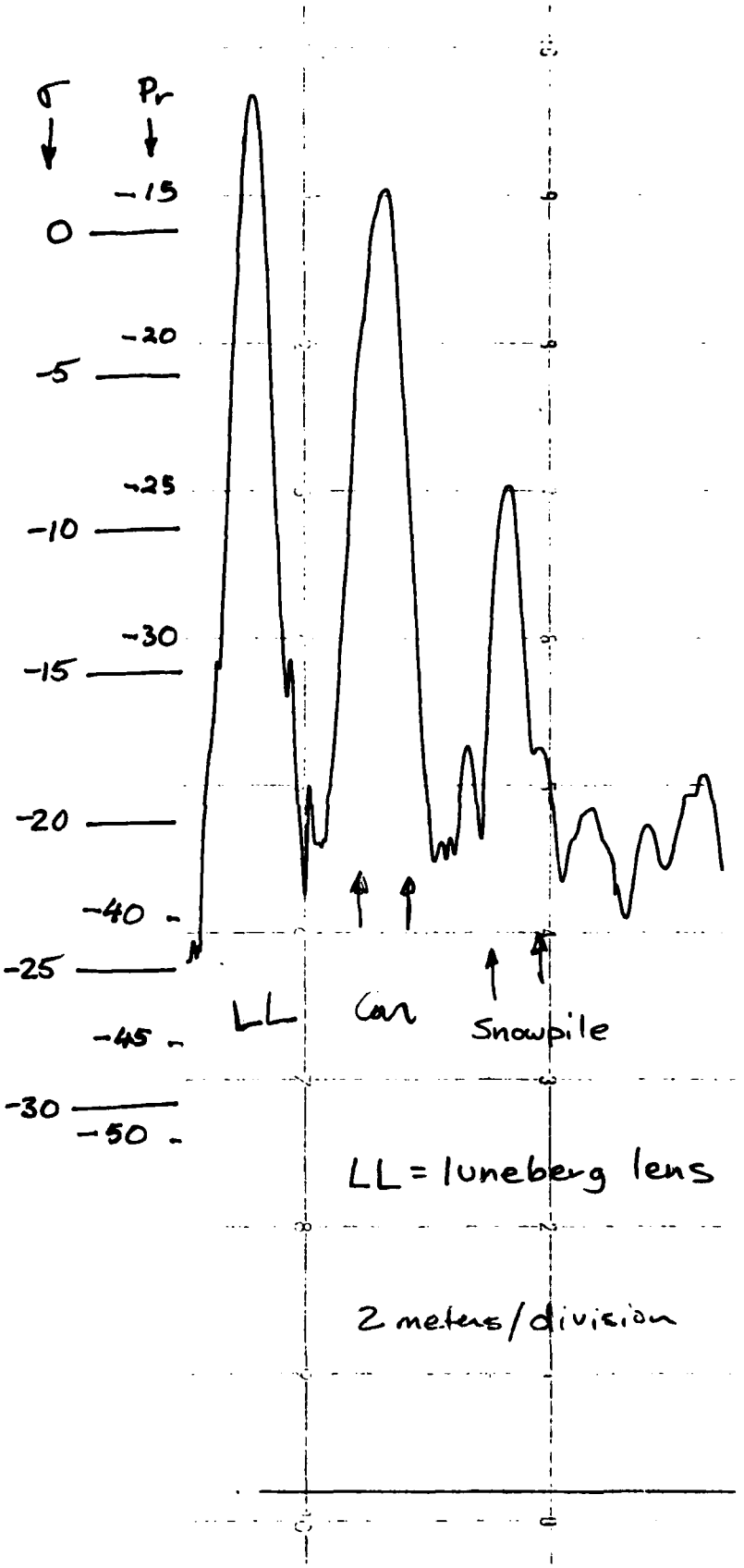

Date: 2/17/80

Steamboat High Parking Lot

F = 8.6

RR, 30°

FM = 371

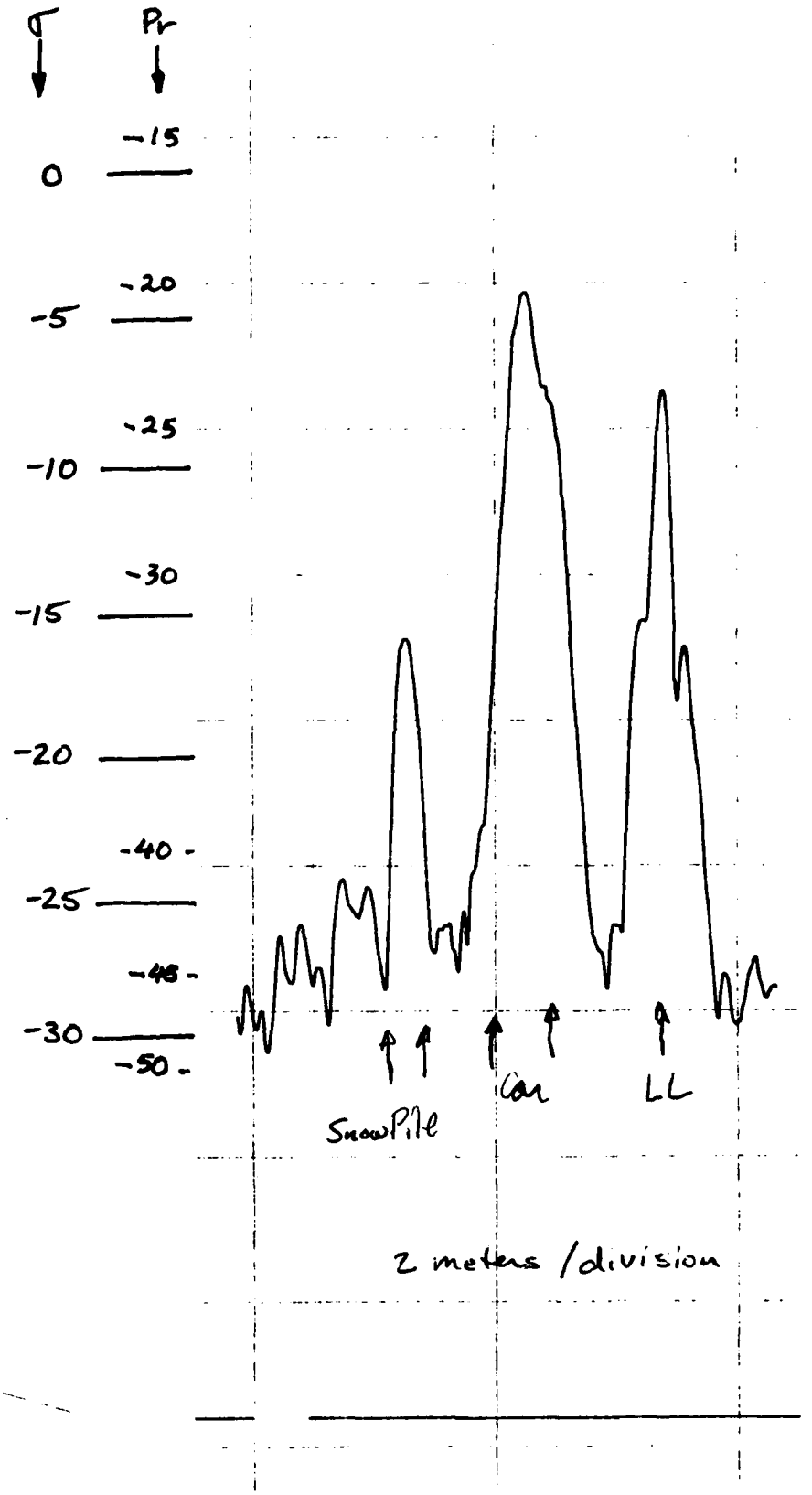

Date: 2/17/80

Steamboat High Parking Lot.

F = 10.2

RL, 30°

FM = 371

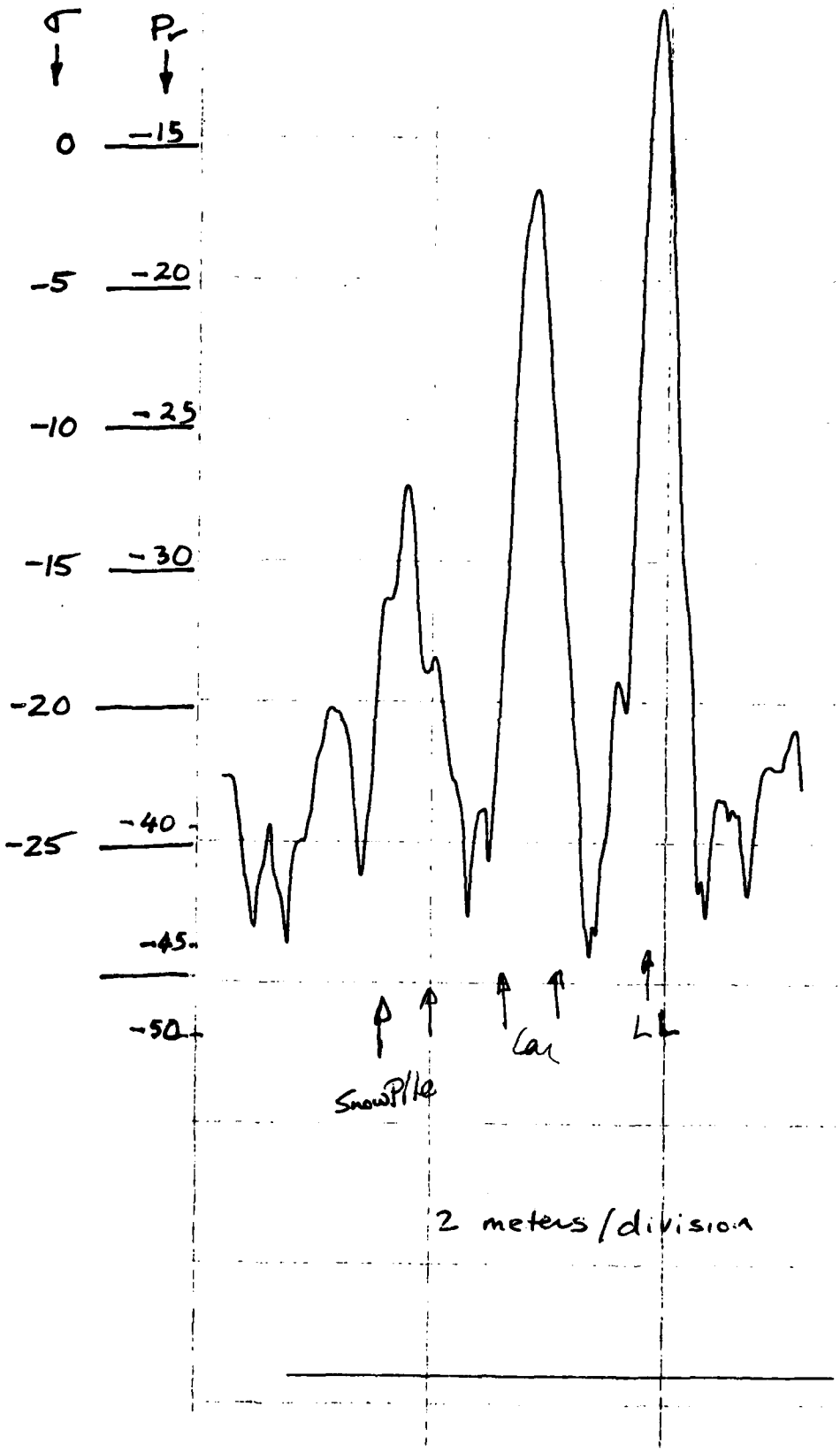

Date: 2/17/80
Steamboat High Parking Lot.

F = 10.2

RR , 30°

FM = 371

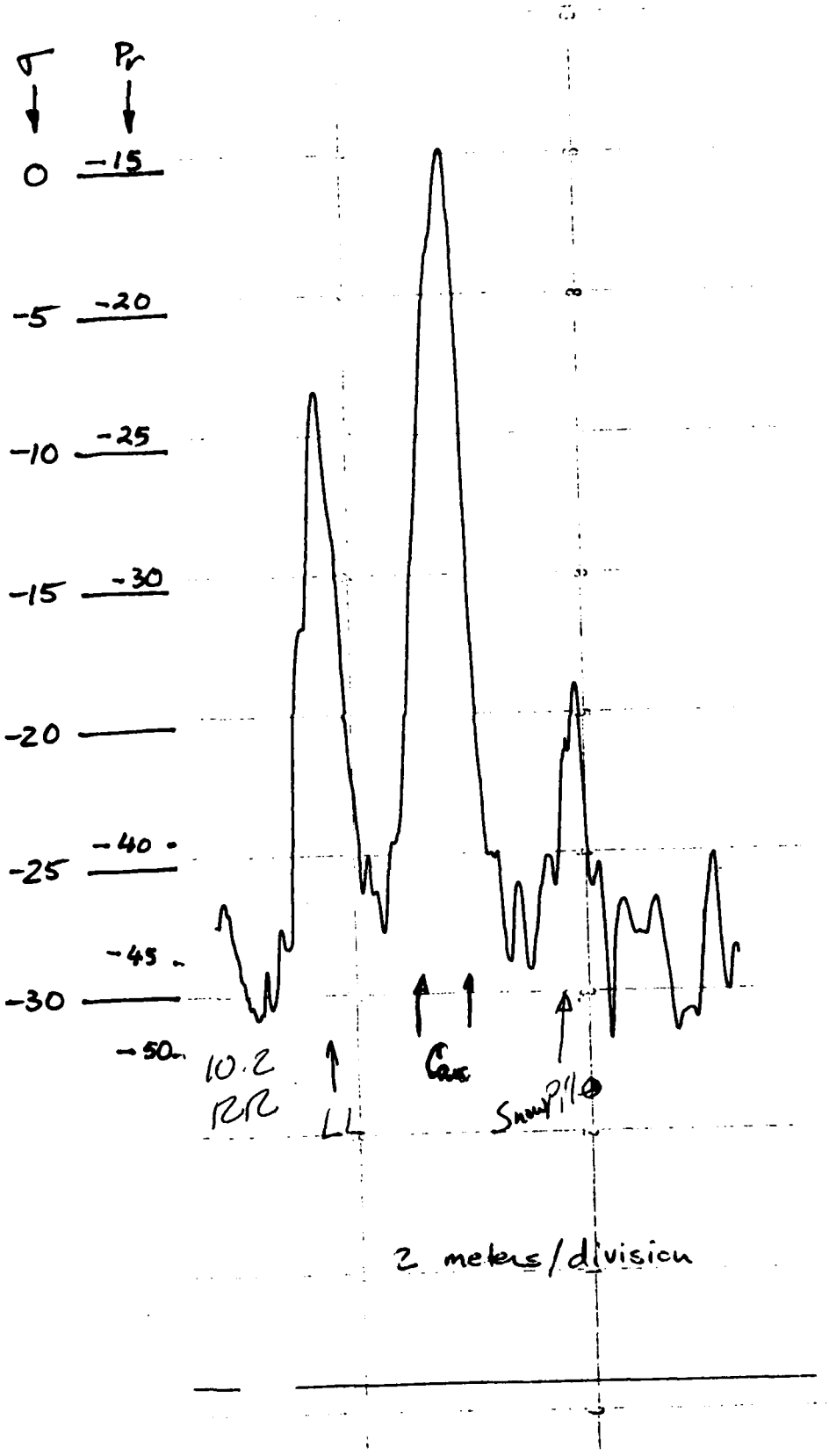

Date: 2/17/80

Steamboat High Parking Lot

F= 11.8

RL ,30°

FH=371

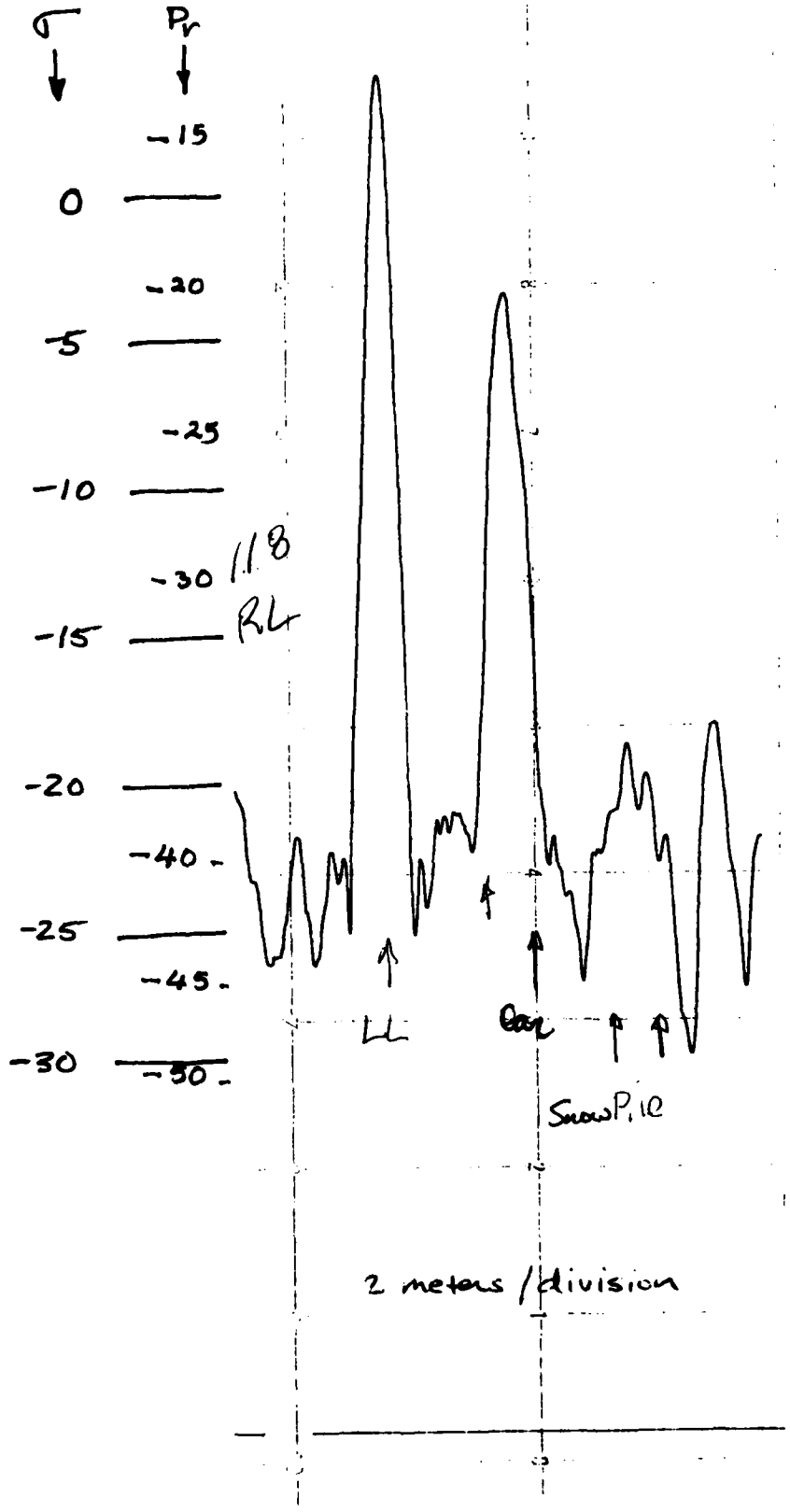

Date: 2/17/80
Steamboat High Parking Lot

F = 11.8

RR, 30°

FM = 371

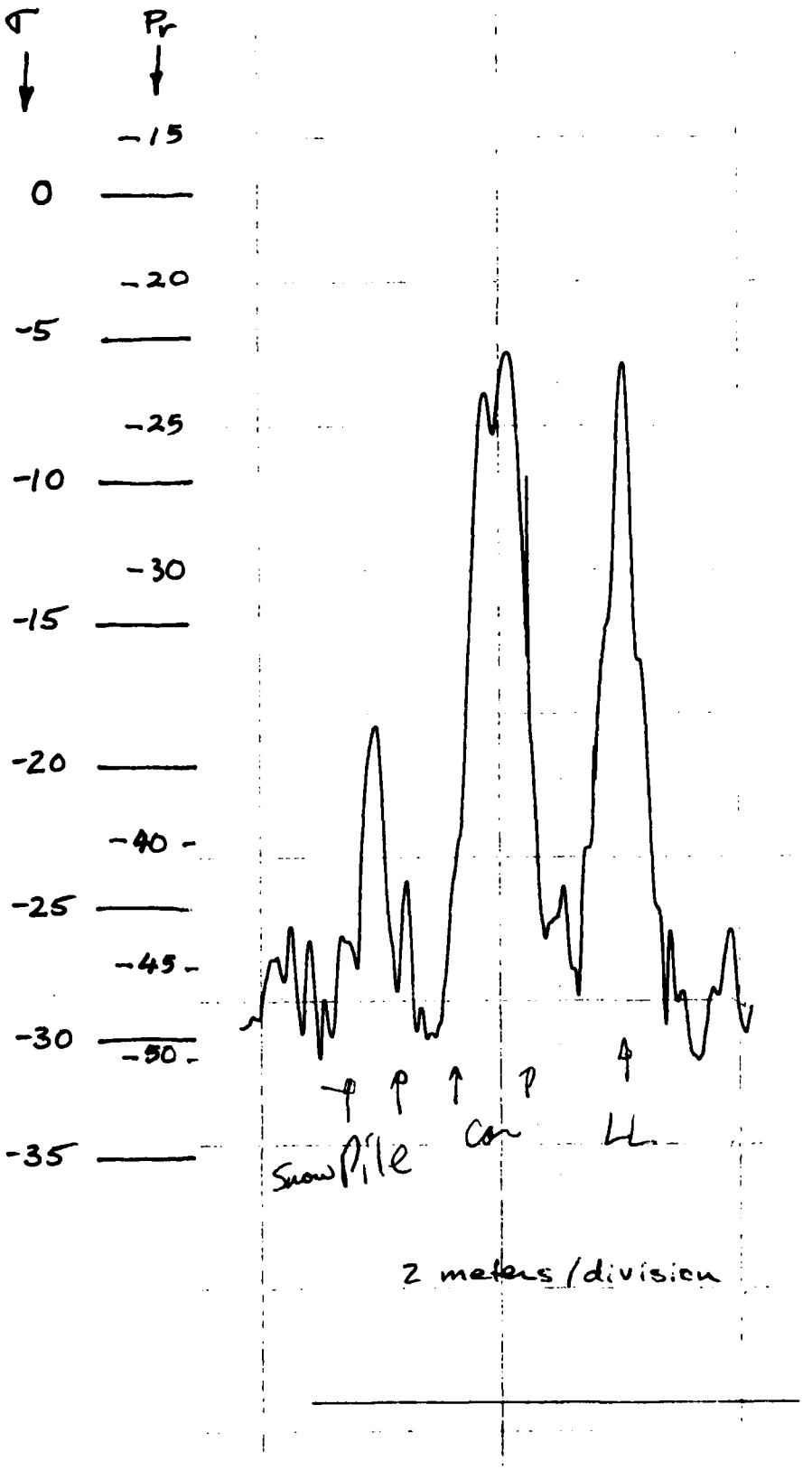

Date: 2/17/80

Steamboat High Parking Lot

F = 13.8

RL, 30°

FM = 371

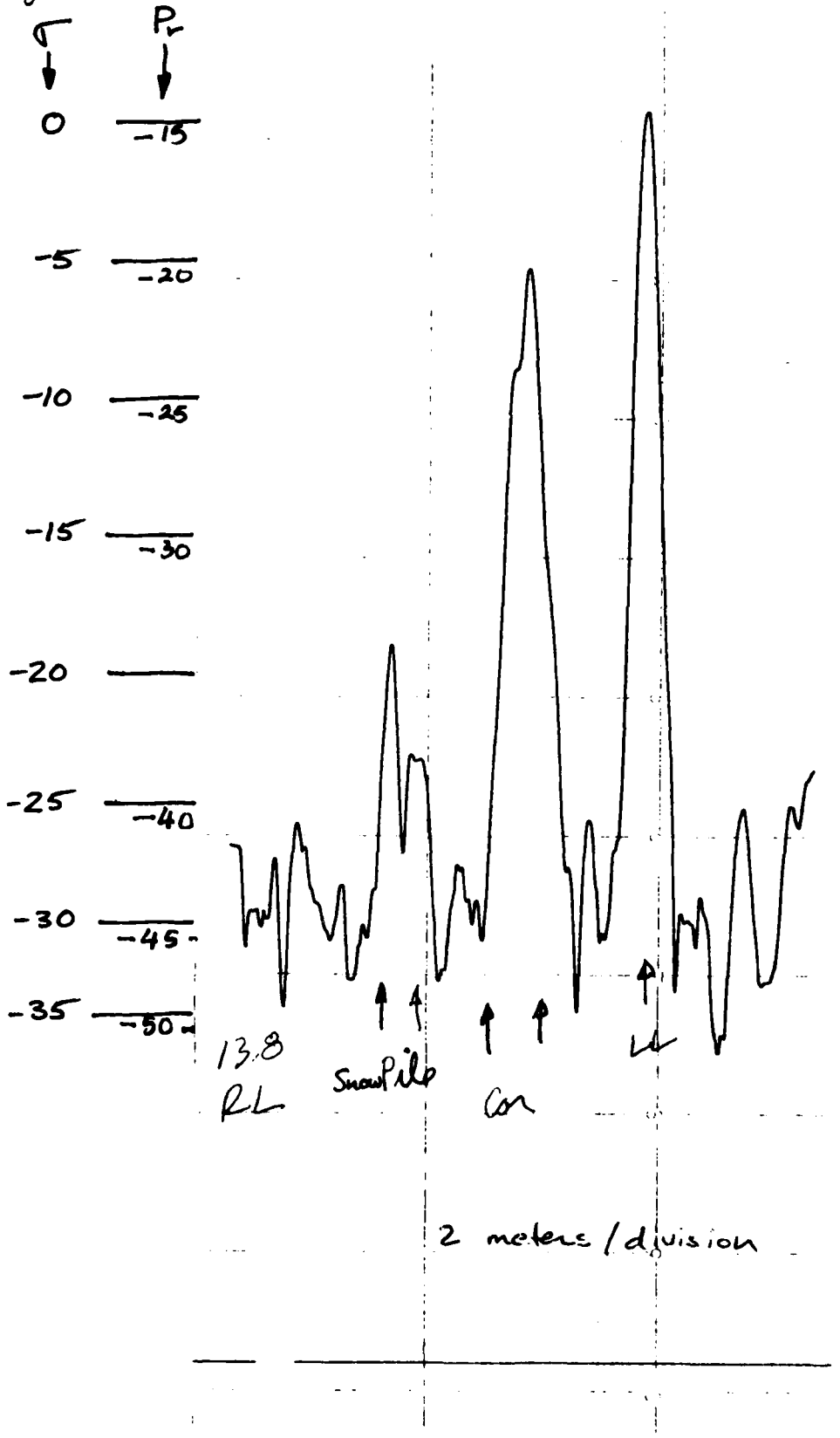

Date: 2/17/80
Steamboat High Parking Lot

F = 13.8

RR, 30°

FH = 371

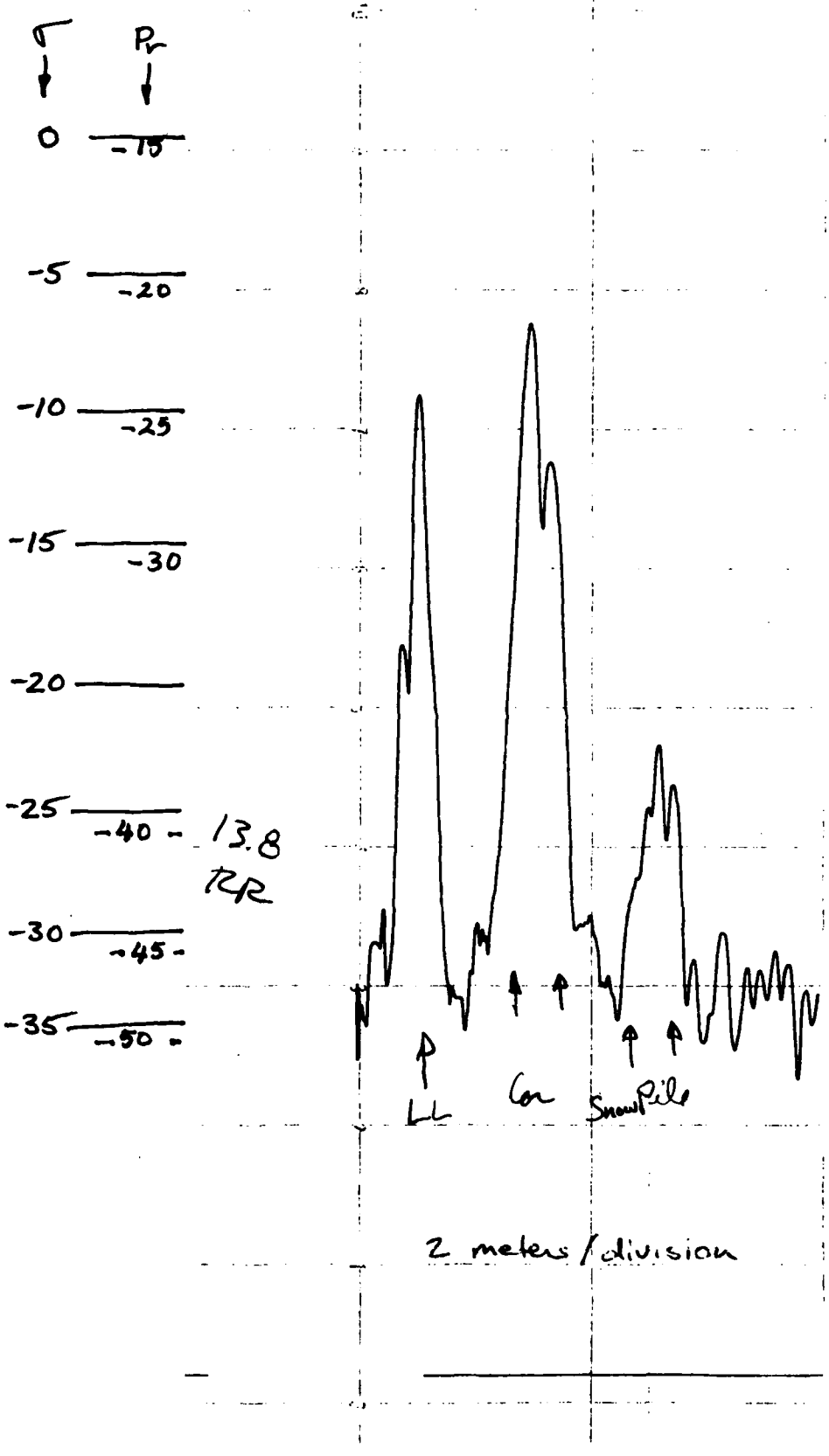

Date: 2/17/80
Steamboat High Parking Lot

F = 16.2

RL ,30°

FH = 371

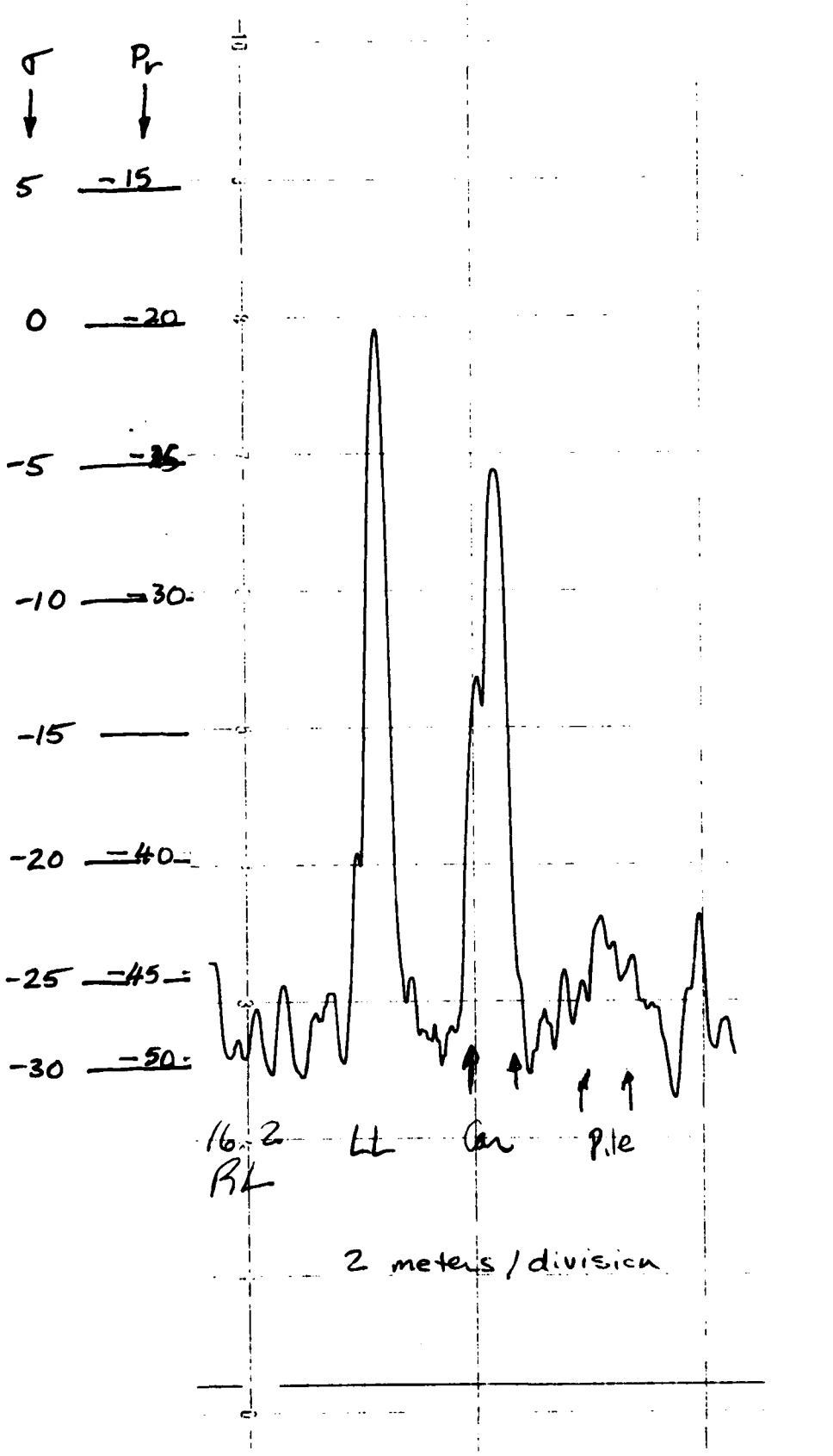

Data: 2/17/80
Steamboat High Parking Lot

F = 16.2

RR , 30°

FM = 371

σ	Pr
5	-15
0	-20
-5	-25
-10	-30
-15	
-20	-40
-25	-45
-30	-50

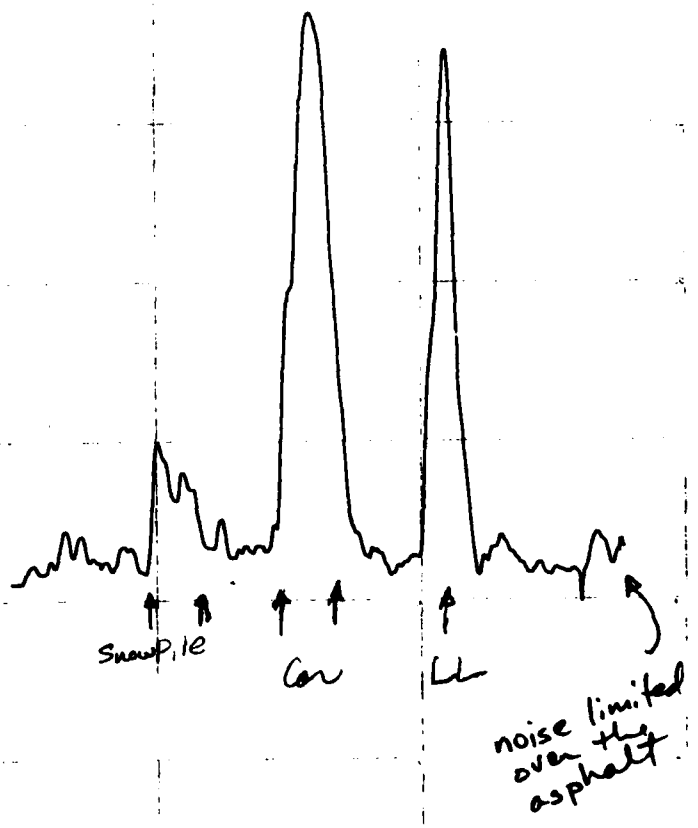

2 meters / division

Date: 2/17/80
Steamboat High Parking Lot

F = 17.0

RL , 30°

FM = 371

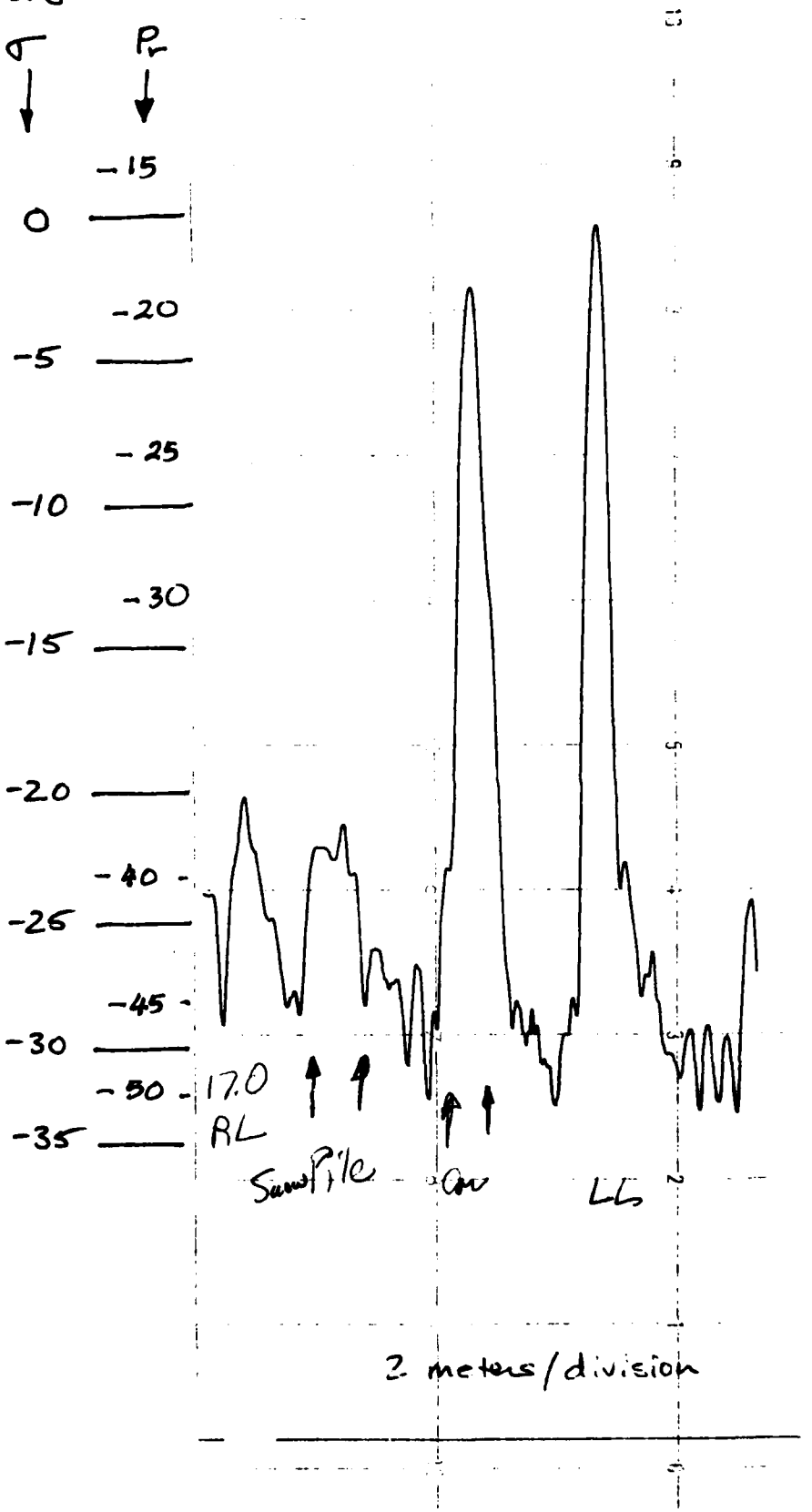

Date: 2/17/80

Steamboat High Parking Lot

FM = 17.0

RR , 30°

σ	P_r
	-15
0	
	-20
-5	
	-25
-10	
	-30
-15	
-20	
	-40
-25	
	-45
-30	
	-50
-35	

FM = 371

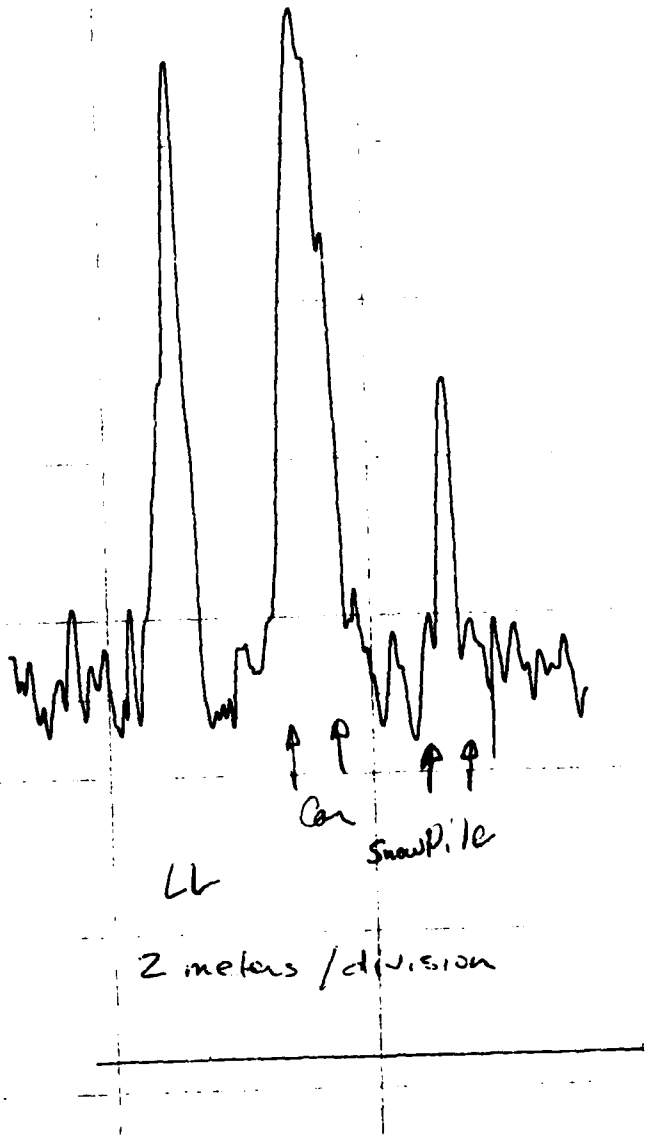

Date: 2/17/80

steamboat High Parking Lot

F = 8.6

RL

FM 431

car FM = 527

70°

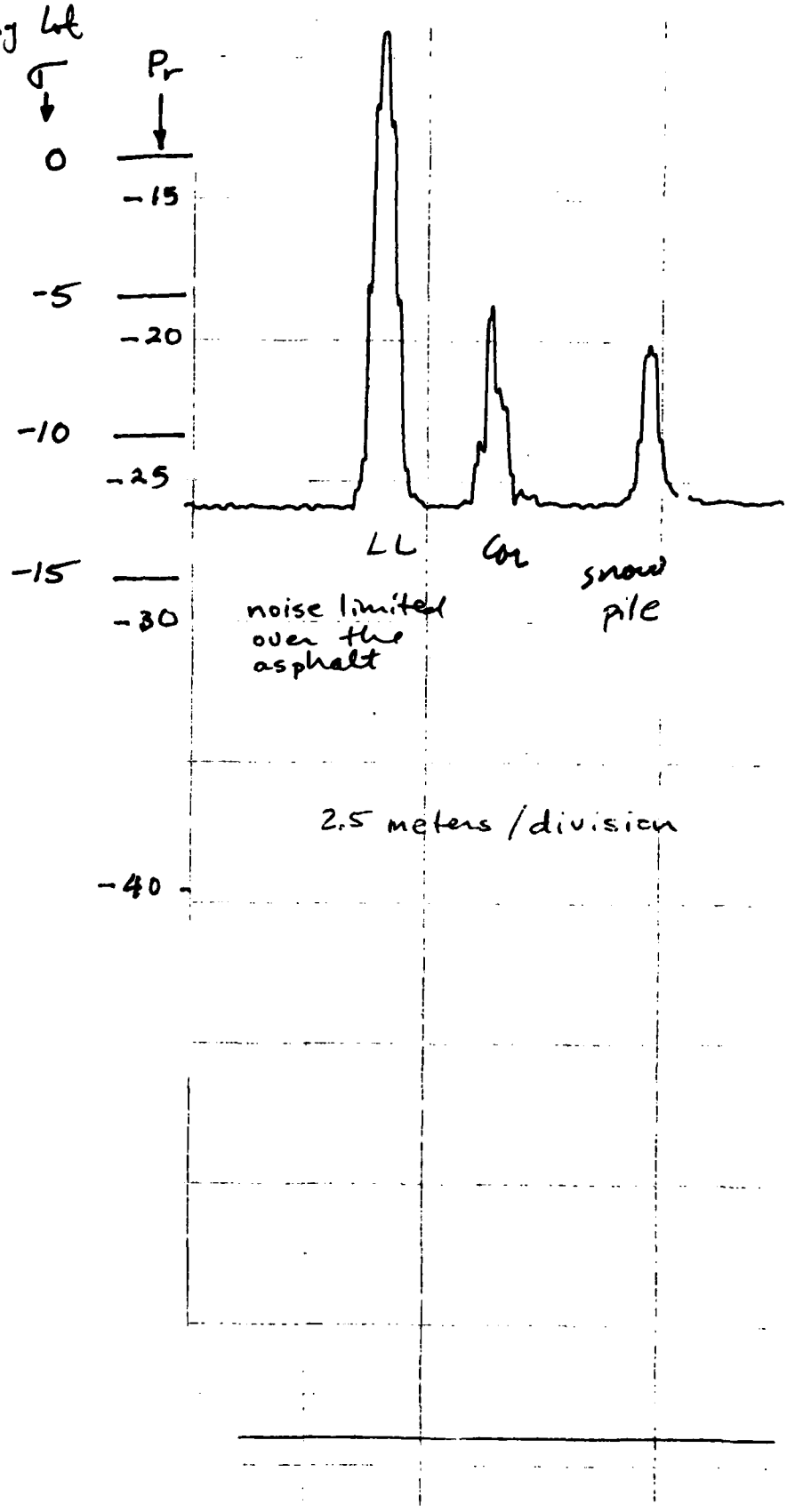

Date: 2/17/80

Steamboat High Parking Lot

F = 8.6

RR , 70°

Lens FM = 432

Car FM = 527

Pile FM = 446

FM = 431

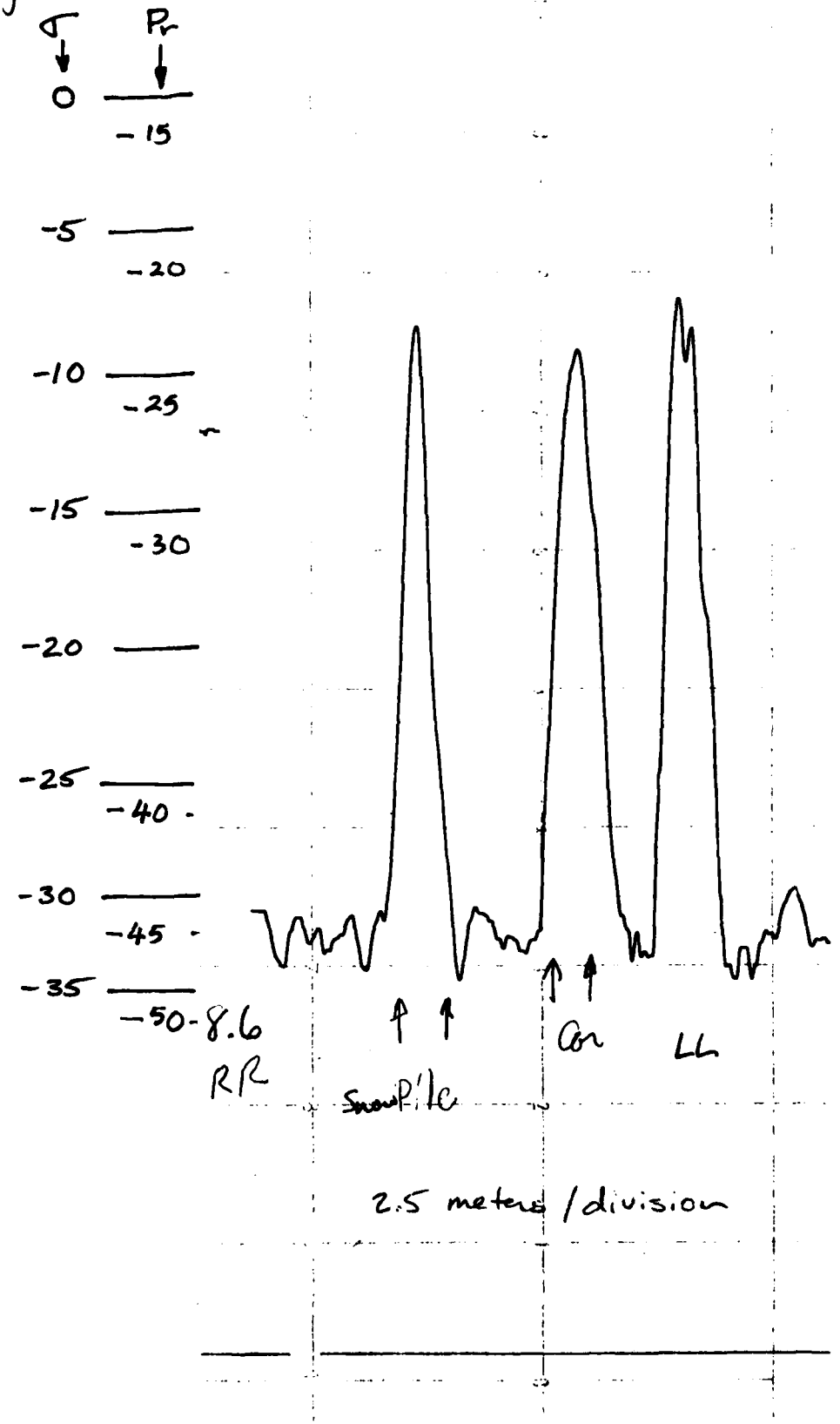

Date 2/17/80
Steamboat High Parking Lot

F = 10.2
RL , 70°

Lens FM = 432
Car FM = 527
Pile FM = 446

FM = 431

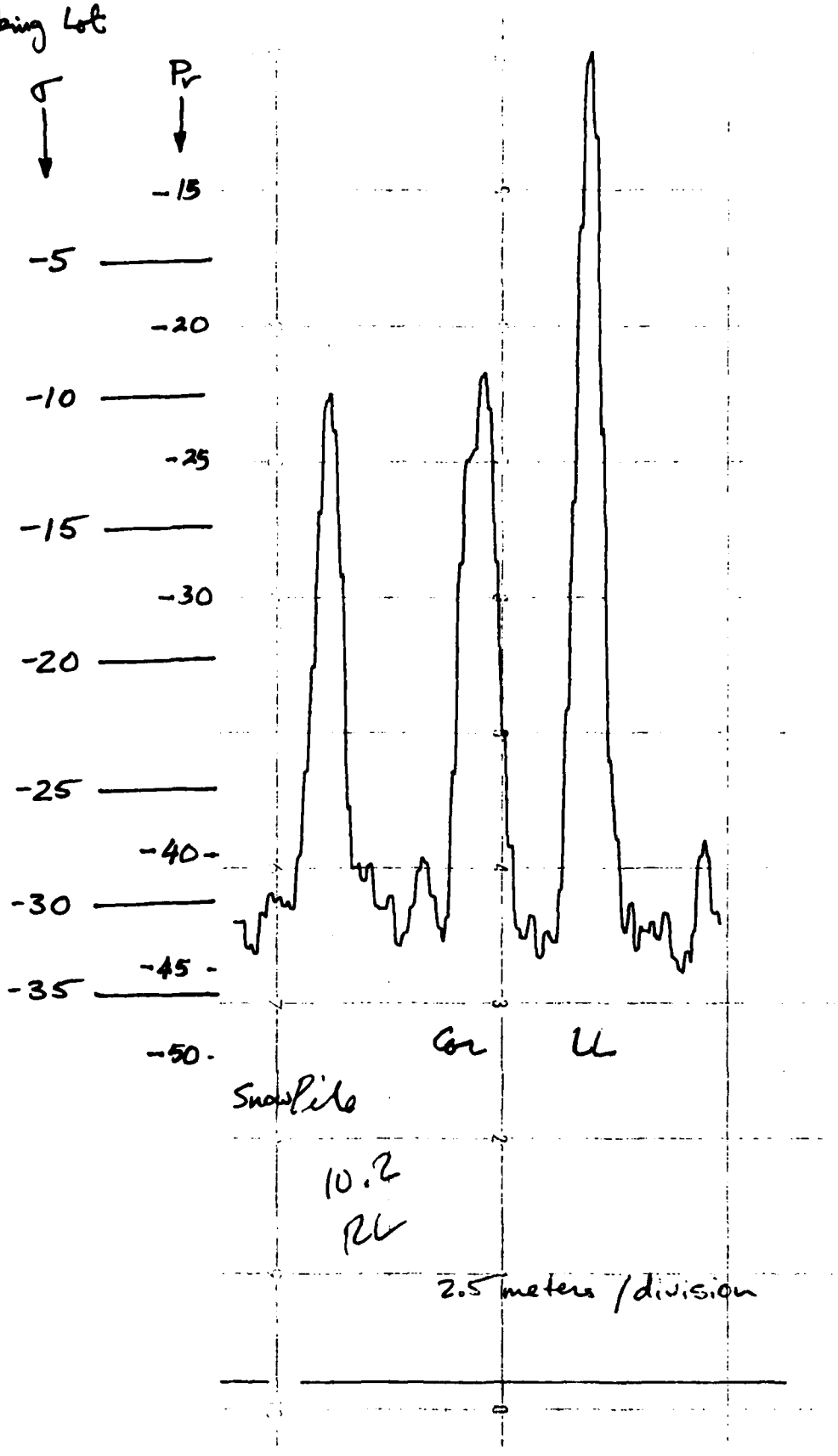

Date: 2/17/80
Steamboat High Parking lot

$F = 10.2$

RR , 70°

Lens FM = 432
Car FM = 527
Pile FM = 446

FM = 431

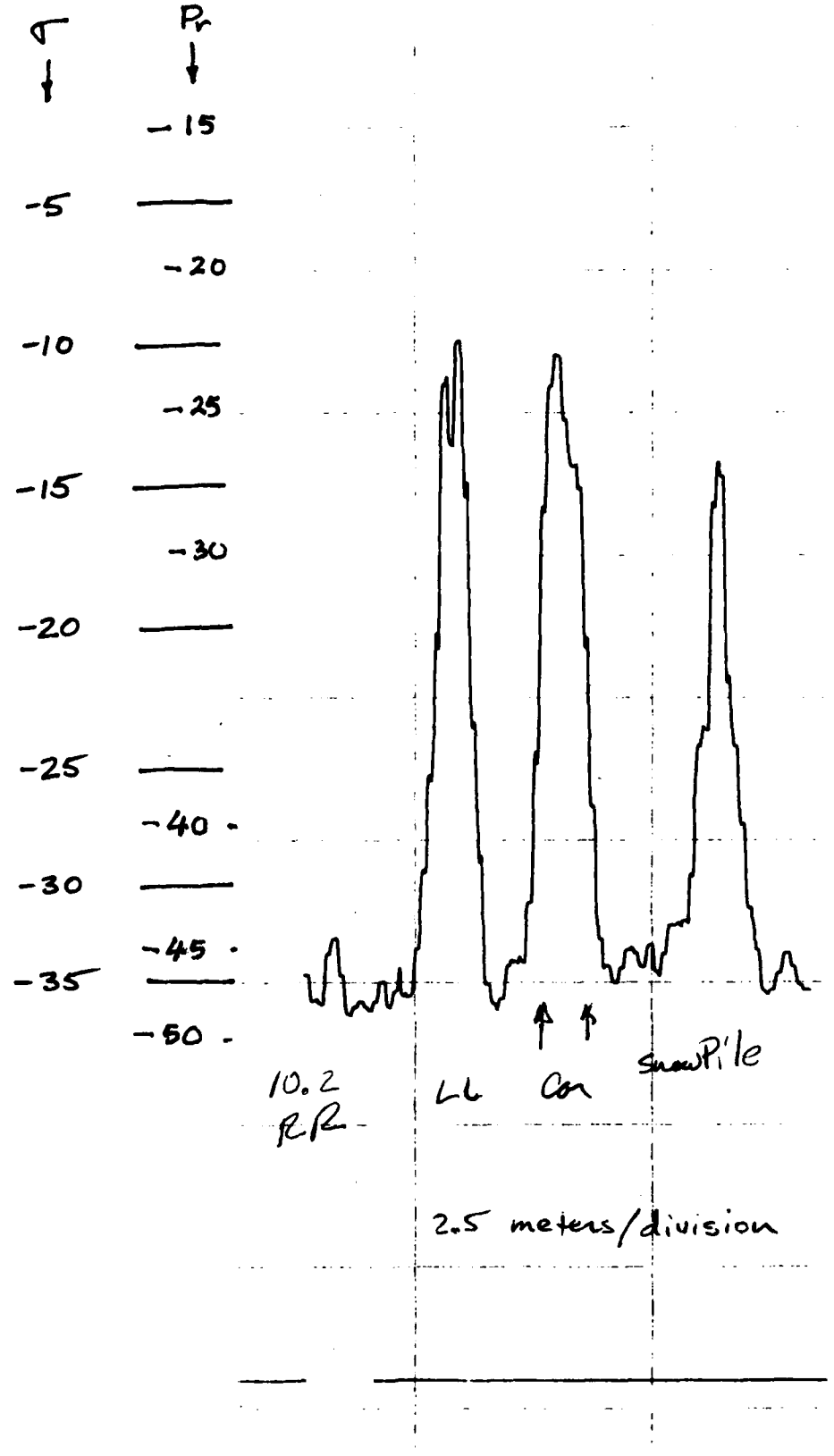

Date: 2/17/80

steamboat Peak Parking Lot

f = 11.8

RL , 70°

Less FM = 432

Car FM = 527

Pile FM = 446

FM = 431

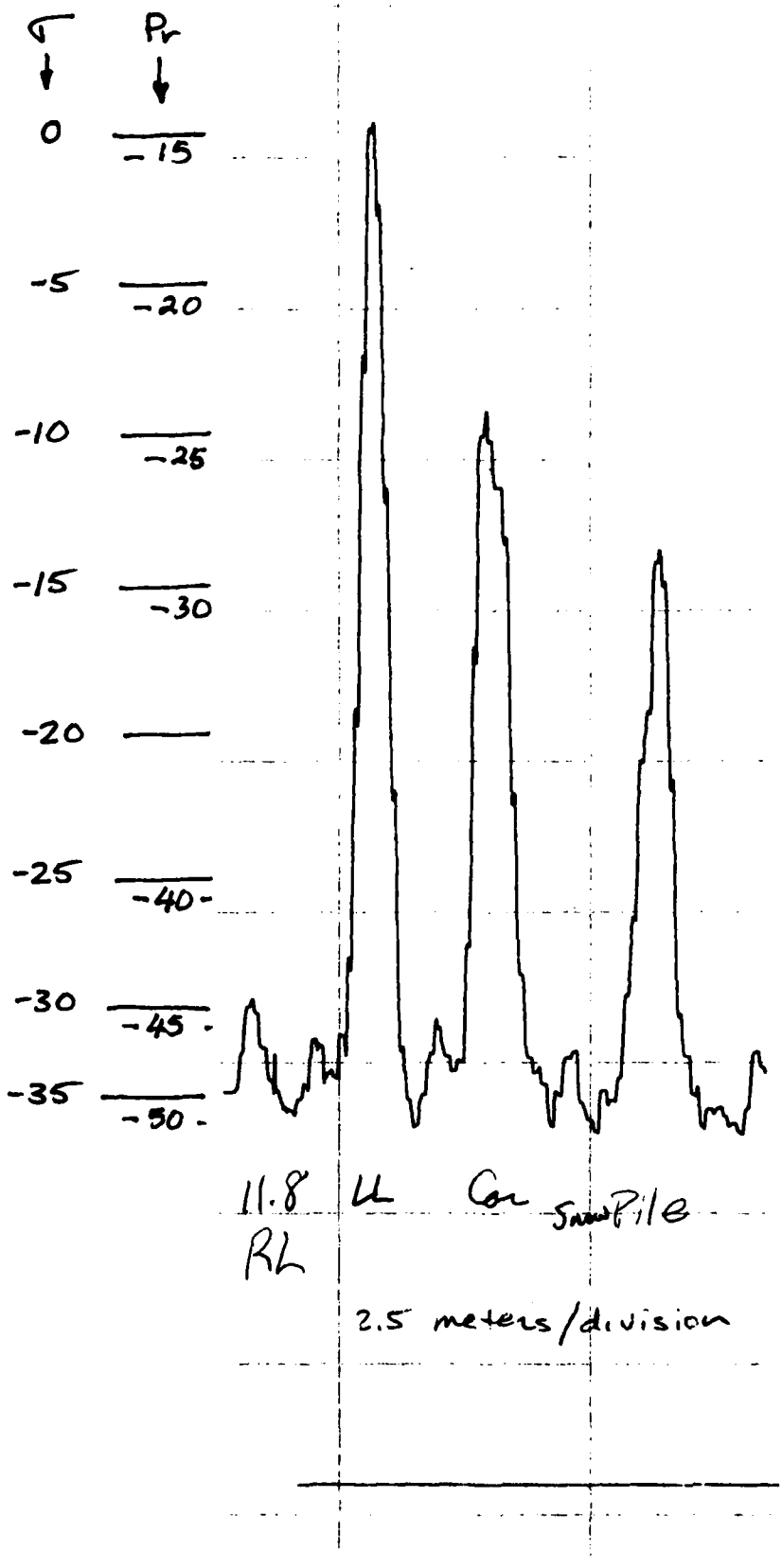

Date: 2/17/80

Steamboat High Parking Lot

F = 11.8

RR , 70°

Lens FM = 432

Car FM = 527

Pile FM = 446

FM = 431

T	Pr
0	-15
-5	-20
-10	-25
-15	-30
-20	
-25	-40
-30	-45
-35	-50

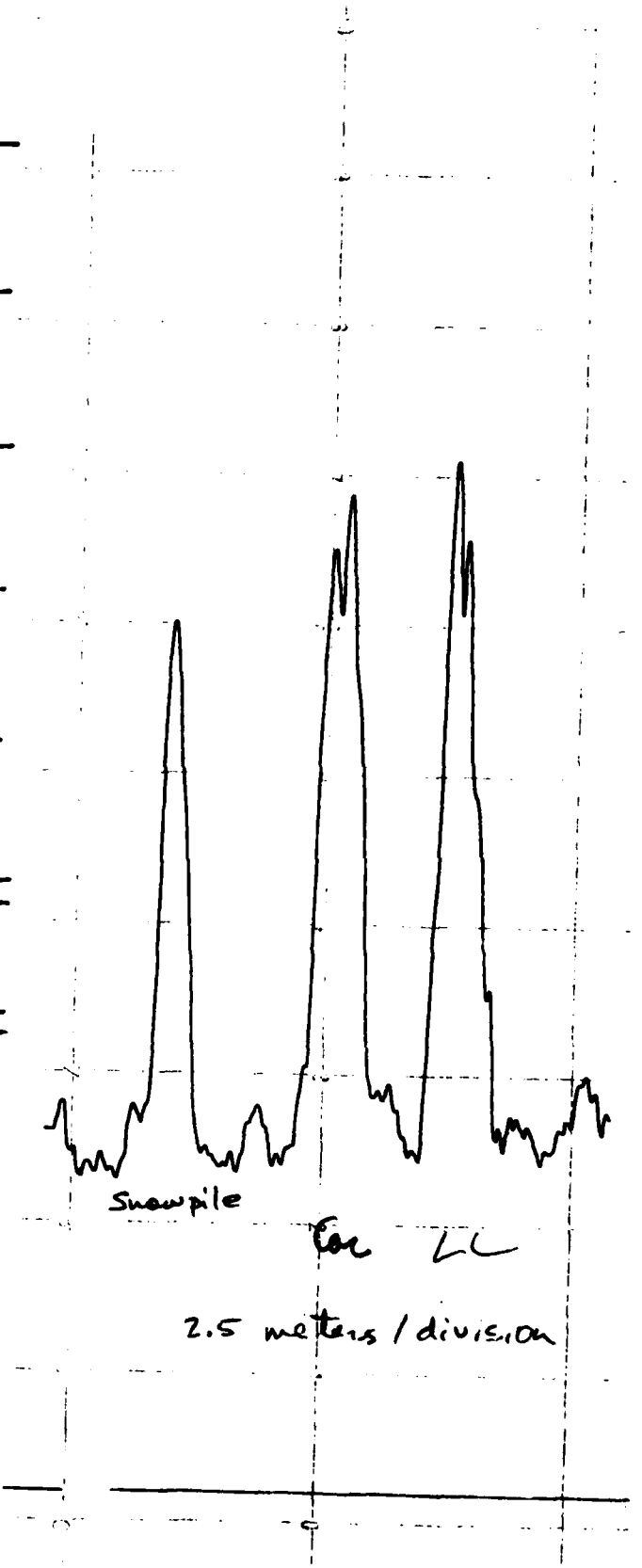

Date: 2/17/80

Steamboat High Parking Lot

f = 13.8

RL , 70°

Lens FM = 432

Car FM = 527

Pile FM = 446

FM = 431

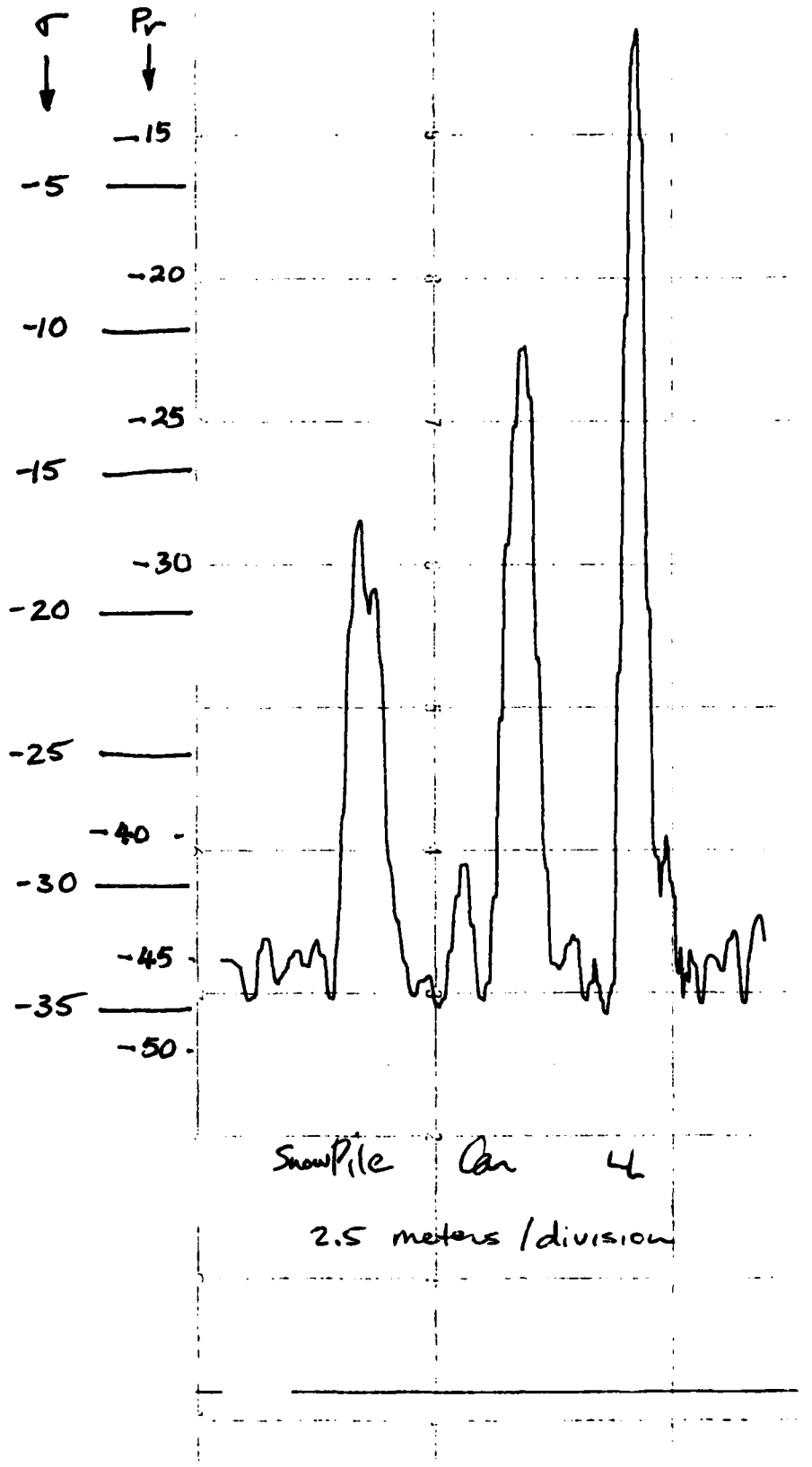

Date: 2/17/80
Steamboat High Parking lot

f = 13.8

RR ,70°

Lens FM = 432

Car FM = 527

Pile FM = 446

FM = 431

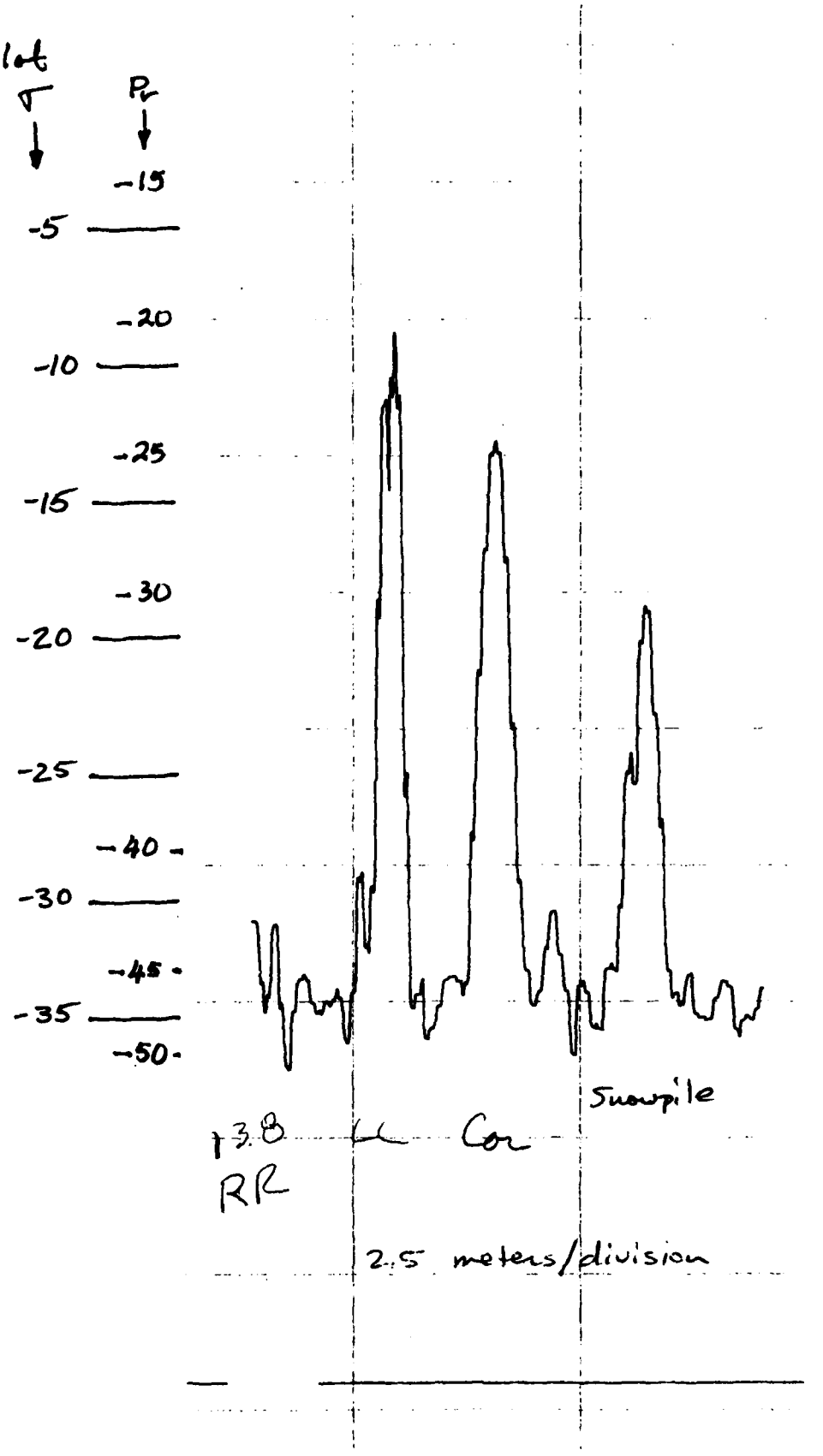

Date: 2/17/80

Steamboat High Parking Lot

f = 16.2

R L , 70°

Lens FM = 432

Car FM = 527

Pile FM = 446

FM = 431

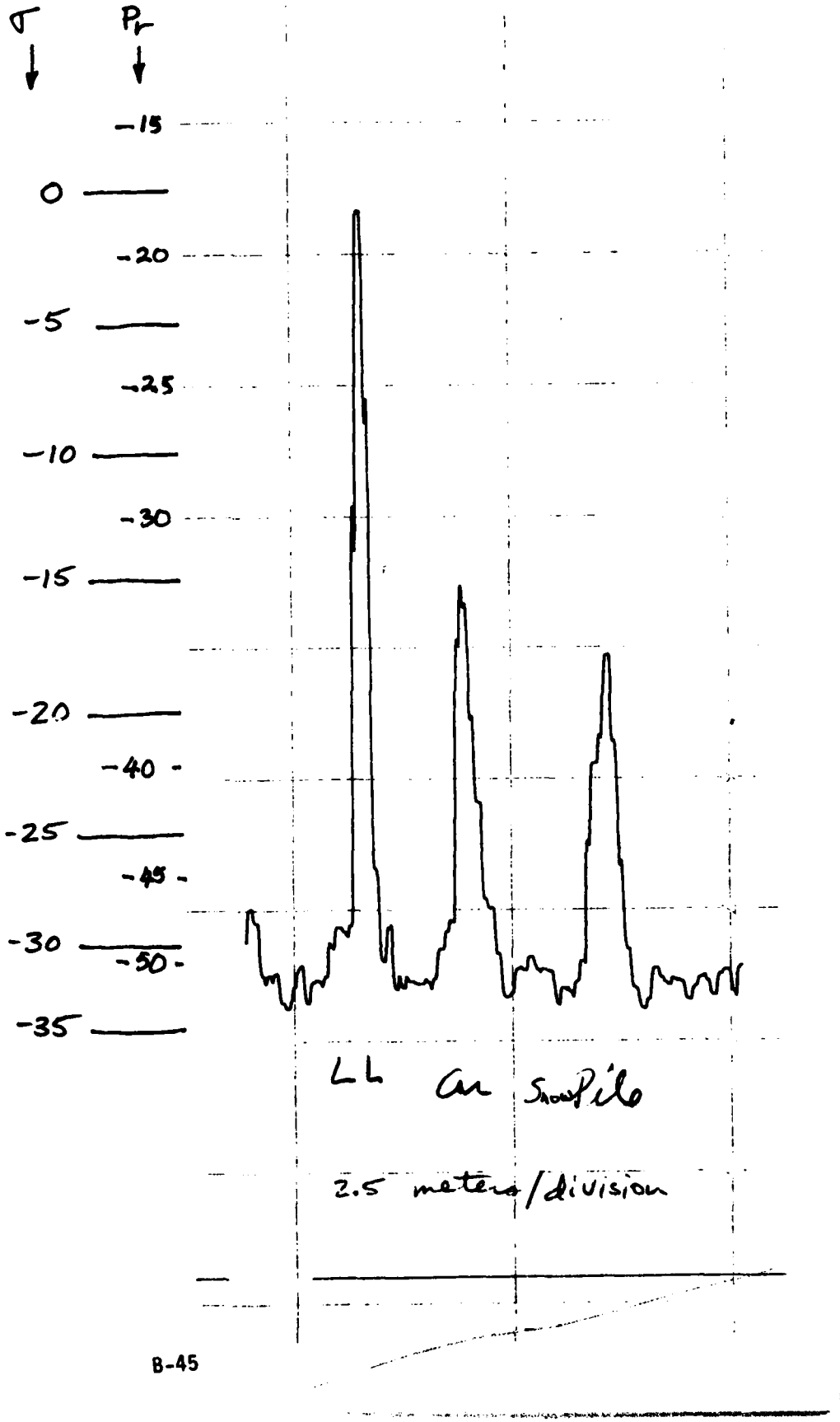

Date 2/17/80
Steamboat High Parking Lot

F = 16.2

RR) 70°

Lens FM = 432

Car FM 527

Pile FM 446

FM = 431

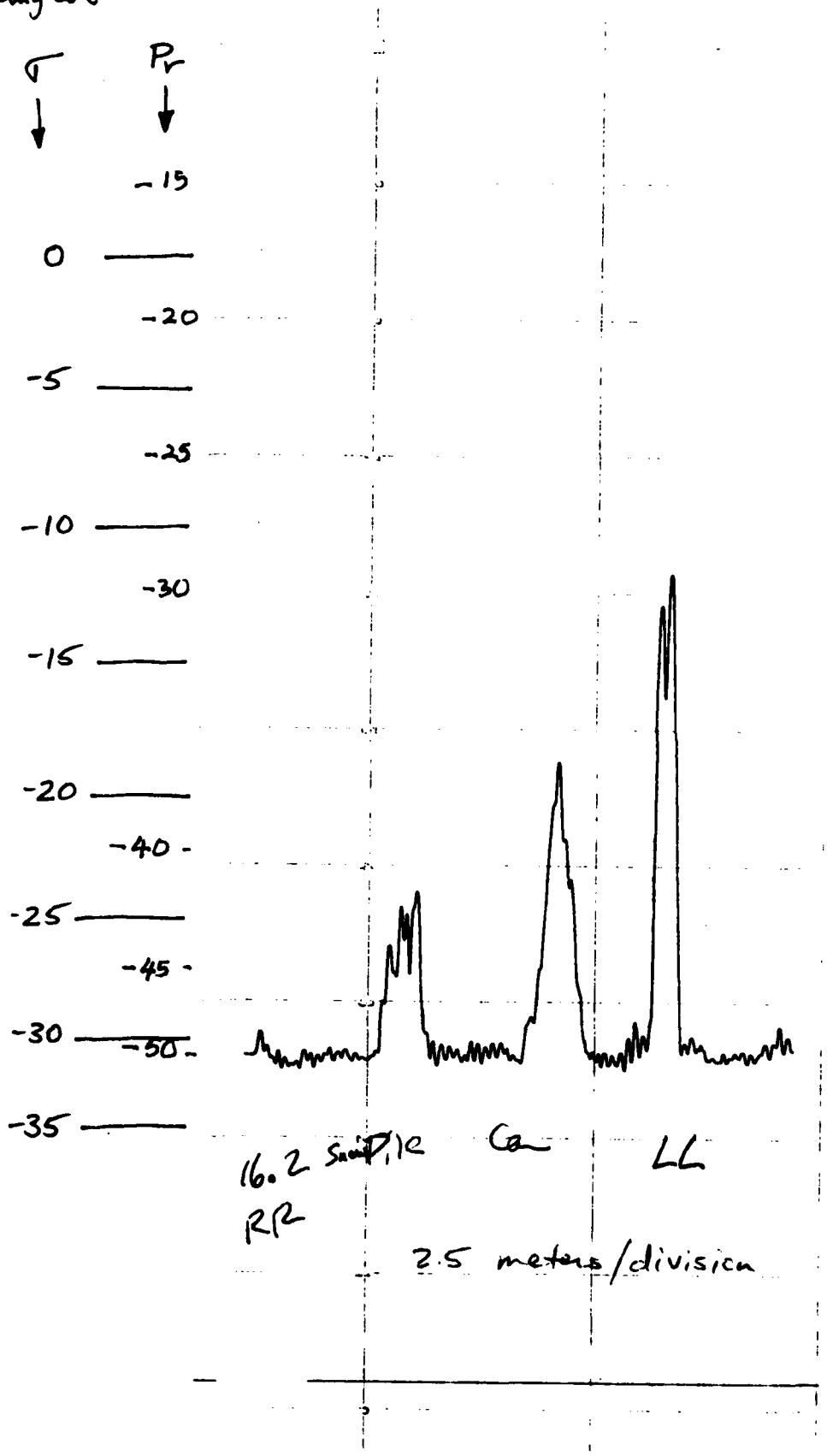

Date 2/17/80
steamboat High Parking lot

f = 17.0
RL , 70°

Lens FM 432
Con FM 527
Pile FM 446

FM = 431

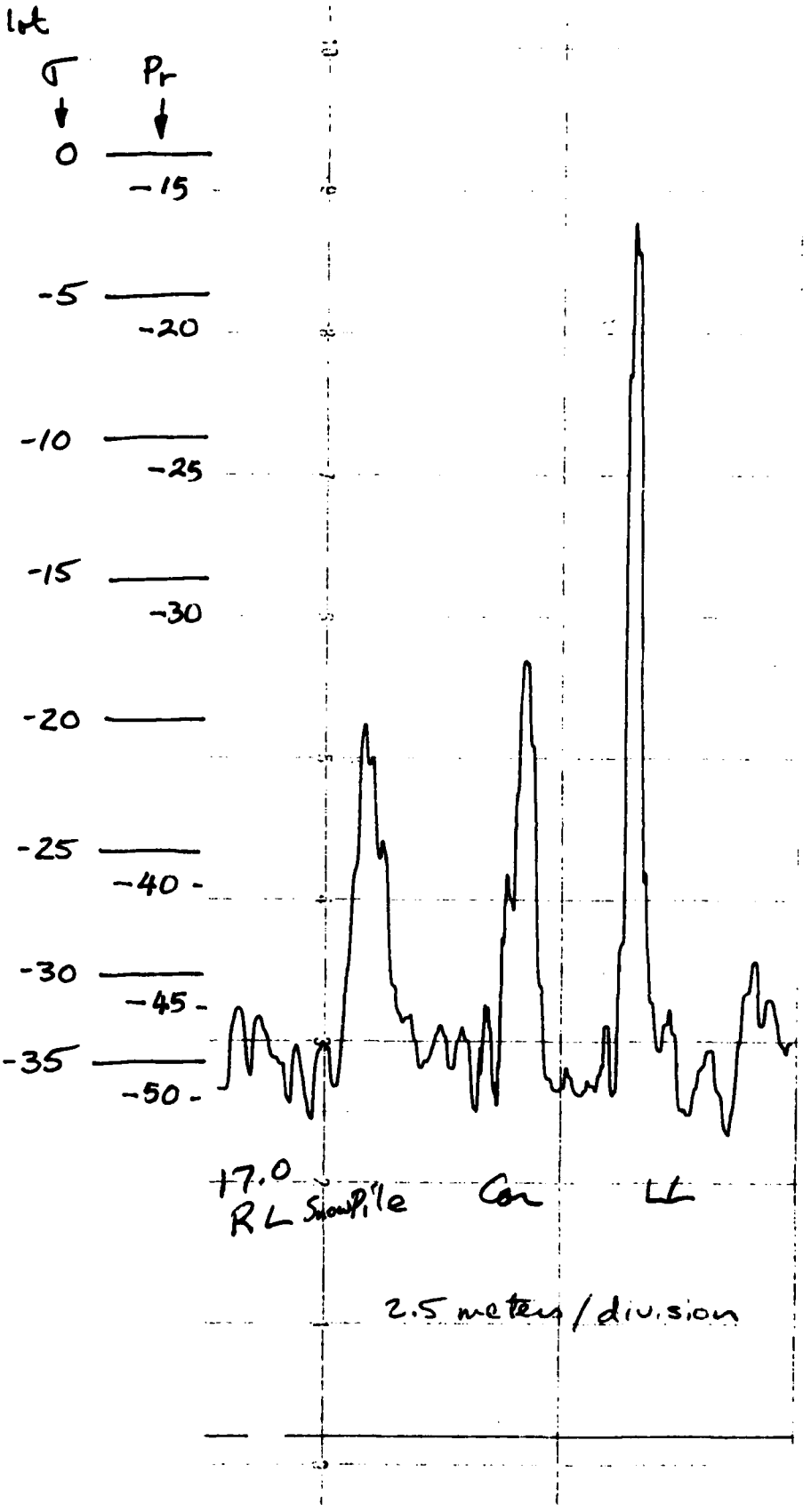

2/17/80

Steamboat High Parking Lot

F = 17.0

RR ,70°

Lens FM 432

Car FM 527

Pile FM 446

FM=431

T	Pr
0	-15
-5	-20
-10	-25
-15	-30
-20	
-25	-40
-30	-45
-35	-50

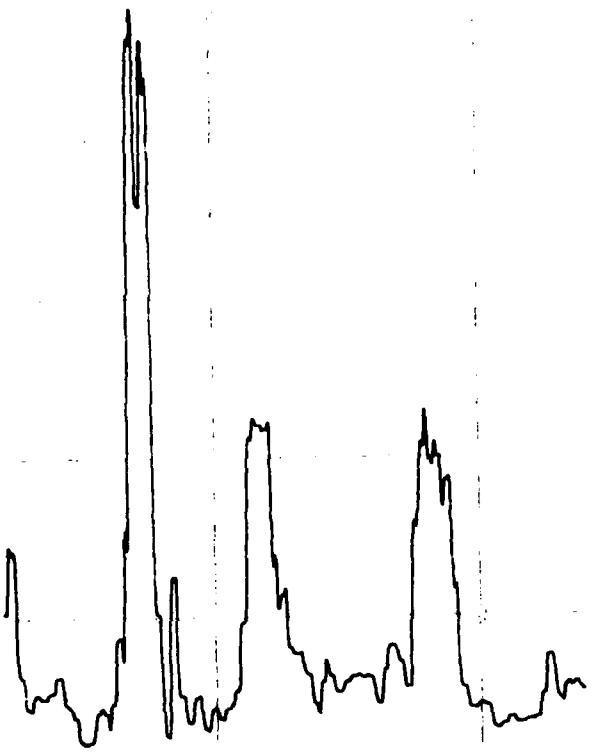

17.0 Car Pile

RR LL

2.5 meters/division

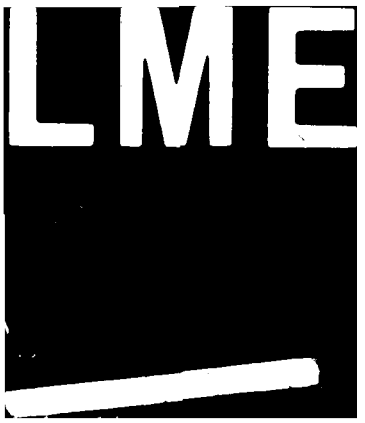
LME